STUDIES TOWARDS AN ASTROGRAVIMETRIC GEOID FOR CANADA

CHARLES L. MERRY

February 1975

TECHNICAL REPORT
NO. 31

PREFACE

In order to make our extensive series of technical reports more readily available, we have scanned the old master copies and produced electronic versions in Portable Document Format. The quality of the images varies depending on the quality of the originals. The images have not been converted to searchable text.

STUDIES TOWARDS AN ASTROGRAVIMETRIC GEOID FOR CANADA

by

Charles L. Merry

Technical Report No. 31

University of New Brunswick
Department of Surveying Engineering
Fredericton, N.B., Canada

February, 1975

ABSTRACT

The determination of geoidal heights from astrogeodetic deflections of the vertical is limited in reliability by the lack of available data, and its generally poor distribution. In order to overcome this problem, one possible method is to use gravity data to assist in predicting deflections in areas where none have been, or can be, observed.

This thesis investigates such a procedure, and evaluates the capabilities of a high order approximating polynomial to represent the geoid. The influence of the additional predicted deflections on the shape of the geoid is studied, and various alternatives for the determination of the detailed shape of the geoid in a small area investigated.

Satisfactory results have been obtained for the deflection prediction. However, not all error sources have been accounted for, and further refinements, together with an improved gravity field, will result in more reliable predictions.

The use of the approximating polynomial has several advantages over the usual approach. Fewer deflection stations are needed than in the classical technique, and geoidal heights, together with their error covariance matrix, can be computed at any points in the region of interest. Geoidal heights, obtained from other sources, may be used as constraints on the solution.

The techniques developed here should contribute significantly towards enabling deflections to be predicted at geodetic stations, and towards providing a reliable tool for geoid computation.

ACKNOWLEDGEMENTS

This work was carried out under the supervision of Dr. P. Vaníček, whose guidance was deeply appreciated. I would also like to express my appreciation to Professors A.C. Hamilton and E.J. Krakiwsky for their constructive criticism of this report.

Data for the investigation was made available through the good graces of Mr. G. Corcoran of the Geodetic Survey of Canada, Mr. D.A. Rice of the United Stated National Geodetic Survey, Dr. J.G. Tanner of the Canadian Earth Physics Branch, and Dr. W.P. Durbin of the United States Defense Mapping Agency.

I would also like to thank Ms. W. Wells for her excellent typing of this report, and Ms. C. Merry for her assistance in the draughting of the diagrams.

This work was partially funded through research contract no. SP2.23244-3-3665 with the Geodetic Survey of Canada. This report constitutes a virtually unaltered reprinting of the author's Ph.D thesis, submitted to the Surveying Engineering Department in October, 1974.

TABLE OF CONTENTS

	Page
Abstract	ii
List of Figures	v
List of Tables	vii
Acknowledgements	viii
1. Introduction	1
1.1 The geoid and its application	1
1.2 Co-ordinate systems	5
1.3 Accuracy requirements	11
1.4 Scope of the investigation	13
2. Deflection Prediction	14
2.1 Introduction	14
2.11 Survey of prediction methods	14
2.12 Two-dimensional interpolation	15
2.2 Gravity data	16
2.21 Data requirements	16
2.22 Point gravity anomalies	18
2.23 $1/3^\circ \times 1/3^\circ$ mean gravity anomalies	18
2.24 $1^\circ \times 1^\circ$ mean gravity anomalies	26
2.25 Evaluation of gravity data	27
2.3 Gravimetric deflections	31
2.31 The Vening-Meinesz formulae	31
2.32 Outer zone contribution	38
2.33 Middle zone contribution	39
2.34 Inner zone contribution	41
2.35 Error propagation	44
2.4 Astrogeodetic deflections	46
2.41 Astrogeodetic data	46
2.42 Sources of error	47
2.5 Two-dimensional interpolation	50
2.51 Mathematical model used	50
2.52 Choice of zone boundaries	53
2.53 Test results	58
2.54 Error evaluation	61
3. Geoid Computation	73
3.1 Survey of computational methods	73
3.2 The surface-fitting technique	74
3.21 Model using deflections	74
3.22 Model using deflections and geoidal heights	79
3.3 Evaluation	82
3.31 Preliminary testing	82
3.32 Geoid comparisons	84
3.33 Density and distribution of deflection data	92
3.34 Inclusion of predicted deflections	94
3.35 Sequential use of the technique	100

TABLE OF CONTENTS - cont'd

	Page
4. Conclusions and Recommendations	105
4.1 Deflection prediction	105
4.2 Geoid computation	106
Appendices:	
I The Method of Least Squares	109
II Derivation of expression for mean gravity anomaly	112
III Derivation of equations for inner zone contribution to gravimetric deflections of the vertical	114
IV Programme descriptions	121
V Data base description	124
References	126

LIST OF FIGURES

No.		Page
1.1	The Geoid and its Relationship to other surfaces	2
1.2	Ellipsoidal Co-ordinate Systems	6
1.3	Cartesian Co-ordinate Systems	8
1.4	Astronomic Latitude and Longitude	10
2.1	Error Function - 1/3° x 1/3° Blocks	24
2.2	Error Function - 1° x 1° Blocks	28
2.3	Mean Free-air Gravity Anomalies	29
2.4	Circular Templates and Rectangular Blocks	34
2.5	Different-sized Rectangular Blocks	36
2.6	Vening-Meinesz Function	37
2.7	Inner Zone - x, y co-ordinates	43
2.8	Variation in Deflection Values as a Function of Area Covered by 1/3° x 1/3° Blocks	55
2.9	Variation in Deflection Values as a Function of Integration Distance	57
2.10	Interpolation Areas	59
2.11	Error Vectors (observed - predicted)	67
2.12	Distribution of Gravity data - New Brunswick	68
2.13	Distribution of Gravity data - St. Laurence and Gaspe	69
2.14	RMS Error as a Function of RMS Deflection	71
3.1	Variance Factor as a Function of Number of Coefficients	83
3.2	UNB74-1: Astrogeodetic Geoid in North America	85
3.3	UNB74-1: Standard Deviations of Geoidal Heights	86
3.4	AMS67 minus UNB74-1 Geoid	89

LIST OF FIGURES - cont'd

No.		Page
3.5	UNB74-1 minus GSFC72 Geoid	90
3.6	Variation in Deflection Station Spacing	93
3.7	Astrogeodetic Geoid in Eastern Canada	95
3.8	Astrogravimetric Geoid in Eastern Canada	96
3.9	Astrogravimetric minus Astrogeodetic Geoid in Eastern Canada	97
3.10	Standard Deviations - Astrogeodetic Geoid	98
3.11	Standard Deviations - Astrogravimetric Geoid	99
3.12	Standard Deviations - Astrogravimetric Geoid with 10 Constraints	104

LIST OF TABLES

No.		Page
2.1	$\sigma_{\Delta g}$ as a function of ΔH.	19
2.2	Error in numerical integration of $\frac{dS(\ )}{d\psi}$ for $1/3^\circ \times 1/3^\circ$ blocks	40
2.3	Summary of deflection interpolation results	62
2.3A	Deflection interpolation results	62A
2.4	Error correlations	64

CHAPTER 1

INTRODUCTION

1.1 The Geoid and its Application

Before the geoid and its applications can be discussed, a few brief definitions are necessary, in order that the terminology used be fully understood.

The geoid is that particular equipotential surface of the earth's gravity field which coincides with mean sea level, in the mean sense. The geoid may be closely approximated by an ellipsoid, and the separation between these two surfaces is known as the geoidal height, N, positive when the geoid is above the ellipsoid (Figure 1.1).

The plumbline is perpendicular to the geoid, and to the other equipotential surfaces of the gravity field. The angle between the tangent to the plumbline at a point, and the normal to the ellipsoid, passing through the same point, is called the deflection of the vertical. Deflections of the vertical at the terrain are surface deflections, and differ by the amount of the curvature of the plumbline from the corresponding deflections at the geoid (Figure 1.1).

The deflection of the vertical at a point is customarily split into two scalar quantities, ξ, η. ξ is the deflection component in the north-south direction, and is called the deflection in the meridian. η is the component at right angles to ξ, and is known as the deflection in the prime vertical. The sign convention is such that ξ is positive

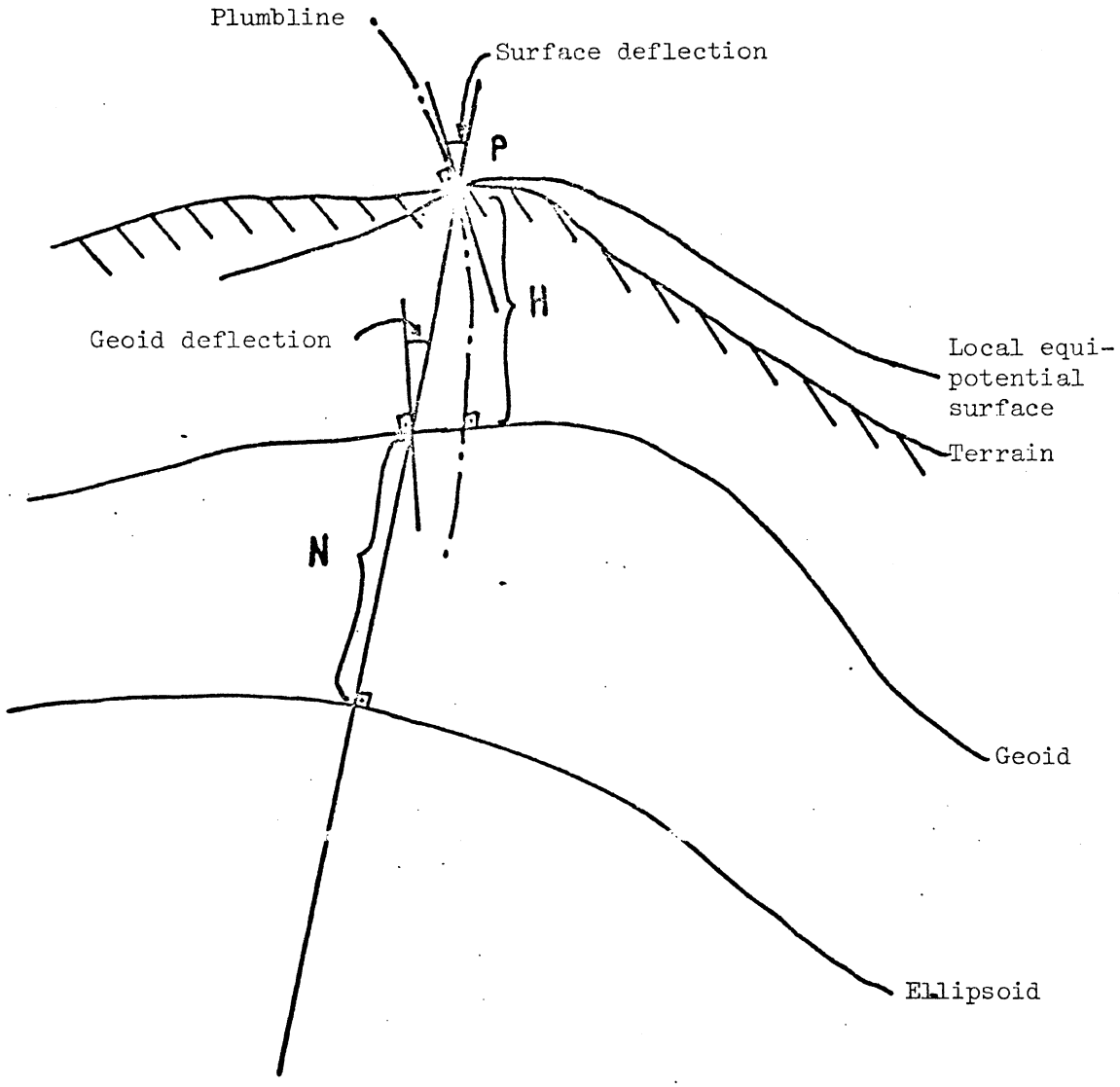

Figure 1.1

The Geoid and its Relationship to other Surfaces

when the geoidal height is increasing towards the south, and η is positive when the geoidal height is increasing towards the west.

The geoid is a physical, but intangible, reality which affects the field of surveying in several ways. Conventional surveying instruments are aligned with their vertical axes parallel to the tangent to the local plumbline. In the classical approach to geodesy, calculations are carried out on a reference ellipsoid, using observations reduced from the terrain to this surface. This reduction requires a knowledge of the geoidal heights and of the surface deflections of the vertical (Merry and Vaníček, 1973).

The process of spirit levelling, with appropriate corrections for variations in gravity, yields height differences between equipotential surfaces (Heiskanen and Moritz, 1967). These heights are customarily referred, by means of tide-gauges, to mean sea level, and thus the geoid effectively becomes the datum surface for heights. However, mean sea level is not completely coincident with the geoid, as variations in its level, due to temperature, pressure, and salinity changes, and to other effects, cause it to depart from an equipotential surface by an amount estimated to be 1 to 2 metres (Lisitzin and Pattulo, 1961). The question as to whether mean sea level can be used as an approximation to the geoid for geodetic purposes, or whether the geoid may be used as a datum from which to measure sea level variations, is yet to be settled (see, for instance, Proc. of Symp. on Applic. of Marine Geodesy, 1974).

The geoid itself is a dynamic surface, with its radius vector from the centre of gravity of the earth changing cyclically, due to the gravitational attraction of the sun and the moon. This change is of the

order of 1 metre (Melchior, 1966).

Several geodesists have investigated means of working without the geoid (e.g. Hotine, 1969; Dufour, 1968). Using the classical observations to terrestrial targets, this still appears to be an impossibility, due to the uncertain effects of atmospheric refraction upon vertical angles, and the fact that these are also affected by deflections of the vertical. One technique that is independant of the geoid is geometric satellite geodesy. However, it is not imaginable that satellite observations will be made at all geodetic stations, and the classical observations will be complemented by, rather than replaced by, observations to satellites. As shall be shown in the next section, geoidal heights form a vital link relating the co-ordinate systems in which these two types of observations are used.

Although there is only one equipotential surface that may be called the geoid, there are several different ways in which geoidal heights may be computed. This has resulted in several "types" of geoid, which are briefly described below:

(1) The satellite geoid is based upon the analysis of orbit perturbations of artificial earth satellites. For a description of the methods used, see Kaula (1966) or Gaposchkin and Lambeck (1969). This representation has the characteristic that, although of uniform quality, it is a somewhat smoothed version of the geoid, referred to a geocentric ellipsoid.

(2) The calculation of the gravimetric geoid uses the magnitude of the earth's gravity, measured at the terrain, to obtain geoidal heights (Heiskanen and Moritz, 1967). It is usually referred to a geocentric ellipsoid and, due to lack of gravity data in certain areas of the world,

is not of consistent quality.

(3) The combined satellite-gravimetric geoid combines the best features of (1) and (2). The detailed variations in geoidal height are described using the gravity anomalies, and the large scale variations by using the satellite data (Vincent et al, 1972).

(4) The calculation of the astrogeodetic geoid uses the direction of gravity (rather than the magnitude) to obtain geoidal heights relative to the reference ellipsoid to which the direction is related. This reference ellipsoid is not necessarily geocentric. Due to the nature of the observations it can only be computed for the land masses, and requires a good distribution of data. For an example, see Fischer (1960).

(5) The astrogravimetric geoid combines the best features of (2) and (4). It is basically an astrogeodetic geoid, with supplementary deflections obtained via gravity anomalies. As this type of geoid is the main topic of this thesis, it will be described in more detail in later sections. No systematic use of this idea has been made in North America, although Fischer et al (1967) used some gravity data in their geoid computation.

1.2 Co-ordinate Systems

In order to describe the use of the geoid in transformations between co-ordinate systems, a brief review of those systems used in geodesy is given here. They are of two types:

(1) Ellipsoidal.

(2) Cartesian.

(1) The ellipsoidal co-ordinate system consists of triplets of numbers: (ϕ, λ, h) defined on a particular rotational ellipsoid. ϕ is the

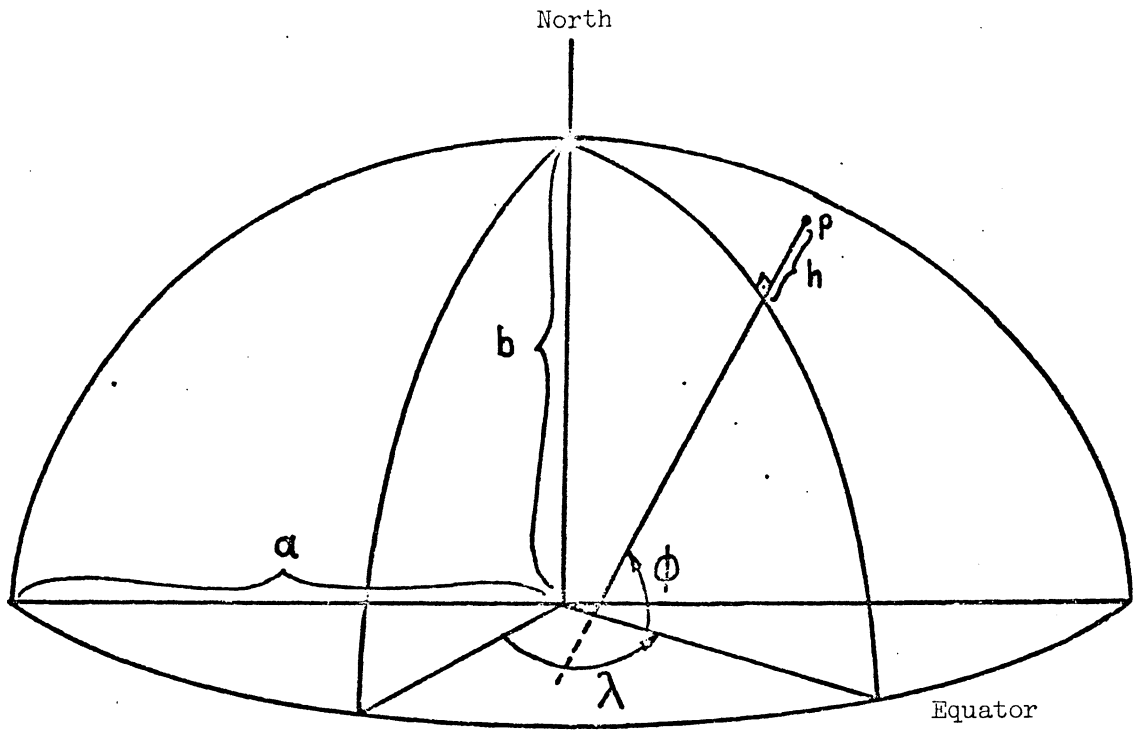

Figure 1.2

Ellipsoidal Co-ordinate System

geodetic latitude, measured north from the equator, λ is the geodetic longitude, measured east from an arbitrary reference plane, and h is the height above the ellipsoid, measured along the outward normal to the ellipsoid (Figure 1.2). For the co-ordinate system to be completely specified, the size and shape parameters of the ellipsoid must be given, generally as a and f. f is the flattening, $f = \frac{a-b}{a}$, and a and b are respectively the semi-major and semi-minor axes of the ellipsoid. The h component is usually considered in two parts: H, the height above the geoid, and N, the geoidal height (Figure 1.1). The classical two-dimensional geodetic system consists of the (ϕ, λ) co-ordinate pairs only. In order to obtain a three-dimensional geodetic system, it is apparent that both H and N are needed.

(2) The cartesian co-ordinate system consists of triplets of numbers (x, y, z), describing the positions of points with respect to three orthogonal axes (Figure 1.3). When the origin of this co-ordinate system coincides with the centre of the ellipsoidal system, and the z-axis is coincident with the minor axis of the ellipsoid, and the x-z plane is the reference meridian plane then the cartesian system is related to the ellipsoidal system by the equations:

$$\begin{bmatrix} x \\ y \\ z \end{bmatrix} = \begin{bmatrix} (N(\phi) + h) \cos\phi \cos\lambda \\ (N(\phi) + h) \cos\phi \sin\lambda \\ ((1 - e^2) N(\phi) + h) \sin\phi \end{bmatrix} \qquad 1.1$$

(Heiskanen and Moritz, 1967), where $N(\phi)$ denotes the radius of curvature of the ellipsoid in the prime vertical, and e is the first eccentricity of the ellipsoid.

When the ellipsoidal (and its corresponding cartesian) system is used as a basis for geodetic calculations, it is known as a geodetic

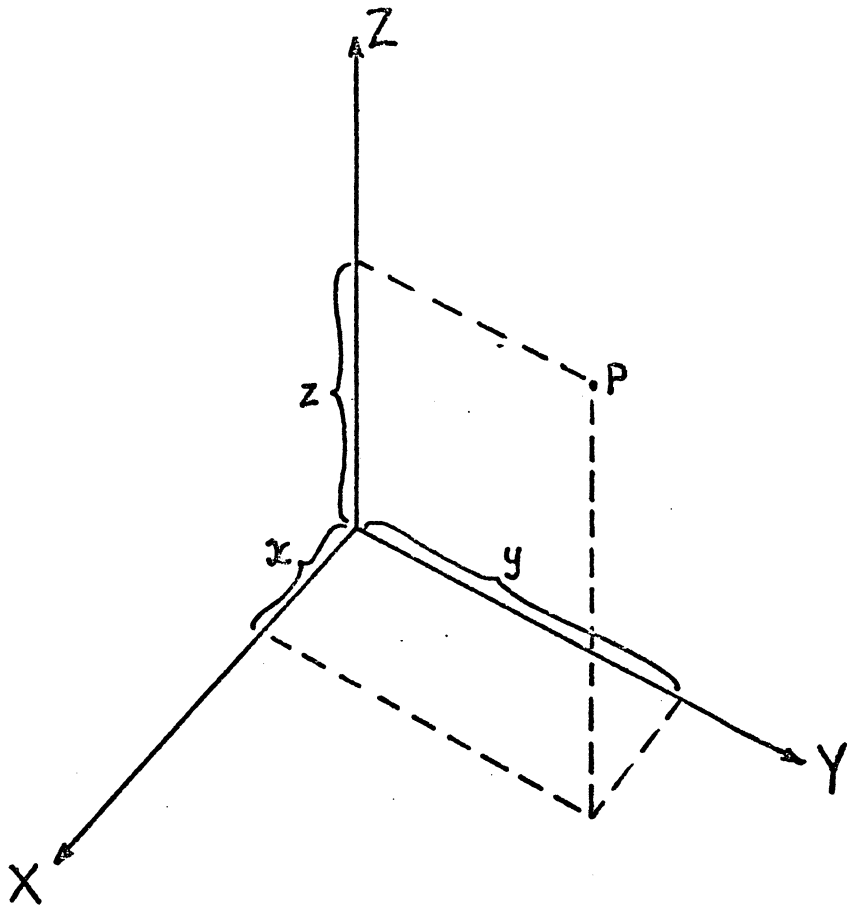

Figure 1.3

Cartesian Co-ordinate System

system, and the ellipsoid as a geodetic reference ellipsoid. When a cartesian system is located in such a way that its origin is at the centre of gravity of the earth, the z-axis coincides with the mean rotation axis of the earth, and the x-z plane contains the Greenwich mean observatory (i.e. it coincides with the Greenwich meridian plane), then it is known as a geocentric system (obviously, there is a corresponding geocentric ellipsoidal system). The geodetic and geocentric co-ordinate systems will not generally coincide, and the origins may be shifted with respect to each other (translated) and their axes may not be parallel (rotated). It is also conceivable that different scales may be used within the systems. In practice these translations, rotations and scale changes are small, causing co-ordinate changes of the order of 100 metres (Mueller et al, 1972).

Calculations involving observations to terrestrial objects are customarily carried out in the two dimensional geodetic system, while those involving observations to satellites are carried out in the cartesian geocentric system. In order to relate the co-ordinates in these two systems, the translation components, rotations, scale change and heights H and N are needed.

The astronomic co-ordinates (Φ, Λ) should also be mentioned here. The astronomic latitude, Φ, of a point P, is the angle formed between the normal to the geoid, passing through P, and the mean equator (at right angles to the mean rotation axis of the earth) (Figure 1.4a). The astronomic longitude Λ, is measured in the plane of the equator from the Greenwich meridian plane east to the plane, containing the mean rotation axis, which is parallel to the normal to the geoid at P (Figure 1.4b).

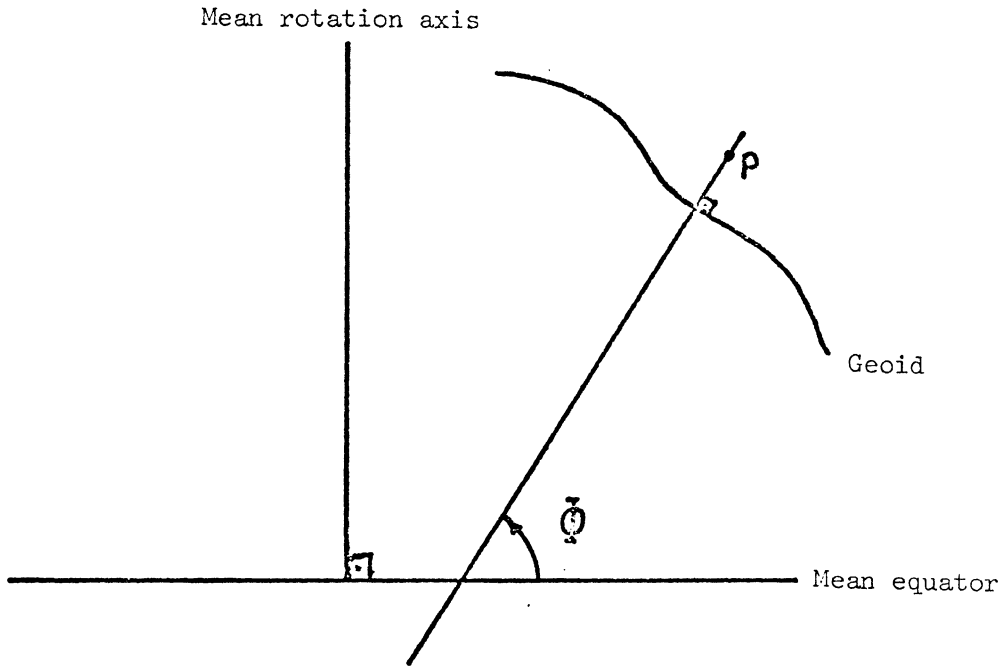

Figure 1.4a

Astronomic Latitude

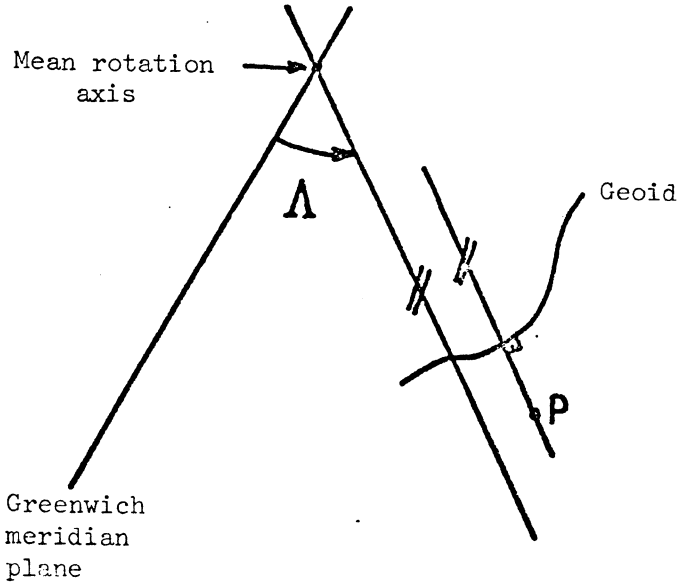

Figure 1.4b

Astronomic Longitude

Provided that the geodetic cartesian system is parallel to the geocentric cartesian system, then the components of the astrogeodetic deflection of the vertical are given by:

$$\xi^A = \Phi - \phi$$
$$\eta^A = (\Lambda - \lambda)\cos\phi \qquad 1.2$$

(Heiskanen and Moritz, 1967).

1.3 Accuracy Requirements

The uses of the astrogravimetric (or astrogeodetic) geoidal heights may be itemised as:

(1) To reduce observed distances and directions from the terrain to the geodetic reference ellipsoid.

(2) To transform the classical two-dimensional geodetic system to a three-dimensional geodetic co-ordinate system.

(3) To relate the geodetic co-ordinate system to a geocentric co-ordinate system (i.e determine translation components and rotations).

(4) To serve as a datum from which variations in mean sea level may be determined.

(1) The accuracy requirements for the reduction of distances and directions will be a function of the accuracy requirements for the first-order horizontal control networks. In Canada, the accuracy requirements are 5 parts per million (ppm) for distances and 2" for first-order directions (Klinkenberg, 1972). In order that errors in geoidal height and deflections of the vertical do not unduly affect the accuracy of the reduced distances and directions, their effects should be considerably smaller than 5 ppm and 2". Assuming the errors in the geoidal heights and deflections to be random (which may not be the case,

especially for geoidal heights), then a reasonable upper bound for their effects is 2.5 ppm and 1". Using the formulae of Merry and Vaníček (1973) this implies that the accuracy of geoidal heights should be better than 16 metres and that of deflections of the vertical better than 1" cotg Z (where Z is the zenith distance of the target for the particular observation).

(2) is in fact a subset of (3) and they may be considered together. No established guidelines are available for accuracy standards in the transformation from geodetic to geocentric co-ordinate systems. A useful rule-of-thumb is that the parameters used in the transformation be no less accurate than the data being transformed. With the rapid changes taking place in satellite technology, it is difficult to place a figure on the accuracy of the geocentric co-ordinates. The optical satellite systems, with an accuracy of 10 to 15 metres (Lambeck, 1971), are rapidly giving way to the Doppler systems, with an accuracy of 1 to 2 metres (Wells, 1974). These, in turn, may be replaced by laser systems with sub-metre accuracy (Bender et al, 1968). No rigorous and complete analysis of the North American networks has been performed, but they do not appear to have reached the same standard of accuracy as the Doppler system, and distortions in the networks in excess of 10 metres are evident (Seppelin, 1974; McLellan, 1974). It appears that for the immediate future needs, an accuracy for geoidal heights of the order of 2 metres is adequate for transformation purposes.

(4) As mentioned earlier, mean sea level variations reach 1 to 2 metres and, in order for these variations to be completely studied, geoidal heights with an accuracy one order better (i.e. 0.1 m to 0.2 m) would be required. It is not anticipated that the astrogravimetric

geoid will be of much help in this field, as it is limited to land masses and enclosed bays.

1.4 Scope of the Investigation

This thesis can be treated in two main parts. The first part deals with the prediction of astrogeodetic deflections using observed deflections and gravity data. The second part deals with the calculation of geoidal heights from deflections of the vertical.

(1) The idea of using gravity data to aid in the prediction of astrogeodetic deflections is not new, and was first used by Molodensky et al (1962). The method used in this investigation differs considerably from those of Molodensky and others, such as Strange and Woollard (1964), who use a linear one-dimensional interpolation between pairs of astrogeodetic deflection stations, and Fischer (1965), who uses a non-linear graphical interpolation along a chain of deflection stations. In the technique developed in this thesis, a non-linear two-dimensional approximation polynomial is used for interpolation. Modified gravimetric deflections are computed using the available gravity anomalies, and a new derivation for the integration in the inner zone is developed.

(2) The model for geoidal heights differs radically from the traditional linear integration between adjacent deflection stations, using Helmert's formula (Heiskanen and Moritz, 1967). In this thesis a surface-fitting technique is employed to fit all available deflections. This model has also been enlarged to incorporate geoidal heights as additional observations. This procedure for computing an astrogravimetric geoid is evaluated, bearing in mind present day accuracy requirements, and the amount of available data.

CHAPTER 2

DEFLECTION PREDICTION

2.1 Introduction

2.11 Survey of prediction methods

There are several possible methods of predicting astrogeodetic deflections, all of which have particular advantages and disadvantages. These methods should be evaluated on the basis of their reliability, ease of use, and the availability of the necessary data. These methods have been categorised by Heiskanen and Moritz (1967) as:

(1) Measurement of zenith distances

(2) Use of torsion balance

(3) Use of topographic-isostatic deflections

(4) Astrogravimetric levelling.

(1) The measurement of zenith distances, although a direct simple approach, is affected by atmospheric refraction to such an extent that it cannot be considered reliable. Under the best topographic conditions (in high mountains), an accuracy of the order of 20" has been achieved in the Rockies (Bacon, 1966), although Hradilek (1968) claims that an accuracy of 2" is possible.

(2) The torsion balance is not easy to use and the reduction of data is a laborious process, although (with limited tests) the method appears to have an accuracy of the order of 1" (Mueller, 1964).

(3) The use of topographic-isostatic deflections is based upon the assumption that the geodetic and gravimetric reference ellipsoids are concentric and are of equal dimensions. Unless the topographic-isostatic deflections are appropriately corrected, the results will be erroneous. The procedure is also laborious and time-consuming, and requires knowledge of the surrounding topography and gravity field to a considerable distance from the computation point (Szabo, 1962). Consequently, it cannot be recommended as a method of deflection prediction.

(4) The method of astrogravimetric levelling, as proposed by Molodensky et al (1962), does require a knowledge of the surrounding gravity field, but not to the same extent as method (3) above. Using a linear interpolation between two adjacent astrogeodetic deflection stations, Strange and Woollard (1964) were able to predict deflections in the Rockies and the Alps with an error of the order of 0".6. The astrogravimetric levelling technique does appear, therefore, to be the most promising of the available techniques.

2.12 Two-dimensional interpolation

This technique, developed in this thesis, is an extension and modification of Molodensky's astrogravimetric levelling. The same basic data is used, but the interpolation between adjacent deflection stations is non-linear and two-dimensional. The procedure is as follows.

Gravimetric deflections of the vertical are calculated at all astrogeodetic deflection stations ("control" points) in a region of interest, and at points for which predicted astrogeodetic deflections are desired. The integration in the Vening-Meinez formulae for the gravity deflections is not extended over the whole earth, as required,

but only over the neighbourhood of the computation point, forming "modified" gravimetric deflections. These modified deflections will not agree with the astrogeodetic deflections at the control points due to the following reasons:

(1) The integration for the gravimetric deflections is not complete. This error should be nearly constant for points not too far apart.

(2) The two types of deflections refer to ellipsoids of different size, shape, and position. This effect will vary smoothly in a near-linear fashion for points not too far apart.

The two effects mentioned above can be modelled using a two-dimensional second order correction polynomial, the coefficients of which are determined from a comparison of the two types of deflections at the control points. This polynomial can then be used to correct the modified gravimetric deflections at the other points, to obtain predicted astro-geodetic deflections. The remainder of this chapter describes the data, and mathematical models used, and evaluates some test results.

2.2 Gravity Data

2.21 Data requirements

For the calculation of gravimetric deflections of the vertical, a homogeneous field of gravity anomalies is required. The gravity anomaly, Δg_P, at a point P on the geoid is given by:

$$\Delta g_P = g_P - \gamma_Q \quad , \qquad 2.1$$

where g_P is the actual value of gravity at P and γ_Q is the normal gravity at Q, the corresponding point on the ellipsoid. The normal gravity is that generated by this ellipsoid, which should have the same potential as the geoid, enclose a mass numerically equal to the mass of

the earth, and be geocentric (Heiskanen and Moritz, 1967). Gravity observed at the surface of the earth must be reduced to the geoid, and the effect of topographic masses above the geoid removed. To this end, several different types of gravity reductions have been developed, resulting in different types of gravity anomalies. Of these, the most widely available and commonly used is the free-air anomaly, given by:

$$\Delta g_P = g_s + 0.3086h - \gamma_Q \quad , \qquad 2.2$$

where g_s is observed at the surface point, s, h is the height of s above P, in metres, and 0.3086 is the normal gradient of gravity, in mgal m^{-1}. (1 gal = 1 cm sec^{-2}.)

The other two most common types of gravity anomaly, the Bouguer and Isostatic, both produce an indirect effect upon the deflections of the vertical, which is difficult to evaluate (Heiskanen and Moritz, 1967).

The choice of a gravity reference system for the purpose of deflection prediction is arbitrary. A constant change in the absolute value of gravity will introduce a constant shift in anomaly values, which has no effect upon the computed deflections. Differences in size and shape between the gravity reference ellipsoid and the reference ellipsoid for astrogeodetic deflections are accounted for in the prediction technique. Consequently, the most readily available system - at this time - has been used. This is the 1930 reference system, based upon the International Ellipsoid (Heiskanen and Moritz, 1967). At present, very little data has been transformed to the newly recommended 1967 Reference System (Int. Assoc. of Geodesy, 1971a).

For the purposes of the technique used in section 2.3, three different gravity data sets are needed. These are:

(1) a point gravity anomaly set,

(2) $1/3^\circ \times 1/3^\circ$ mean gravity anomalies, and

(3) $1^\circ \times 1^\circ$ mean gravity anomalies.

(By $1/3^\circ \times 1/3^\circ$ mean anomalies, I imply mean gravity anomaly values for elements on the surface of the earth with sides of $1/3^\circ$ latitude and $1/3^\circ$ longitude. Similarly for the $1^\circ \times 1^\circ$ mean values.)

2.22 Point gravity anomalies

This data (approximately 100,000 values, in Canada) was made available by the Gravity Division of the Earth Physics Branch (EPB), Ottawa (Buck and Tanner, 1972). No accuracy estimates were obtained with this data, and these estimates were made, following Vanicek et al (1972), using the equation:

$$\sigma_{\Delta g}^2 = \sigma_m^2 + (0.09406\Delta H)^2 \quad , \qquad 2.3$$

where $\sigma_{\Delta g}$ is the standard deviation of the gravity anomaly (in mgals), σ_m is the measurement error (=0.05 mgal.), and ΔH is the height error (in feet). Δg is only weakly dependant upon horizontal position errors, and these have not been considered here. (Note, the term standard deviation is not used with its rigorous statistical meaning. It is described further in Appendix I: The Method of Least Squares.) The various values of $\sigma_{\Delta g}$, as a function of the values of ΔH provided by the EPB are shown in Table 2.1.

2.23 $1/3^\circ \times 1/3^\circ$ mean gravity anomalies

These anomalies have been computed from the point gravity data. The mean gravity anomaly, $\overline{\Delta g}$, for a region of area A, is given by:

$$\overline{\Delta g} = \frac{1}{A} \iint \Delta g dA \quad , \qquad 2.4$$

(Heiskanen and Moritz, 1967), where Δg is the gravity anomaly, known at

$\sigma_{\Delta g}$ (mgals)	ΔH (feet)
0.05	0.1
0.1	1.0
0.3	3.0
0.9	10.0
2.4	25.0
9.4	100.0
12.0	unknown

Table 2.1

$\sigma_{\Delta g}$ (standard error of a gravity anomaly) as a function of ΔH (estimated height error).

every point in the region. In practice, the anomalies are only available for a few points in the region, and the complete evaluation of the surface integral is not possible.

Several solutions may be used for this problem:

(1) Direct arithmetic mean,

(2) Prediction of point anomalies in the region

(3) Representation of the gravity anomalies by an integrable function.

(2) and (3) are essentially the same, except that in the case of (2) the integration of equation 2.4 would be numerically evaluated. (1) has the disadvantage that it may be a poor representation of $\overline{\Delta g}$, but, in the case of scanty data, it is the only alternative. As the purpose of this thesis is not to evaluate procedures for determining an optimal gravity field, a simplistic approach has been adopted, using methods (3) and (1). When there is sufficient data, the gravity field in the region can be represented by a polynomial of second order as proposed by Nagy (1963). Then, for any point i:

$$\tilde{\Delta g}_i = \sum_{j,k=0}^{2} c_{jk}\, x_i^j\, y_i^k \quad , \qquad 2.5$$

where Δg_i is the estimated gravity anomaly at i, c_{jk} are the coefficients of a second-order algebraic polynomial, and (x,y) form a co-ordinate pair in a local orthogonal system, with the x-axis directed north, and the y-axis east, and the origin at the centre of the region.

This polynomial can be integrated to determine $\overline{\Delta g}$:

$$\overline{\Delta g} \doteq c_{oo} + \frac{c_{02}}{3} b^2 + \frac{c_{20}}{3} a^2 + \frac{c_{22}}{9} a^2 b^2 \quad , \qquad 2.6$$

where 'a' is half the north-south extent of the region, and 'b' half the

east-west extent (assuming the region to be trapezoidal in shape). The detailed derivation of 2.6 is given in Appendix II.

The coefficients of the polynomial are found from a least squares approximation procedure:

$$\sum_{j=1}^{9} \langle \phi_k, \phi_j \rangle \; c_j = \langle \Delta g, \phi_k \rangle \qquad k=1,\ldots,9 \quad , \qquad 2.7$$

where $\phi_1(x_i,y_i) = 1, \phi_2(x_i,y_i) = y_i, \phi_3(x_i,y_i) = y_i^2, \ldots, \phi_9(x_i,y_i) = x_i^2 y_i^2$

and the scalar product $\langle \phi_k, \phi_j \rangle$ is defined by:

$$\langle \phi_k, \phi_j \rangle = \sum_{i=1}^{n} w(x_i,y_i) \cdot \phi_k(x_i,y_i) \cdot \phi_j(x_i,y_i) \quad , \qquad 2.8$$

where n = number of data points used.

The weight function $w(x_i,y_i)$ is given as:

$$w(x_i,y_i) = \sigma_{\Delta g_i}^{-2} \qquad 2.9$$

where $\sigma_{\Delta g_i}$ is the standard deviation of the point gravity anomaly, Δg_i, given by equation 2.3.

Equations 2.7 can be written in matrix form:

$$G \underset{\sim}{c} = \underset{\sim}{\ell}$$

from which:

$$\underset{\sim}{c} = G^{-1} \underset{\sim}{\ell} \qquad 2.10$$

Residuals can be computed at the observed data points:

$$V_i = \Delta g_i - \tilde{\Delta g}_i \qquad 2.11$$

where $\tilde{\Delta g}_i$ is given by equation 2.5.

Then the variance factor σ_o^2 is determined from:

$$\sigma_o^2 = \frac{\langle V, V \rangle}{n-9} \quad . \qquad 2.12$$

The error covariance matrix of the coefficients is then:

$$\Sigma_c = \sigma_o^2 \, G^{-1} \quad . \qquad 2.13$$

Rewriting equation 2.6 as:

$$\overline{\Delta g} = \underset{\sim}{b} \; \underset{\sim}{c}' \qquad 2.6$$

where $\underset{\sim}{b} = (1, \frac{b^2}{3}, \frac{a^2}{3}, \frac{a^2 b^2}{9})$

2.14

and $\underset{\sim}{c}' = (c_{oo}, c_{o2}, c_{20}, c_{22})$,

then, applying the law of propagation of covariance (Vaníček, 1973), the variance of $\overline{\Delta g}$ is given by:

$$\sigma^2_{\overline{\Delta g}} = \underset{\sim}{b} \; \Sigma_c' \; \underset{\sim}{b}^T \quad , \qquad 2.15$$

where Σ_c' is a reduced covariance matrix containing only the information relative to $\underset{\sim}{c}'$.

(Note that, although the coefficients $\underset{\sim}{c}'$ are needed in equation 2.6, all 9 coefficients $\underset{\sim}{c}$ must be determined, as the functions ϕ_i are not orthogonal.)

It is not possible to use the above-described procedure in all cases, as there is not always sufficient well-distributed point gravity data within individual 1/3° x 1/3° blocks. Practical experience has indicated that there should be at least 50% more data points than unknowns for a reliable solution for the polynomial coefficients. Furthermore, this data should not be clustered in one corner of the 1/3° x 1/3° square. If these criteria are not satisfied (i.e. if there is not data in at least three quadrants or if there are less than 15 data points), then the less sophisticated prodecure of method (1) is used. In this procedure, the weighted arithmetic mean of the point gravity anomalies in the block is used to represent the mean gravity anomaly. The weights used are inversely proportional to the variances of the available anomalies.

This technique corresponds to solving for, and using, only the c_{oo} term of equation 2.6 (i.e. a zero order polynomial representation). In this case the standard deviation of the mean, given by:

$$\sigma_m^2 = \frac{\left\langle \overline{\Delta g} - \Delta g_i , \overline{\Delta g} - \Delta g_i \right\rangle}{(n-1)\langle 1,1 \rangle} \qquad 2.16$$

should not be used as an estimate for $\sigma_{\overline{\Delta g}}$, as it is based upon the premise that

$$\overline{\Delta g} = E(\Delta g_i) \qquad 2.17$$

where E represents the expectation operator (Wells and Krakiwsky, 1971). This premise is no longer valid in the case of gravity anomalies where the mean, $\overline{\Delta g}$, does not represent the expected value of individual anomalies. In order to provide a less biased estimate for the accuracy, the following procedure was used. The standard deviations of the rigorous integral solution are plotted as a function of the number of points used in each block. The resulting second-order curve (Figure 2.1) can then be used to predict the standard deviations for the blocks that have less than 15 data points.

The above two procedures will only account for blocks in which gravity data exists. There are many 1/3° x 1/3° blocks in which no gravity data has been observed. For example, in Eastern Canada only about 70% of the blocks contain gravity information. For the empty areas, some type of prediction method must be resorted to. These methods are generally of three types:

(1) geometric interpolation,

(2) geophysical prediction, and

(3) autocorrelation (collocation).

The investigation, and analysis of these methods are considered beyond the

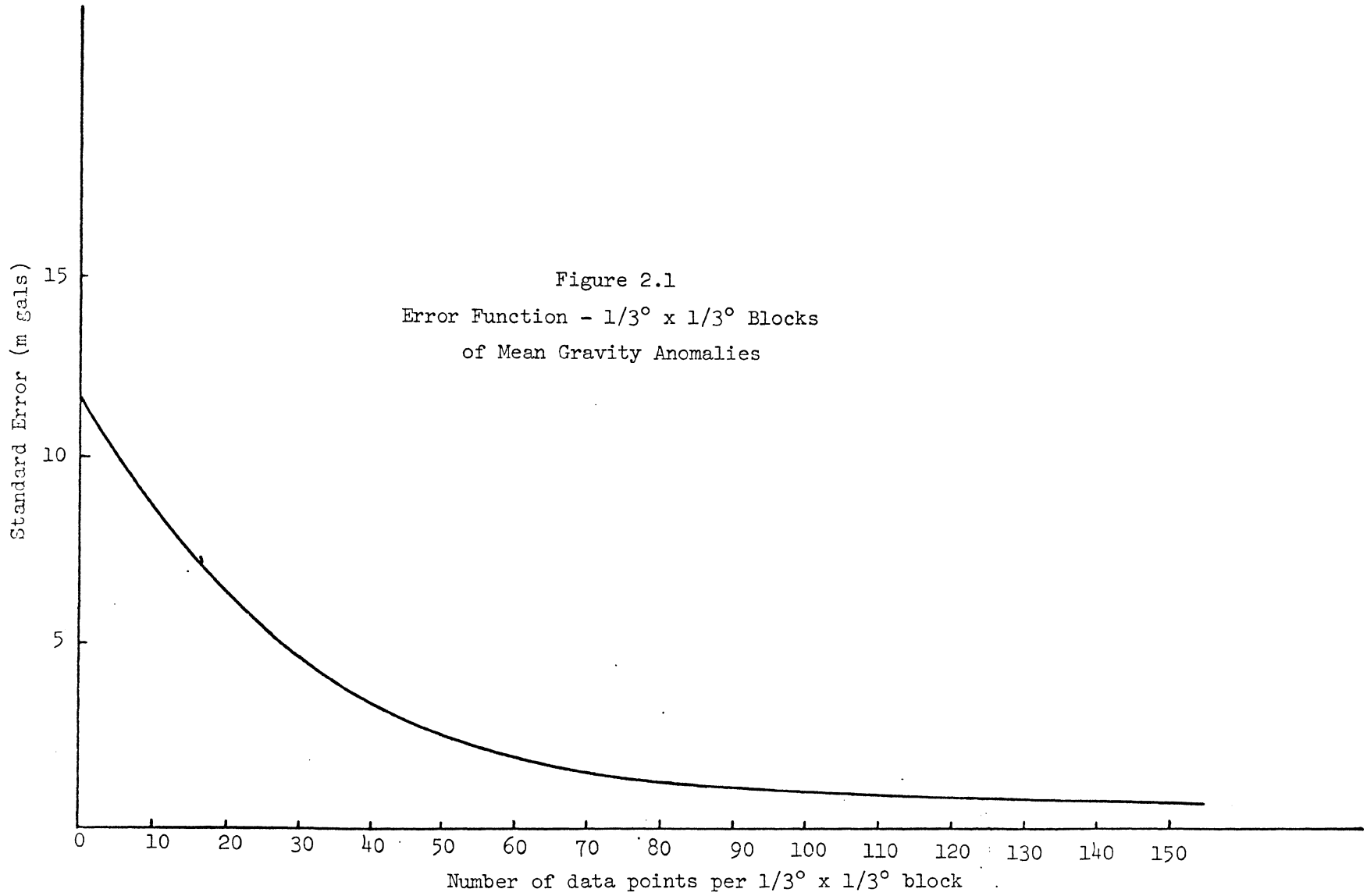

Figure 2.1
Error Function - 1/3° x 1/3° Blocks
of Mean Gravity Anomalies

scope of this thesis.

A version of method (1) has been developed, in which the auto-correlation of the gravity anomalies is partially taken into account. The mean anomaly, $\overline{\Delta g}_P$ is predicted from the neighbouring 1/3° x 1/3° mean anomalies, $\overline{\Delta g}_i$, using the formula:

$$\overline{\Delta g}_P = \frac{\left\langle \overline{\Delta g}_i^{1/2}, \overline{\Delta g}_i^{1/2} \right\rangle}{\langle 1,1 \rangle} \qquad 2.18$$

where the weight function is specified as:

$$w(\psi_{Pi}) = \sigma_{\overline{\Delta g}_i}^{-2} \, e^{-\psi_{Pi}/1/5^\circ} \quad . \qquad 2.19$$

Here, $\sigma_{\overline{\Delta g}_i}$ is the standard deviation of $\overline{\Delta g}_i$, from equation 2.15, and ψ_{Pi} is the angular distance (in degrees) between the points (ϕ_P, λ_P) and (ϕ_i, λ_i). The exponential term takes into account the decrease of the correlation between gravity anomalies with increasing distance between them. The non-linear correlation is best represented by an exponential function of this type (Kaula, 1957). The value 1.5° has been taken from the same reference, in which Kaula uses several gravity profiles in the United States to determine correlation coefficients for mean free-air gravity anomalies. Estimates of the accuracy of the predicted gravity anomalies are found from:

$$\sigma_{\overline{\Delta g}_P}^2 = \sigma_o^2 + \frac{1}{n} \sum_{i=1}^{n} \sigma_{\overline{\Delta g}_P}^2 \qquad 2.20$$

where:

$$\sigma_o^2 = \frac{\left\langle \overline{\Delta g}_P - \overline{\Delta g}_i, \overline{\Delta g}_P - \overline{\Delta g}_i \right\rangle}{(n-1) \langle 1,1 \rangle} \qquad 2.21$$

Equation 2.20 takes into account the fact that the mean, $\overline{\Delta g}_P$, does not represent the expected value of the individual mean anomalies. Hence,

$\sigma_{\overline{\Delta g_P}}$ is the geometric mean of σ_o and the geometric mean of the individual anomalies. Although, from a rigorous statistical viewpoint, this technique is questionable, it does avoid the practical difficulties associated with the large error covariance and auto-covariance matrices required for the more rigorous collocation approach (e.g. Moritz, 1972).

Only the immediately adjacent $1/3^\circ \times 1/3^\circ$ blocks are used for the prediction (i.e. $\psi_{max} = 0.5^\circ$). If there are less than two mean gravity values within this distance, then ψ_{max} is increased successively (in 0.5° increments) until there are at least two adjacent values, or until ψ_{max} exceeds 1.5°. In this case if there are still less than two adjacent values a mean anomaly of 0.0 mgal with a standard deviation of 11.5 mgal (taken from Figure 2.1) is assumed.

2.24 $1^\circ \times 1^\circ$ mean gravity anomalies

These were available in two data sets. The first consisted of 2,131 $1^\circ \times 1^\circ$ blocks in Canada, supplied by the EPB. The second contained 20,113 $1^\circ \times 1^\circ$ blocks distributed over the entire earth, excluding most of Canada, supplied by the Defense Mapping Agency, Aerospace Centre, St. Louis (DMAAC) (Seppelin, 1971). These two data sets were combined into one data set for North America, north of 40° latitude. There are some overlaps of data in the original files, notably along the common border of Canada and the U.S.A., and, for these cases, the weighted mean of the two values for each overlapping degree square was adopted. The original error estimates for the EPB data are optimistic, being based upon the deviation of point values from the mean. In order to make the error estimates for the combined data set as homogeneous as possible, standard deviations were assigned to the EPB data in accordance with the procedure described in Rapp (1972). Rapp obtained an empirical function

relation between the DMAAC error estimates and the number of data points per $1^\circ \times 1^\circ$ block, which is shown diagrammatically in Figure 2.2. The weights used in the combination of common blocks were inversely proportional to the variances.

The combined data set of 3311 $1^\circ \times 1^\circ$ blocks still left some empty areas in Canada (Figure 2.3). Predicted values were calculated for these areas using the same techniques as described earlier for the $1/3^\circ \times 1/3^\circ$ blocks. Again, the blocks used for the prediction were the immediately adjacent ones ($\psi_{max} = 1.5^\circ$). If there were less than two adjacent blocks with known anomalies, then ψ_{max} was increased to 3.0° and then to 4.5°. The entire land mass of Canada and the immediately adjacent areas were covered by observed and predicted $1^\circ \times 1^\circ$ mean free-air anomalies using the above technique.

2.25 Evaluation of gravity data

The determination and evaluation of the gravity field in Canada constitutes a thesis in itself. Consequently, it is recognised that the data sets described here could be improved in quantity and quality. No detailed evaluation of this data has been attempted, but some general comments may be made, with regard to each data set.

(1) The point data in Canada is not evenly distributed and is lacking completely in certain areas - see Figure 1 of Nagy (1973). The quality of the gravity observations is high, but the free-air reduction introduces significant errors (in excess of 10 mgals - Table 2.1) in the free-air gravity anomalies, due to the lack of adequate height information. The data set is not entirely free of blunders, and several incorrect values were detected during the course of this investigation.

Figure 2.2

Error Function - 1° x 1° Blocks

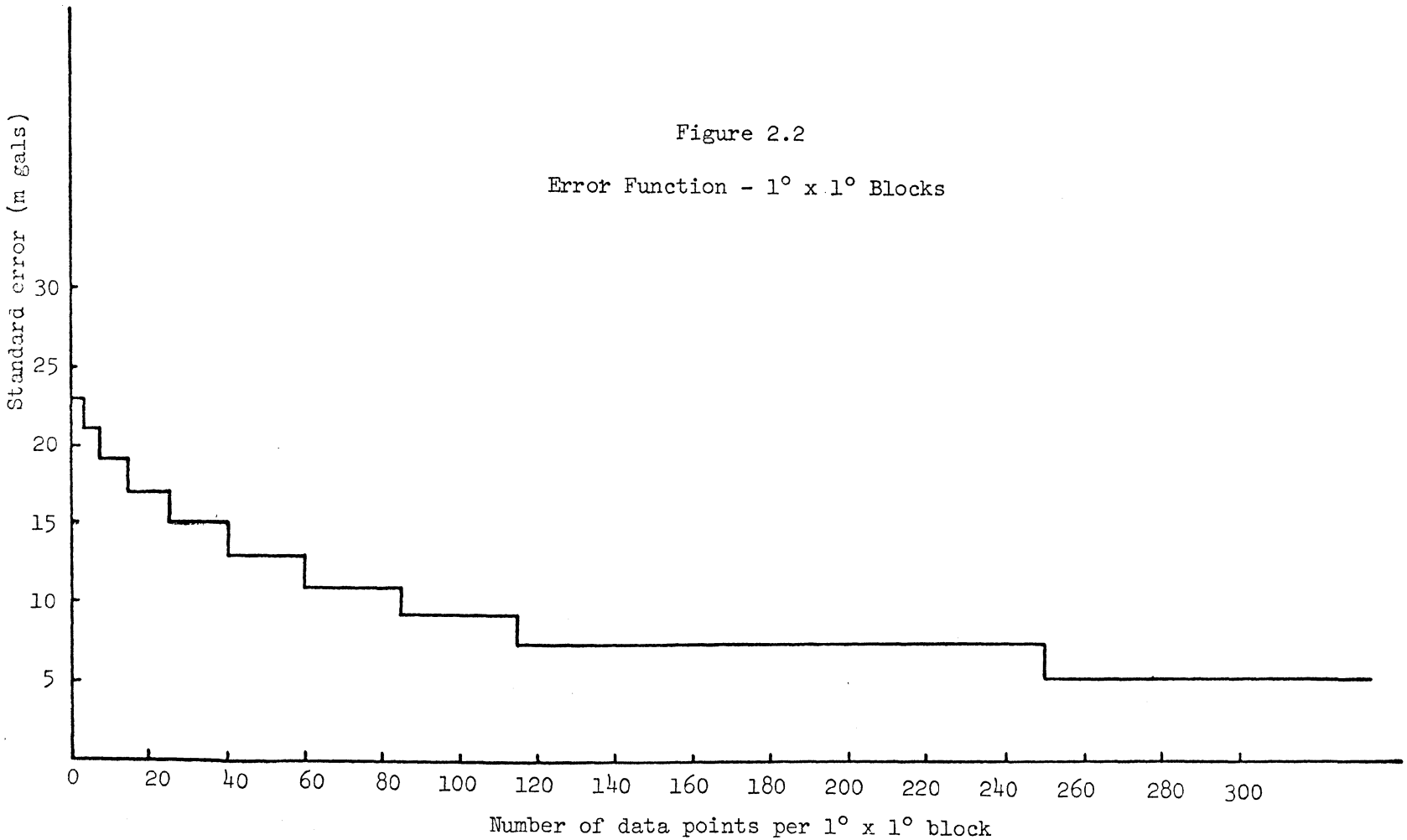

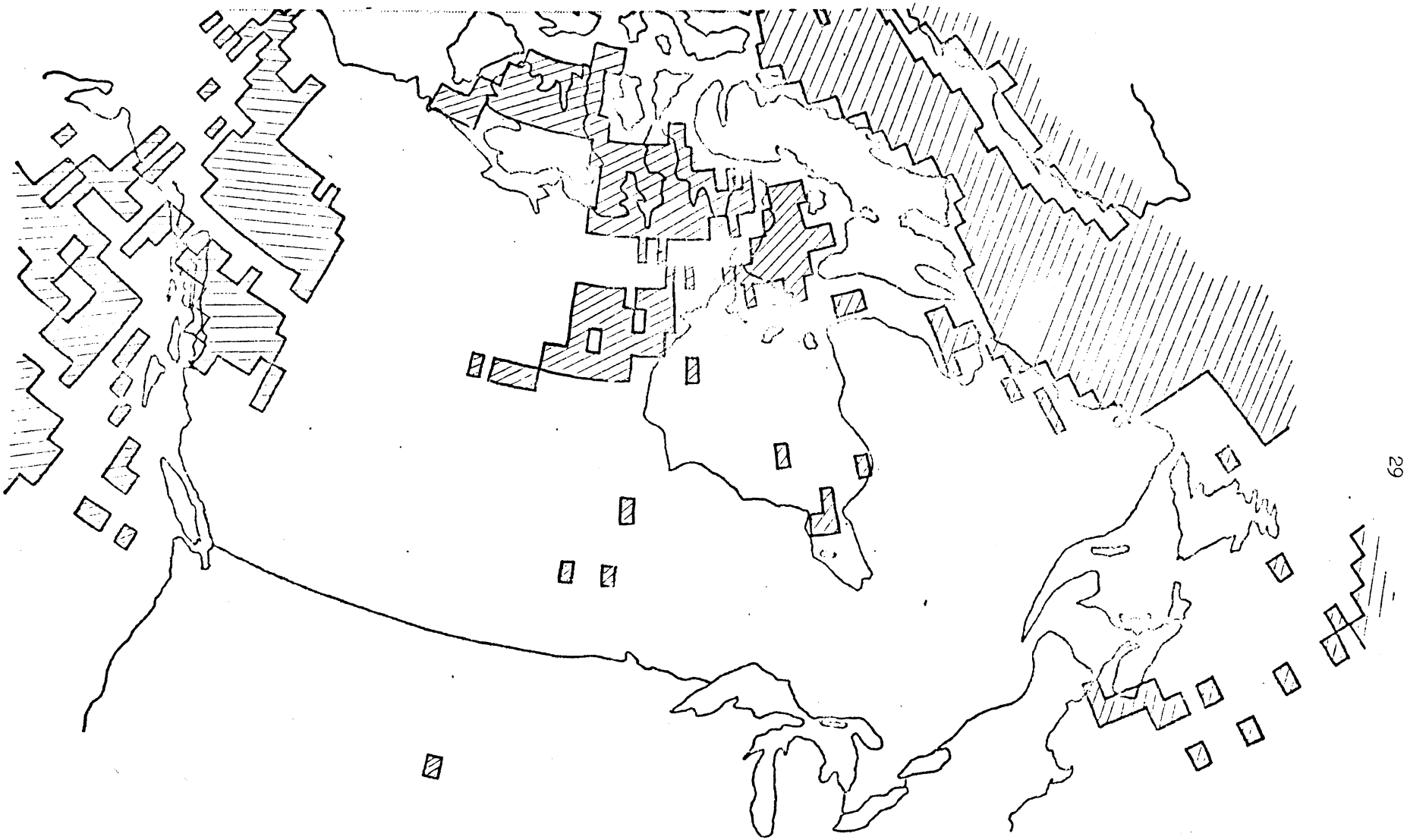

Figure 2.3
1° x 1° Mean Free Air Gravity Anomalies

Empty areas - ▨

(2) The reliability of the $1/3^\circ \times 1/3^\circ$ mean anomalies will depend upon the quality, quantity, and distribution of the point anomalies. The error estimates discussed in section 2.23 take into account the first two of these. Unless the point gravity anomalies are well-distributed within each $1/3^\circ \times 1/3^\circ$ block, the $1/3^\circ \times 1/3^\circ$ mean anomaly values are likely to be biased.

(3) The $1^\circ \times 1^\circ$ mean anomalies supplied by the DMAAC take into account the quality, quantity and distribution of the point gravity anomalies (Seppelin, 1971). The EPB mean anomalies do not take the distribution into account and are likely to be unreliable for this reason. In combining the two data sets some large differences were noted between them at common blocks. These differences, evaluated for 347 blocks, are summarised below:

Mean difference	:	+ 8.31 mgal
RMS difference	:	25.83 mgal
Maximum difference	:	+ 125.58 mgal
Minimum difference	:	- 36.98 mgal

(These differences are taken in the sense: DMAAC-EPB values.)
The differences are significant, in that they exceed, in most cases, the estimated standard deviations of the mean values, and in that the DMAAC values are systematically greater than the EPB values. Some further investigation into the causes of these differences is urgently required.

A further comparison that has been made is that between the $1/3^\circ \times 1/3^\circ$ data set for Eastern Canada, and the corresponding portion of the combined $1^\circ \times 1^\circ$ data set. In this comparison, $1^\circ \times 1^\circ$ mean values were computed from the $1/3^\circ \times 1/3^\circ$ mean values, using a weighted arithmetic mean. The weights used were the inverses of the estimated

variances. The results obtained from 426 comparisons are summarised below:

Mean difference	:	- 1.59 mgal
RMS difference	:	8.19 mgal
Maximum difference	:	+ 35.21 mgal
Minimum difference	:	- 70.50 mgal

(Taken in the sense: $1/3^\circ \times 1/3^\circ$ computed values - $1^\circ \times 1^\circ$ mean values.) The majority of the larger discrepancies occur where only the DMAAC values are available for comparison. This indicates that the Canadian data is consistent within itself, and that the significant differences between the DMAAC and EPB $1^\circ \times 1^\circ$ means may be due to errors in the DMAAC data, rather than in the method used by the EPB. However, this is something that will have to be clarified by the organisations themselves, and the existing data, burdened as it is with unpredictable errors, must be used in the best possible fashion.

2.3 Gravimetric Deflections

2.31 The Vening-Meinesz formulae

Gravimetric deflections are computed by means of the integration formulae of Vening-Meinesz. Essentially, these formulae are the spatial differentials of Stokes' formula for geoidal heights. The classical theory of the gravity potential of the earth, leading to these formulae is described in several texts (e.g. Heiskanen and Vening-Meinesz, 1958; Heiskanen and Moritz, 1967), and will not be discussed here. The formulae of Vening-Meinesz are:

$$\xi^G = \frac{1}{4\pi G} \int_\sigma \int \Delta g \, \frac{dS(\psi)}{d\psi} \cos\alpha \, d\sigma$$

$$\eta^G = \frac{1}{4\Pi G} \iint_\sigma \Delta g \frac{dS(\psi)}{d\psi} \sin\alpha d\sigma \qquad 2.22$$

where the symbols have the following meanings:

ξ^G, η^G are the gravimetric meridian and prime vertical components of the deflection of the vertical.

Δg is a free-air gravity anomaly, as a function of position.

$$\frac{dS(\psi)}{d\psi} = \frac{-\cos(\psi/2)}{2\sin^2(\psi/2)} + 8\sin\psi - 6\cos(\psi/2) - 3\frac{1-\sin(\psi/2)}{\sin\psi}$$

$$+ 3\sin\psi \ln[\sin(\psi/2) + \sin^2(\psi/2)] \quad \text{(Vening-Meinesz function)} \quad 2.23$$

$\Pi = 3.141592653...$

$G = 981$ gals (an average value of gravity on the geoid).

ψ is the spherical distance from the computation point to the particular gravity anomaly, and α is the azimuth of the geodesic connecting the computation point with the point to which the particular gravity anomaly pertains (measured clockwise from north).

The deflections of the vertical obtained by means of equation 2.22 refer to the same ellipsoid as that used to obtain the gravity anomalies, Δg, and are obtained at the geoid. The integration of equation 2.22 is closed, and should be carried out over the surface of the geoid. It is sufficient, in practice, to integrate over the surface of a sphere which has the same volume as the earth. This spherical approximation introduces errors of the order of the flattening, i.e. 0.3%, which, for gravimetric deflections, may be considered negligible (Heiskanen and Moritz, 1967).

The numerical evaluation of Vening-Meinesz formulae requires the replacement of the integration by a summation over discrete data:

$$\xi^G = \frac{1}{4\Pi G} \Sigma \ \Delta g \ \frac{dS(\psi)}{d\psi} \cos\alpha\Delta\sigma$$

$$\eta^G = \frac{1}{4\Pi G} \Sigma \ \Delta g \ \frac{dS(\psi)}{d\psi} \sin\alpha\Delta\sigma \qquad 2.24$$

There are two commonly used techniques of computing the deflections from equation 2.24. One uses elements that are portions of spherical discs, centred at the computation point P, i.e. circular coordinates on the surface of the earth (Figure 2.4a). The other uses quasi-rectangular blocks formed by the intersections of meridians and parallels, i.e. rectangular co-ordinates on the surface of the earth (Figure 2.4b). Both methods require the calculation of mean values of Δg for each element.

(1) When circular co-ordinates are used, the values of Δg must be recomputed every time the computation point (i.e. the origin of the co-ordinate system) is moved. This method was originally useful when access to high speed computers was difficult or impossible. Circular templates were used in conjunction with contour maps of gravity anomalies (e.g. Rice, 1952; Derenyi, 1965). This work required a great deal of time and effort, and consequently very few deflections could be computed.

(2) The rectangular block mean values do not change with the computation point, and can be precomputed, stored, and used repeatedly. This method has been described in Uotila (1960), where the author recommends a combination of blocks and circular templates, the templates to be used for the inner area, and blocks of $1^\circ \times 1^\circ$ and $5^\circ \times 5^\circ$ for the outer area. This technique has been used for computing gravimetric deflections of the vertical in North America by Nagy (1963) and Fischer (1965). However, the practical application of their methods allow gravimetric deflections to be computed only at block corners, or at the geometric centres of blocks.

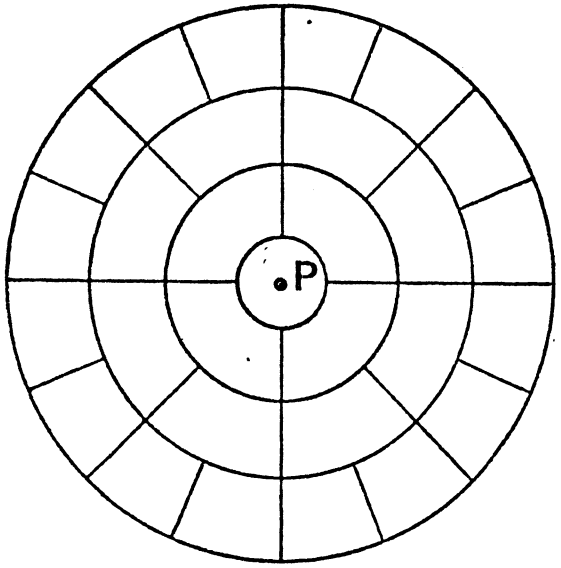

Figure 2.4a

Circular Templates

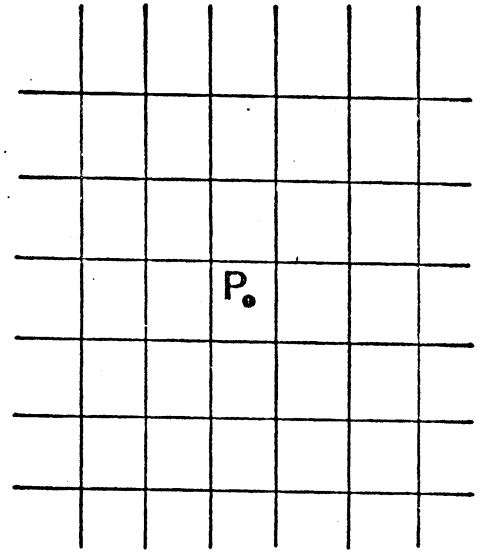

Figure 2.4b

Rectangular Blocks

Fischer overcomes this problem by computing "curvature" components (spatial derivatives of the deflections) and uses these to account for the effect of moving the computation point. This procedure requires a uniform, dense gravity coverage in the immediate vicinity, and would not therefore be feasible for most conditions.

(3) A more general approach, involving an analytical solution for the deflection contribution from the immediate vicinity of the computation point, and a series approximation for the gravity field in this vicinity, has been developed here. The summation in equation 2.24 is broken into three parts:

$$\xi^G = \xi_1 + \xi_2 + \xi_3$$
$$\eta^G = \eta_1 + \eta_2 + \eta_3 \qquad 2.25$$

where each of the subscripted values is determined from a different region and involves different block sizes (Figure 2.5). The block sizes used are: $1^\circ \times 1^\circ$ for the outer zone; $1/3^\circ \times 1/3^\circ$ for the middle zone. In the inner zone, point gravity anomalies are used. The choice of $1^\circ \times 1^\circ$ blocks was predetermined by the fact that these were the smallest blocks for which mean values were readily available (Decker, 1972).

The Vening-Meinesz function, $\frac{dS(\psi)}{d\psi}$, goes to infinity at the computation point (Figure 2.6), and it is evident that even smaller elements should be used for the vicinity of the computation point. A $1/3^\circ \times 1/3^\circ$ size has been chosen as a compromise between a theoretically preferable smaller block size and the reality that the available gravity data has a density of one point per 10 km or less (Nagy, 1973). The innermost $1/3^\circ \times 1/3^\circ$ block in which the computation point is contained is treated in a different way, using point data to determine the

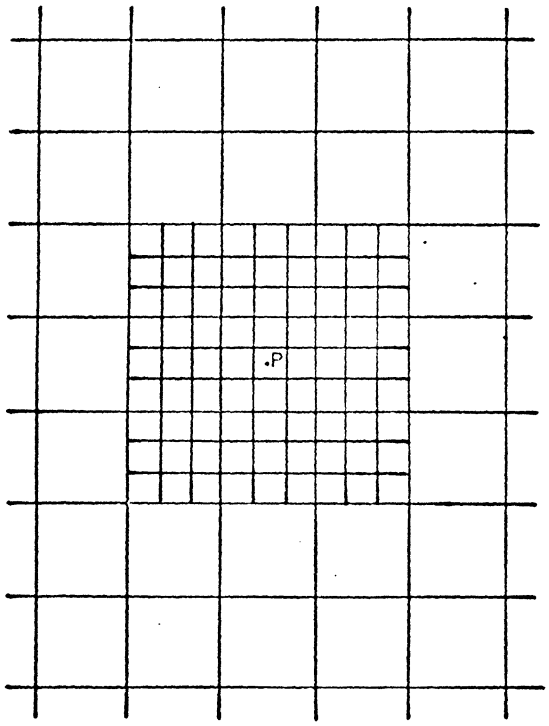

Figure 2.5

Different-sized Rectangular Blocks

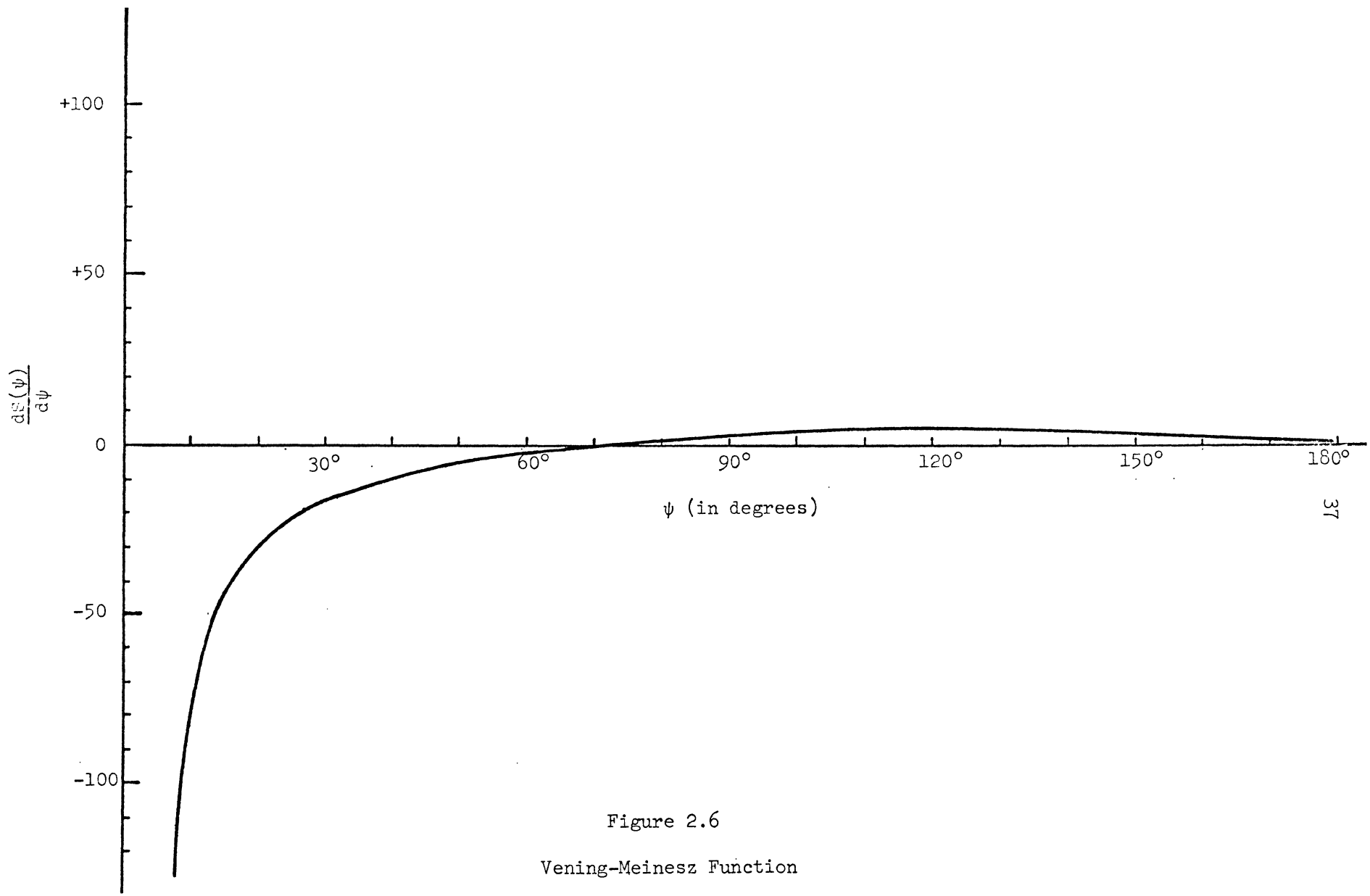

Figure 2.6

Vening-Meinesz Function

coefficients of a two-dimensional polynomial approximating the gravity field. The analytical expression for the Vening-Meinesz integral of this series has been derived, using approximations for the Vening-Meinesz function, as is shown later. The determination of each of the components is outlined in the next sections.

2.32 Outer zone contribution

The part of equation 2.24 pertinent to the outer zone can be written as:

$$\xi_1 = \frac{1}{4\Pi G} \sum_{i=1}^{n} \overline{\Delta g_i} \left(\frac{dS(\psi)}{d\psi}\right)_i \cos\phi_i \cos\alpha_i \Delta\phi_1 \Delta\lambda_1$$

$$\eta_1 = \frac{1}{4\Pi G} \sum_{i=1}^{n} \overline{\Delta g_i} \left(\frac{dS(\psi)}{d\psi}\right)_i \cos\phi_i \sin\alpha_i \Delta\phi_1 \Delta\lambda_1 \qquad 2.26$$

where $\overline{\Delta g_i}$ is the mean value of the gravity anomaly in the ith block,

$\frac{dS(\psi)}{d\psi}$ is evaluated at the mid-point of the ith block,

ϕ_i is the latitude of this midpoint,

$\Delta\phi_1 = \Delta\lambda_1 = 1^\circ$,

n is the number of $1^\circ \times 1^\circ$ blocks used, and

ψ_i, α_i are given by:

$$\psi_i = \arccos(\sin\phi_P \sin\phi_i + \cos\phi_P \cos\phi_i \cos(\lambda_i - \lambda_P))$$

$$\alpha_i = \arctan\left(\frac{\cos\phi_i \sin(\lambda_i - \lambda_P)}{\cos\phi_P \sin\phi_i - \sin\phi_P \cos\phi_i \cos(\lambda_i - \lambda_P)}\right) \qquad 2.27$$

and (ϕ_P, λ_P) are the latitude and longitude of the computation point, and (ϕ_i, λ_i) the latitude and longitude of the midpoint of the ith block.

2.33 Middle zone contribution

The part of equation 2.24 pertinent to the middle zone is similarly given by

$$\xi_2 = \frac{1}{4\Pi G} \sum_{j=1}^{m} \overline{\Delta g}_j \left(\frac{dS(\psi)}{d\psi}\right)_j \cos\phi_j \cos\alpha_j \Delta\phi_2 \Delta\lambda_2$$

$$\eta_2 = \frac{1}{4\Pi G} \sum_{j=1}^{m} \overline{\Delta g}_j \left(\frac{dS(\psi)}{d\psi}\right)_j \cos\phi_j \sin\alpha_j \Delta\phi_2 \Delta\lambda_2 \qquad 2.28$$

where $\Delta\phi_2 = \Delta\lambda_2 = 1/3°$,

m is the number of $1/3° \times 1/3°$ blocks, and the other symbols have the same meaning as before.

For the $1/3° \times 1/3°$ blocks near the computation point, it is no longer sufficient to use a value of $\frac{dS(\psi)}{d\psi}$, evaluated at the centre of each block, due to the rapid change in this function near the computation point (Figure 2.6). A more rigorous approach is to integrate over the block (Heiskanen and Moritz, 1967):

$$\overline{\frac{dS(\psi)}{d\psi}} = \frac{1}{A} \iint \frac{dS(\psi)}{d\psi} dA \qquad 2.29$$

where $\overline{\frac{dS(\psi)}{d\psi}}$ denotes the mean value of $\frac{dS(\psi)}{d\psi}$ for the block, and A is the block area. For those blocks within 0°.5 of the computation point, equation 2.29 is integrated numerically and this value used instead of the value of $\frac{dS(\psi)}{d\psi}$ for the block centre.

One disadvantage of allowing the computation point to be at an arbitrary position within a $1/3° \times 1/3°$ block is that equation 2.29 becomes unstable when the computation point approaches the edges of its $1/3° \times 1/3°$ block. The error in the numerical integration that may occur is illustrated in Table 2.2. In order to keep this error below 10% of the deflection value, the co-ordinates of the computation point are

For $\bar{\Delta}g$ = 50 mgal in adjacent block

Angular distance from computation point to edge of block	Contribution to deflection	Error (seconds of arc)	Error (percentage)
0°.17	1".32	0".01	1
0°.10	2".38	0".03	1
0°.07	3".30	0".05	2
0°.04	5".03	0".18	4
0°.02	7".44	0".51	7
0°.01	8".95	0".90	10
0°.001	13".80	3".20	23

Table 2.2

Error in numerical integration of $\frac{dS(\psi)}{d\psi}$ for (1/3° x 1/3°) blocks adjacent to block containing computation point.

changed slightly (if necessary) so that it is always at least 0°.01 (approximately 1 km) away from the edge. The change in deflection value caused by this position shift, is not likely to be significant.

2.34 Inner zone contribution

The contribution of the innermost 1/3° x 1/3° block is given by:

$$\xi_3 = -\frac{1}{2\pi G}(\Delta g_P \cdot f_1 + g_x f_2 + g_y f_3) - \frac{3}{4\pi GR}(\Delta g_P g_1 + \frac{1}{2} g_x g_2 + \frac{1}{4} g_y g_3)$$

$$\eta_3 = -\frac{1}{2\pi G}(\Delta g_P \cdot f_1' + g_y f_2' + g_x f_3') - \frac{3}{4\pi GR}(\Delta g_P g_1' + \frac{1}{2} g_y g_2' + \frac{1}{4} g_x g_3') \qquad 2.30$$

where Δg_P is the gravity anomaly at the computation point P, and $g_x \cdot g_y$ are the horizontal gradients of gravity at P, evaluated in an (x, y) local plane co-ordinate system in which the x-axis is directed north, the y-axis east, and the origin is at P. R is a mean radius of curvature for the earth and:

$$f_1 = \ln(y_2 + \sqrt{(x_1^2+y_2^2)}) - \ln(y_2 + \sqrt{(x_2^2+y_2^2)}) - \ln(y_1 + \sqrt{(x_1^2+y_1^2)}) + \ln(y_1 + \sqrt{(x_2^2+y_1^2)})$$

$$f_2 = y_2 \ln(x_2 + \sqrt{(x_2^2+y_2^2)}) - y_2 \ln(x_1 + \sqrt{(x_1^2+y_2^2)}) - y_1 \ln(x_2 + \sqrt{(x_2^2+y_2^2)}) + y_1 \ln(x_1 + \sqrt{(x_1^2+y_1^2)})$$

$$f_3 = \sqrt{(x_1^2+y_2^2)} - \sqrt{(x_2^2+y_2^2)} - \sqrt{(x_1^2+y_1^2)} + \sqrt{(x_2^2+y_1^2)}$$

$$g_1 = \frac{1}{2}(y_2 \ln(x_2^2+y_2^2) + y_1 \ln(x_1^2+y_1^2) - y_2 \ln(x_1^2+y_2^2) - y_1 \ln(x_2^2+y_1^2))$$

$$+ x_2 \arctan \frac{y_2}{x_2} + x_1 \arctan \frac{y_1}{x_1} - x_2 \arctan \frac{y_1}{x_2} - x_1 \arctan \frac{y_2}{x_1} \qquad 2.31$$

$$g_2 = x_2 y_2 - y_2^2 \arctan \frac{x_2}{y_2} + x_2^2 \arctan \frac{y_2}{x_2} - x_1 y_2 + y_2^2 \arctan \frac{x_1}{y_2} -$$

$$- x_1^2 \arctan \frac{y_2}{x_1} - x_2 y_1 + y_1^2 \arctan \frac{x_2}{y_1} - x_2^2 \arctan \frac{y_1}{x_2} + x_1 y_1 - y_1^2 \arctan \frac{x_1}{y_1} +$$

$$+ x_1^2 \arctan \frac{y_1}{x_1}$$

$$g_3 = (x_2^2 + y_2^2)\ln(x_2^2 + y_2^2) - (x_1^2 + y_2^2)\ln(x_1^2 + y_2^2) - (x_2^2 + y_1^2)\ln(x_2^2 + y_1^2) +$$

$$+ (x_1^2 + y_1^2)\ln(x_1^2 + y_1^2) \ .$$

The equations for the primed quantities are identical to those above, except that the x and y co-ordinates are interchanged. x_1, y_1, x_2, y_2 are the co-ordinates of the four corners of the innermost ($1/3^\circ$ x $1/3^\circ$) block, relative to the point P (Figure 2.7). Equations 2.30 and 2.31 are derived in Appendix III. Values for Δg_P, g_x, g_y are found by fitting a plane to the point gravity data in the innermost block. The plane is defined by the following expression:

$$\tilde{\Delta g}_i = \Delta g_P + g_x\Big|_P x_i + g_y\Big|_P y_i \qquad 2.32$$

a truncated series expansion at P. Putting:

$c_1 = \Delta g_P$; $c_2 = g_x$; $c_3 = g_y$; $\phi_1(x,y) = 1$; $\phi_2(x,y) = x$; $\phi_3(x,y) = y$

$$\tilde{\Delta g}_i = \sum_{j=1}^{3} c_j \phi_j \qquad 2.33$$

The coefficients c_j are found from the solution of the matrix equation:

$$G \underset{\sim}{c} = \underset{\sim}{\ell} \qquad 2.34$$

where the matrix G has elements: $g_{kj} = \langle \phi_k, \phi_j \rangle$, and the vector $\underset{\sim}{\ell}$ has elements: $\ell_k = \langle \Delta g, \phi_k \rangle$ $j,k=1,\ldots,3$. The weight function in the scalar products is given by:

$$w(x_i, y_i) = \sigma_{\Delta g_i}^{-2} \qquad 2.35$$

The inner zone yields most of the information concerning the influence of local variations in the gravity field, and it is important

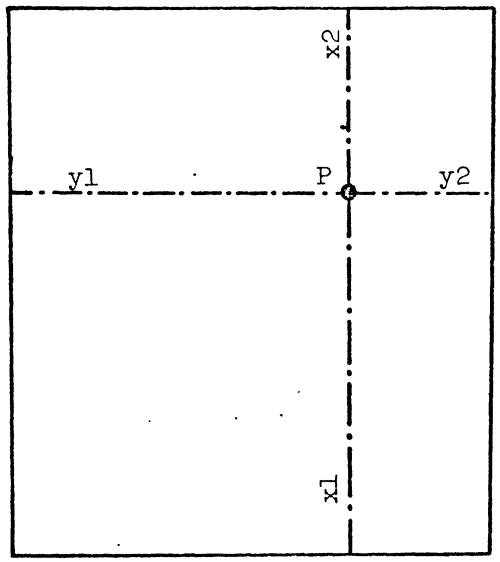

Figure 2.7

Inner Zone - x, y co-ordinates

that there be sufficient well-distributed data in this zone in order to get a reliable estimate of the deflections. Consequently, several criteria have been set up to ensure that the data has these characteristics. Sufficiency is ensured when there are at least four data points in the region. The distribution is checked by ensuring that there is at least one data point in each of at least three of the four quadrants around the computation point. If these criteria are not met, no deflection components are computed for that point.

2.35 Error propagation

In order to obtain some estimate of the reliability of the results, propagation of the gravity anomaly errors has been included in this study. It has been shown (e.g. Heiskanen and Moritz, 1967), that gravity anomalies are correlated with each other as a function of distance, and much research has been done into the representation of this correlation by means of auto-covariance functions and empirical covariance matrices (e.g. Kaula, 1957; Lauritzen, 1973). However, the practical problems involved in using the necessarily large covariance matrices associated with the anomalies have not been successfully overcome, as yet. Consequently, for the purpose of this thesis, the gravity anomalies, both point and mean, have been assumed to be uncorrelated, thus resulting in diagonal weight matrices. The propagation of errors for the components ξ_1, ξ_2, η_1, η_2 is then fairly straight-forward:

$$\sigma_{\xi_j} = \frac{1}{4\pi G} \sqrt{\left[\sum_{i=1}^{n} \left(\left(\frac{dS(\psi)}{d\psi}\right)_i \cos\phi_i \cos\alpha_i \, d\phi_j \, d\lambda_j \right)^2 \cdot \sigma^2_{\Delta g_i} \right]}$$

$$\sigma_{\eta_j} = \frac{1}{4\pi G} \sqrt{\left[\sum_{i=1}^{n} \left(\left(\frac{dS(\psi)}{d\psi}\right)_i \cos\phi_i \sin\alpha_i \, d\phi_j \, d\lambda_j \right)^2 \cdot \sigma^2_{\Delta g_i} \right]} \text{ for } j=1,2 \quad . \qquad 2.36$$

The propagation of errors for the inner zone proceeds in two steps. The error covariance matrix of the coefficients c_j (equation 2.33) is derived from:

$$\Sigma_c = \sigma_o^2 \, G^{-1} \qquad 2.37$$

where

$$\sigma_o^2 = \frac{\sum_{i=1}^{n} (\Delta g_i - \tilde{\Delta g}_i)^2 \cdot w(x_i, y_i)}{n-3} \qquad 2.38$$

The variances of ξ_3 and η_3 are given by:

$$\sigma_{\xi_3}^2 = \underset{\sim}{d}_1 \, \Sigma_c \, \underset{\sim}{d}_1^T$$

$$\sigma_{\eta_3}^2 = \underset{\sim}{d}_2 \, \Sigma_c \, \underset{\sim}{d}_2^T \qquad 2.39$$

where $\underset{\sim}{d}_1$ and $\underset{\sim}{d}_2$ are the linear operators on: $\underset{\sim}{q} = (\Delta g, g_x, g_y)$ in equation 2.30:

$$\xi_3 = \underset{\sim}{q} \, \underset{\sim}{d}_1 \; ; \; \eta_3 = \underset{\sim}{q} \, \underset{\sim}{d}_2 \qquad 2.30$$

$\underset{\sim}{d}_1$ and $\underset{\sim}{d}_2$ are given by:

$$\underset{\sim}{d}_1^T = \frac{1}{2\Pi G} \left(-f_1 - \frac{3}{2R} g_1 ; \; -f_2 - \frac{3}{2R} g_2 ; \; -f_3 - \frac{3}{2R} g_3\right)$$

$$\underset{\sim}{d}_2^T = \frac{1}{2\Pi G} \left(-f_1' - \frac{3}{2R} g_1' ; \; -f_3' - \frac{3}{2R} g_3' \; -f_2' - \frac{3}{2R} g_2'\right) \qquad 2.40$$

The complete estimates for the standard deviations of ξ^G, η^G are given by:

$$\sigma_{\xi^G} = \sqrt{(\sigma_{\xi_1}^2 + \sigma_{\xi_2}^2 + \sigma_{\xi_3}^2)}$$

$$\sigma_{\eta^G} = \sqrt{(\sigma_{\eta_1}^2 + \sigma_{\eta_2}^2 + \sigma_{\eta_3}^2)} \qquad 2.41$$

2.4 Astrogeodetic Deflections

2.41 Astrogeodetic data

The astrogeodetic deflection components at a point are given by:

$$\xi^A = \Phi - \phi$$
$$\eta^A = (\Lambda - \lambda)\cos\phi \qquad 2.42$$

where (Φ,Λ) are the astronomic latitude and longitude of the deflection station, and (ϕ,λ) are the corresponding geodetic quantities. (Longitude is considered positive eastwards.)

The above definitions are valid for all points if the minor axis of the geodetic reference ellipsoid is parallel to the mean rotation axis of the earth, and the Greenwich meridian plane of the geodetic system is parallel to the astronomic Greenwich meridian plane. If this is not the case, the deflections should be corrected for the rotations between the two systems. There have been several attempts at determining these rotations (e.g. Lambeck, 1971; Mueller at al, 1972; Thomson and Krakiwsky, 1974), with some small rotations being evident. An apparent rotation between the Greenwich meridian planes has been documented, and is due to the redefinition of the Greenwich mean astronomic meridian by the Bureau International de l'Heure in 1962 (Stoyko, 1962). This resulted in the longitude of the U.S. Naval Observatory changing by 0".765, while that of the Canadian Dominion Observatory did not alter. However, in order to avoid the resultant discontinuity in astronomic longitude values, all post-1962 longitudes are still referred to the old Greenwich mean meridian (D.A. Rice, personal communication, 1972). This essentially means that the astronomic and geodetic co-ordinate systems

in North America remain parallel to each other, but are not parallel to any other system based upon the post-1962 Greenwich mean meridian (such as satellite systems).

Independent of the rotation in longitude described above, there may be an additional rotation of the geodetic co-ordinate system about the normal to the ellipsoid at the initial geodetic point. This rotation is due to incomplete satisfaction of Laplace's azimuth condition at this point (Vanicek and Wells, 1974).

The astrogeodetic deflection data available for this study consisted of 870 deflections in Canada and 3050 deflections in the U.S.A. This data was supplied by the Geodetic Survey of Canada and the U.S. National Geodetic Survey. Approximately 100 of the Canadian deflections were considered to be of low order, due to either poor astronomic determinations or large uncertainities in the geodetic co-ordinates (in the Arctic Islands). The observations were generally made with a first-order universal theodolite (such as the Wild T4 or Kern DKM3A) or with a portable transit (Bamberg), in accordance with the procedures set out in Hoskinson and Duerksen (1952). Different star catalogues have been used during the period of observation (some observations date back to the late 19th century), the principal ones being the General Catalogue, the FK3, and the FK4. Longitude, prior to 1925, was obtained using telegraph timing techniques. After 1925, time comparisons by means of radio superseded the telegraphic technique.

2.42 Sources of error

In estimating the accuracies of the observed astrogeodetic deflections, three different kinds of errors can be distinguished:

(1) errors in the astronomic co-ordinates,

(2) errors in the geodetic co-ordinates,

(3) error in neglecting the curvature of the plumbline.

(1) The errors inherent in the observing techniques have been estimated at 0".5 in latitude and 0".6 in longitude (Rice, 1962). Pre-1925 longitudes will have an additional error of 1".5, due to errors in the telegraph timing method. The systematic differences between the various star catalogues used are not expected to affect the astronomic positions by more than 0".4 (G. Corcoran, personal communication, 1972)* Reduction of the co-ordinates to the mean pole of 1900-1905 (Conventional International Origin) has, in most cases, not been carried out. This affects latitude by 0".2 and longitude by 0".2tanϕ (Mueller, 1969).

(2) Observational errors propagate from the initial point of the geodetic datum in a random fashion and an approximate formula for the errors in the North American networks has been suggested by Simmons (1950):

$$\text{Proportional error} \doteq M^{1/3}/20{,}000 \qquad 2.43$$

where M is the distance in miles from the initial point (Meades Ranch). This formula may be transformed to an estimate for the standard deviation (in arc seconds):

$$\sigma_G \doteq 1.89 \times 10^{-5} \cdot k^{2/3} \qquad 2.44$$

where k is the distance in metres from the origin.

Systematic errors of two types are also present in the North American geodetic networks. The non-rigorous adjustment technique initially used has led to systematic distortions of newly-added networks that were forced to fit the older results. In Canada, misclosures of up to 36 metres (approximately 1".0) have been reported (Dept. of Energy, Mines and Resources, 1972), and errors of 0".2 in relative position across New

---

* All the U.S. data has been reduced to either the FK3 or FK4 (W. Strange, personal communication, 1974).

Brunswick, due solely to the adjustment constraints, have been found (Krakiwsky and Konecny, 1971).

A further source of systematic error is that due to the reduction procedure applied to the observations used in the original adjustment of the networks. The horizontal directions were not corrected for the deflection of the vertical, and the distances were, in effect, reduced to the geoid, and not to the ellipsoid. The effect of this last approximation has been estimated not to exceed 0".5 in position, in Canada (Merry and Vaníček, 1973).

(3) The astronomic co-ordinates should be reduced from the terrain to the geoid, prior to the evaluation of the deflection components Such a reduction, due to the curvature of actual plumbline between the terrain and the geoid, has not been carried out. Consequently, the derived astrogeodetic deflections of the vertical are surface astrogeodetic deflections. The curvature of the plumbline will be mainly due to topographic irregularities and crustal density variations. Investigations in the Alps have shown that curvature in mountainous terrain may reach 11" (Kobold and Hunziker, 1962). Evaluation of the curvature is a difficult task, made more difficult by the fact that (in Canada at least) the necessary gravity or other geophysical data is seldom available in sufficient quantity (Ndyetabula, 1974). Based upon the above discussion, a general model for the errors can be written as:

$$\sigma_{\xi^A} = \sqrt{(\sigma_o^2 + \sigma_c^2 + \sigma_P^2 + \sigma_G^2)}$$

$$\sigma_{\eta^A} = \sqrt{(\sigma_o^2 + \sigma_c^2 + \sigma_P^2 + \sigma_G^2 + \sigma_T^2)} \qquad 2.45$$

where σ_o is an estimate for the observing precision - 0".5 for latitude and 0".6 for longitude (for second order deflections, σ_o = 1".5); σ_c

represents the error due to use of different star catalogues (0".4 for old observations, 0".0 for post-1964 observations); σ_P represents the error due to the effect of polar motion - 0".2 for latitude and 0".2tanϕ for longitude (for post-1962 U.S. data, σ_P = 0".0, as the correction for polar motion has been applied); σ_G is given by equation 2.44; and σ_T is an estimate for the telegraph timing error - 1".5 for pre-1925 longitude, 0".0 for post-1925 longitudes.

The above model provides accuracy estimates ranging from 0".5 near the initial point to 2".0 in the Canadian Arctic. These estimates are likely to be too optimistic, as systematic errors, due to network distortion, improper distance and angle reductions, and neglect of plumbline curvature, have not been modelled. The effects of these errors must be considered unpredictable at this stage, but may vary from 0".0 to as much as 10".0.

2.5 Two-dimensional Interpolation

2.51 Mathematical model used

The modified gravimetric deflections ξ^G, η^G differ from the observed astrogeodetic deflections ξ^A, η^A due to two causes:

(1) the two types of deflection are related to two ellipsoids of different size, shape and position.

(2) the modified gravimetric deflections do not account for the influence of the gravity field beyond the outer zone, and for the error in numerical integration.

These differences, $\delta\xi$, $\delta\eta$, can be approximated by two second-order, two-dimensional, polynomial expressions:

$$\delta\xi = \xi^A - \xi^G \doteq \tilde{\delta\xi} = \sum_{\ell=1}^{9} c_\ell \, \phi_\ell(x,y) \qquad 2.46$$

$$\delta\eta = \eta^A - \eta^G \doteq \tilde{\delta\eta} = \sum_{\ell=1}^{9} c'_\ell \, \phi_\ell \, (x,y)$$

or, in a more specific form:

$$\tilde{\delta\xi} = \sum_{\substack{i=0\\j=0}}^{2} a_{ij} \, x^i y^j$$

$$\tilde{\delta\eta} = \sum_{\substack{i=0\\j=0}}^{2} b_{ij} \, x^i y^j \qquad 2.47$$

where (x,y) form a local orthogonal co-ordinate pair, and are given by:

$$x = \phi - \phi_o$$

$$y = \lambda - \lambda_o \qquad 2.48$$

and (ϕ_o, λ_o) are the latitude and longitude of an arbitrary origin located close to the centre of the area. The coefficients a_{ij}, b_{ij} are found using the least squares approximation technique described earlier:

$$\sum_{\substack{i=0\\j=0}}^{2} \left\langle x^k \cdot y^\ell, \, x^i \cdot y^j \right\rangle a_{ij} = \left\langle \delta\xi, \, x^k \cdot y^\ell \right\rangle$$

$$\sum_{\substack{i=0\\j=0}}^{2} \left\langle x^k \cdot y^\ell, \, x^i \cdot y^j \right\rangle b_{ij} = \left\langle \delta\eta, \, x^k \cdot y^\ell \right\rangle \qquad 2.49$$

$$k,\ell = 0,1,2.$$

The weighting functions, used in the scalar products, are:

$$w(\delta\xi) = (\sigma^2_{\xi^A} + \sigma^2_{\xi^G})^{-1}$$

$$w(\delta\eta) = (\sigma^2_{\eta^A} + \sigma^2_{\eta^G})^{-1} \qquad 2.50$$

$\delta\xi$, $\delta\eta$ are obtained at the control points where both astrogeodetic and modified gravimetric deflections are available. Equations 2.49 can be written in matrix notation as:

$$G \underset{\sim}{a} = \underset{\sim}{m}$$
$$G \underset{\sim}{b} = \underset{\sim}{n} \qquad 2.51$$

from which

$$\underset{\sim}{a} = G^{-1} \underset{\sim}{m}$$
$$\underset{\sim}{b} = G^{-1} \underset{\sim}{n} \qquad 2.52$$

The error covariance matrices of the coefficients are found from:

$$\Sigma_a = \sigma^2_{oa} G^{-1}$$
$$\Sigma_b = \sigma^2_{ob} G^{-1} \qquad 2.53$$

where

$$\sigma^2_{oa} = \frac{\sum_{i=1}^{n} (\delta\xi_i - \tilde{\delta\xi}_i)^2 \, w(\delta\xi_i)}{n-9}$$
$$\sigma^2_{ob} = \frac{\sum_{i=1}^{n} (\delta\eta_i - \tilde{\delta\eta}_i)^2 \, w(\delta\eta_i)}{n-9} \qquad 2.54$$

n = number of control points. The error covariance matrices of the quantities $\tilde{\delta\xi}$, $\tilde{\delta\eta}$ are:

$$\Sigma_{\tilde{\delta\xi}} = C \, \Sigma_a \, C^T$$
$$\Sigma_{\tilde{\delta\eta}} = C \, \Sigma_b \, C^T \qquad 2.55$$

where C is the matrix:

$$C = \begin{bmatrix} \phi_1(x_1,y_1) & \cdots & \phi_9(x_1, y_1) \\ \vdots & & \vdots \\ \phi_1(x_m,y_m) & \cdots & \phi_9(x_m,y_m) \end{bmatrix} \qquad 2.56$$

Here $\phi_i(x,y)$ have the same meaning as in equation 2.46, and m is the number of points for which predicted astrogeodetic deflections are needed.

Using the computed coefficients, a_{ij}, b_{ij}, in equation 2.47, values of $\tilde{\delta\xi}$, $\tilde{\delta\eta}$ can be determined at any point in the region, as a function of the local co-ordinates (x,y). Adding these quantities to the gravimetric deflections, ξ^G, η^G, the interpolated astrogeodetic deflections are:

$$\tilde{\xi}^A = \xi^G + \tilde{\delta\xi}$$
$$\tilde{\eta}^A = \eta^G + \tilde{\delta\eta} \qquad 2.57$$

With error covariance matrices:

$$\Sigma_{\tilde{\xi}}A = \Sigma_{\tilde{\delta\xi}} + \Sigma_{\xi}G$$
$$\Sigma_{\tilde{\eta}}A = \Sigma_{\tilde{\delta\eta}} + \Sigma_{\eta}G \qquad 2.58$$

The modified gravimetric deflections have been considered as uncorrelated so that $\Sigma_{\xi}G$ and $\Sigma_{\eta}G$ are diagonal matrices in the expression, with the diagonal elements being:

$$\sigma^2_{\xi_1}G \;,\ldots,\; \sigma^2_{\xi_m}G \;;\; \sigma^2_{\eta_1}G \;,\ldots,\; \sigma^2_{\eta_m} \quad .$$

2.52 Choice of zone boundaries

In the calculation of the modified gravimetric deflections, three zone boundaries need to be established. The first two of these are not dependant upon the interpolation procedure and could have been described in an earlier section. The third zone boundary, that of the outer zone, is dependant upon the interpolation procedure. As a matter of convenience, all three are described here.

(1) Inner Zone Boundary: Ideally, this boundary should be such that the portion of the gravity field contained within it could be adequately represented by a plane. However, practical considerations overrode this requirement. Due to the relatively sparse nature of the gravity coverage in Canada, a minimum size of $1/3^\circ \times 1/3^\circ$ was chosen in order to have sufficient (at least three) data points within this zone, to model a plane.

(2) Middle Zone Boundary: For the numerical integration of equation 2.24, it is desirable that the element size be kept as small as possible. That is, the smallest element size (in this case the $1/3^\circ \times 1/3^\circ$ blocks) should extend as far as possible from the computation point. However, due to the decrease in the value of the Vening-Meinesz function with increase in distance from the computation point (Figure 2.6), it is possible to use larger block sizes (such as $1^\circ \times 1^\circ$) further away. This results in a considerable saving in computer time and storage.

In order to determine the optimum middle zone boundary, the following procedure was used. Gravimetric deflections at 9 points in New Brunswick were computed, and for each of these the area covered by the $1/3^\circ \times 1/3^\circ$ blocks was varied from $1^\circ \times 1^\circ$ to $11^\circ \times 11^\circ$, in 2° increments. Where less than $11^\circ \times 11^\circ$ was covered by $1/3^\circ \times 1/3^\circ$ blocks, $1^\circ \times 1^\circ$ blocks were used instead. Taking the $11^\circ \times 11^\circ$ values as a standard, differences in the deflection values, from this standard, were obtained at the nine points. The root mean square (RMS) differences, as a function of middle zone boundary, are shown in Figure 2.8. A noticeable change in trend occurs at the $5^\circ \times 5^\circ$ value on this graph, and this appears to be the minimum area that should be covered by $1/3^\circ \times 1/3^\circ$ blocks of data, without sacrificing too much accuracy. Consequently, $5^\circ \times 5^\circ$ has

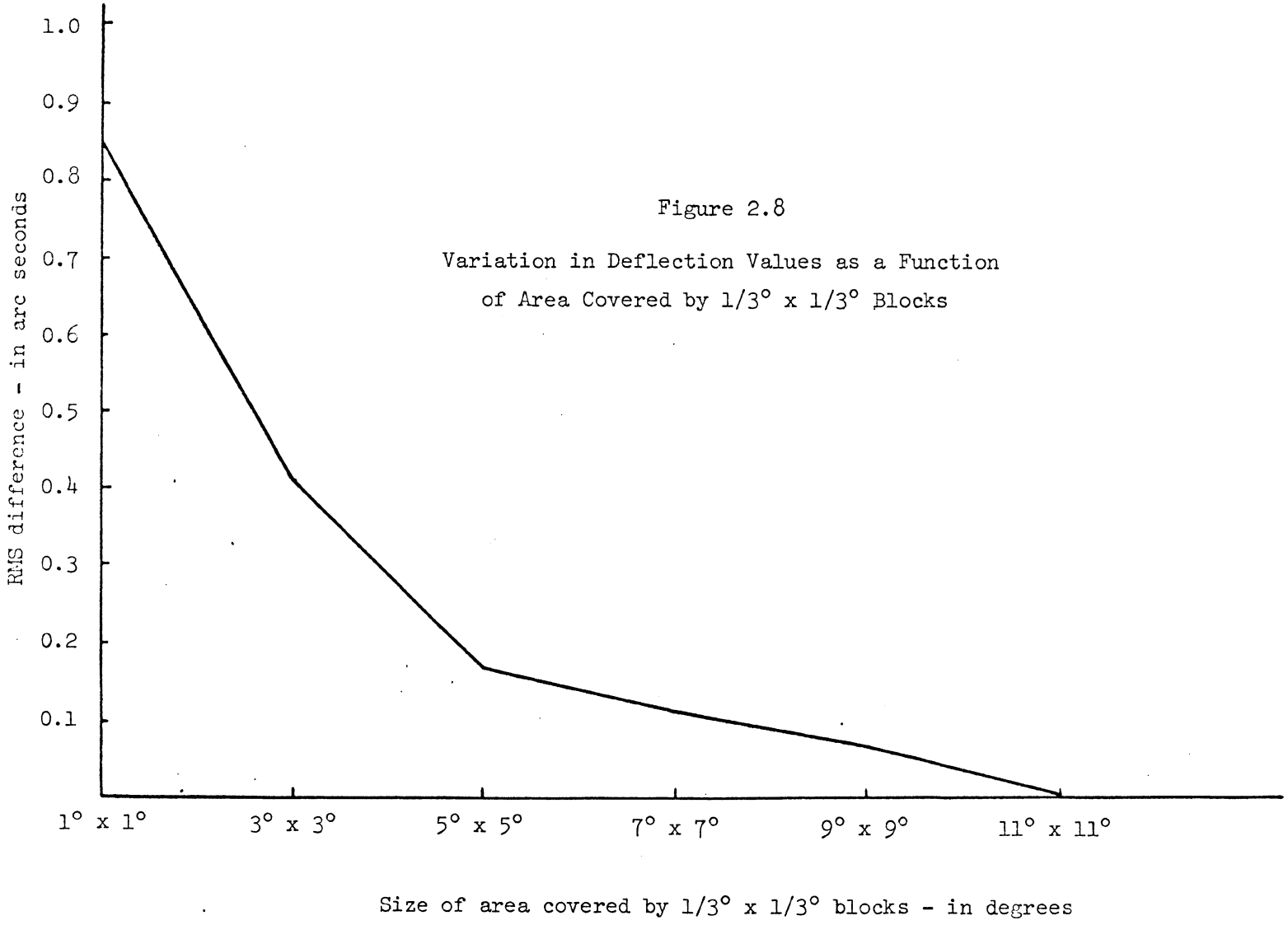

Figure 2.8

Variation in Deflection Values as a Function of Area Covered by 1/3° x 1/3° Blocks

been selected as the area to be covered by the $1/3^\circ \times 1/3^\circ$ blocks of mean gravity anomalies.

(3) Outer Zone Boundary: This boundary should be chosen in such a way that the residual error, due to the neglect of the distant zones, could be modelled by a surface of second order, over the region covered by the control points. Preliminary testing, using the gravimetric deflections, indicated that, for a region 400 km by 400 km in extent, an outer zone boundary 500 km from the computation point would be adequate. This zone boundary was used for some initial investigations (Merry and Vaníček, 1974a).

Further testing, described below, showed that a smaller outer limit could be used. In this test, deflections were predicted at 18 points in New Brunswick, using an outer zone boundary ranging from 300 km to 800 km. The RMS differences between the deflections obtained using the 800 km boundary, and those obtained using smaller values are shown in Figure 2.9. It is apparent that a relative accuracy of 0".1 can be achieved using as short an integration distance as 300 km. The region covered by the control stations, in this test, was 600 km x 500 km. In a similar test, using a slightly larger region of 800 km x 800 km, the integration distance that provided a relative accuracy of approximately 0".1 was 400 km. Hence, it may be concluded that it is adequate to continue the integration out to approximately half the length of the side of the region covered by the control points. This appears to contradict the experience of Molodensky et al (1962) and Strange and Woollard (1964), who recommend that the integration be carried out to at least the distance between control stations. However, it should be remembered that their interpolation was one-dimensional and linear, while a two-dimensional

Figure 2.9

Variation in Deflection Values as a Function of Integration Distance

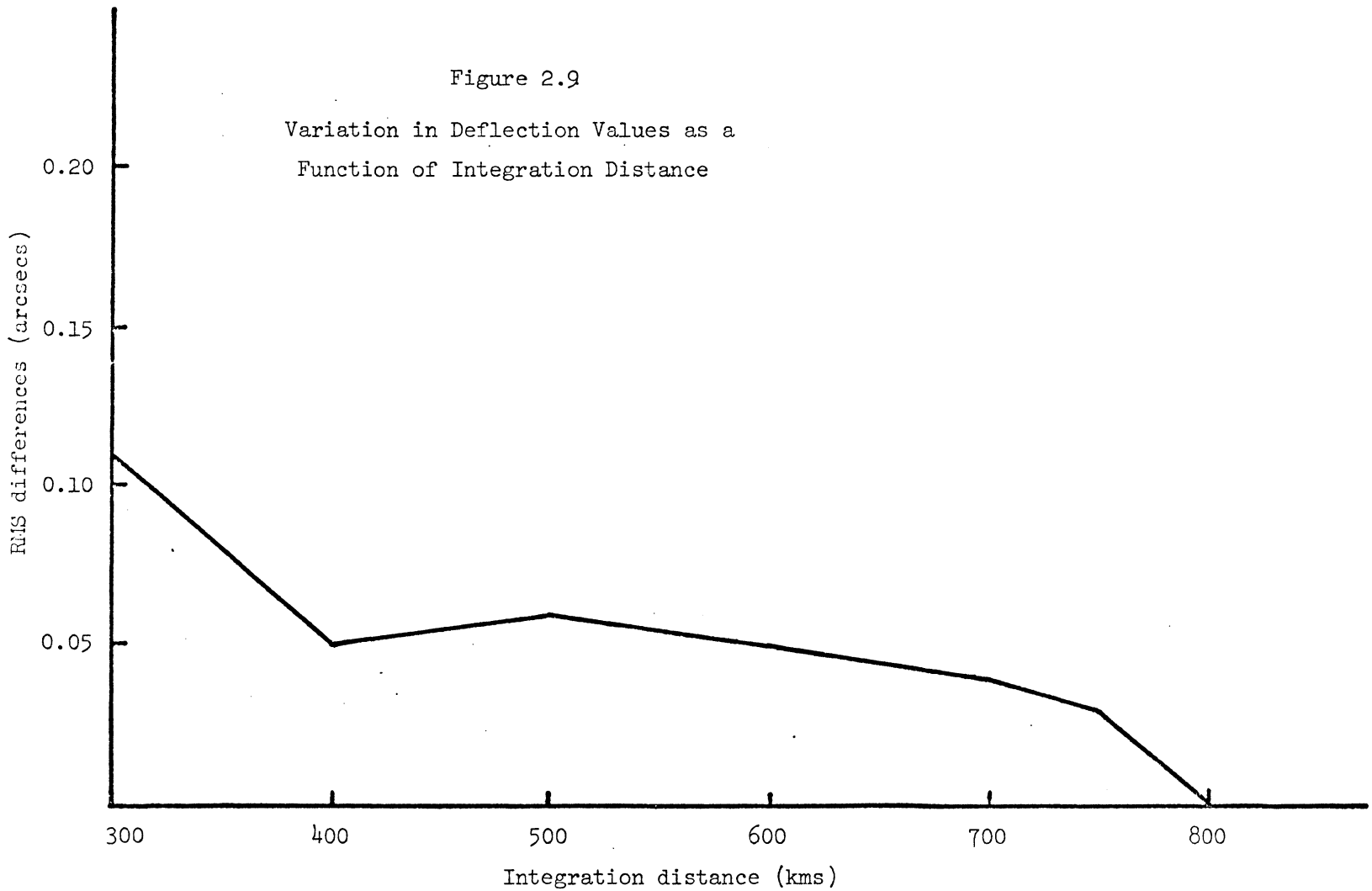

second order correction polynomial is used here. Based upon the foregoing, and erring on the cautious side, the outer zone limit has been set at 400 km for regions smaller than 800 km x 800 km, and at one-half the larger side, for larger regions.

2.53 Test results

In order to test the reliability of the procedure, astrogeodetic deflections were interpolated in a number of different areas:

(1) New Brunswick

(2) St. Lawrence River Valley

(3) Gaspé Peninsula

(4) Rocky Mountains.

The relative positions of these areas are indicated in Figure 2.10. In each area deflections were interpolated at points at which the astrogeodetic deflections had been previously observed. A comparison between the predicted and observed deflections was then made, and the results are summarised in Table 2.3. Table 2.3A gives the detailed comparisons.

(1) New Brunswick and the surrounding regions have the best astrogeodetic deflection coverage in Canada, and consequently there were a large number of control stations available for the interpolation. On the other hand, the gravity data is poorly distributed in this region and some gross errors in this data were detected, with possibly more errors remaining undetected. Therefore, it was not possible to predict deflections at as many deflection stations as had been expected. The RMS error is small (less than 2") but so are the deflections, so that the relative error is large. However, it is encouraging that the predominant upward slope of the geoid towards the east has been detected, and is

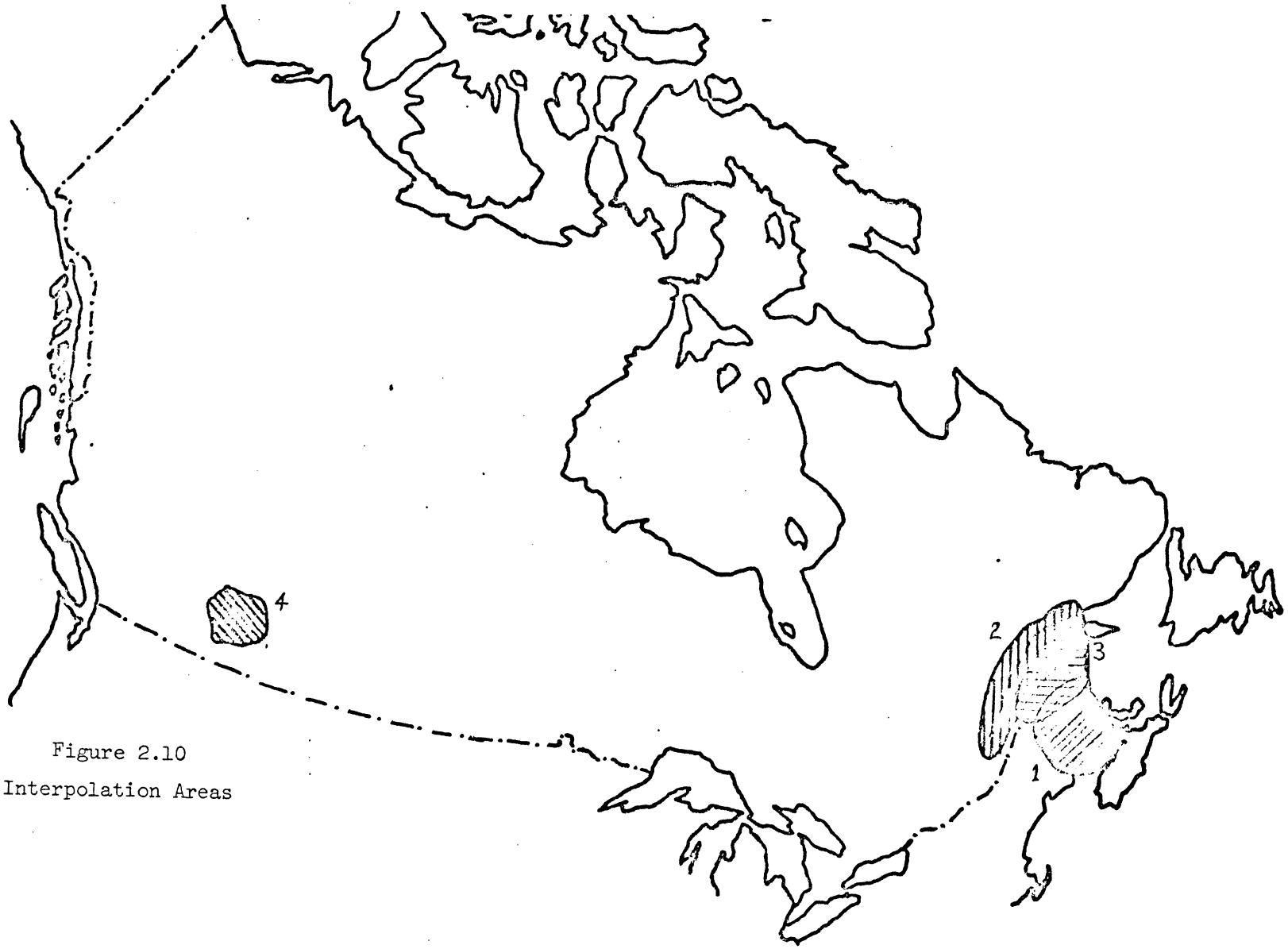

Figure 2.10
Interpolation Areas

evident in the predicted η - components. It should be noted that it is major features, such as this slope, which are more important in terms of correctly reducing observations from the surface of the earth (Meissl, 1973).

(2) In the St. Lawrence region, the gravity data suffers from the same poor distribution as in New Brunswick. Fewer deflection stations are available to provide control, and consequently the RMS errors are larger, as are the deflections themselves.

(3) In the Gaspé region, similar conditions as in the St. Lawrence valley apply, although more control stations are available. Several of the predicted deflection stations are common with those in the other two regions, so that a direct comparison of the predicted deflections may be made. Using three common points with the New Brunswick set, the RMS difference between the predicted values is 0".2. For the five common points with the St. Lawrence region, the RMS difference is 1".0. This difference is not insignificant and indicates that the predicted values are dependant, to some extent, upon the distribution of the particular control stations used. A possible reason for this dependance is that regionally systematic errors in the astrogeodetic deflections (due to network distortion, for example) are being modelled by the correction polynomials in each area.

(4) Rocky Mountains: Due to the nature of the terrain, gravity data is sparse, and concentrated in the valleys. It was only possible to predict deflections at two stations, one of which was extrapolated. Consequently, no conclusions can be based upon these scanty results.

2.54 Error evaluation

For the results obtained in this investigation, the predicted errors (obtained by propagation of errors through the mathematical models) have been smaller than the actual errors (Table 2.3). (The results in the Rockies are not considered here, as there is insufficient data for any meaningful comparison to be made.) In order to determine possible reasons for this, various possible correlations have been investigated.

Correlation of actual errors with:

(1) predicted errors,

(2) data point distribution in inner zone,

(3) topography.

The correlation has been determined in terms of correlation coefficients (Vaníček, 1973), where the correlation between the vectors $\underset{\sim}{x}$ and $\underset{\sim}{y}$ is given by:

$$\rho_{xy} = \frac{S_{xy}}{S_x \, S_y} \qquad 2.59$$

and

$$S_{xy} = \frac{1}{n} \sum_{i=1}^{n} \{(x_i - \bar{x})(y_i - \bar{y})\}$$

$$S_x^2 = \frac{1}{n} \sum_{i=1}^{n} (x_i - \bar{x}) \qquad 2.60$$

$$S_y^2 = \frac{1}{n} \sum_{i=1}^{n} (y_i - \bar{y})$$

where $\bar{x}$, $\bar{y}$ are the mean values of $\underset{\sim}{x}$, $\underset{\sim}{y}$:

Area	Component	Number of Stations	RMS Actual error	RMS Predicted Error	Maximum Error	RMS Predicted Deflection	Percentage Error
New Brunswick	ξ	17	1.17	0.64	-2.34	1.61	73
	η		1.52	0.67	+2.64	3.60	42
St. Lawrence	ξ	9	2.82	1.17	+5.16	7.43	38
	η		3.03	1.19	-5.06	5.43	56
Gaspé	ξ	13	3.25	0.76	+7.23	5.55	59
	η		2.16	0.79	-4.66	5.14	42
Rockies	ξ	2	0.29	7.34	+0.40	8.68	3
	η		0.22	4.12	+0.31	3.44	6

Table 2.3

Summary of Deflection Interpolation Results

Deflection File Number	Observed ξ''	Predicted ξ''	$\delta\xi''$	Observed η	Predicted η	$\delta\eta$
37	-0.2	+1.6	-1.8	-1.6	-1.8	+0.2
38	-2.4	-0.1	-2.3	+0.1	-0.3	+0.4
39	+2.6	+1.9	+0.7	+0.7	-1.9	+2.6
41	-2.2	-3.8	+1.6	-2.3	-4.0	+1.7
45	-1.4	-0.3	-1.1	-1.6	-3.8	+2.2
46	+0.1	-2.0	+2.1	-3.8	-1.8	-2.0
47	+1.4	+1.5	-0.1	-6.1	-7.6	+1.5
49	-1.4	-1.6	+0.2	-2.7	-3.9	+1.2
50	-0.2	-0.5	+0.3	-4.1	-4.8	+0.7
53	-2.0	-1.0	-1.0	-2.9	-5.0	+2.1
56	-0.3	+0.9	-1.2	-1.0	-0.8	-0.2
57	-1.2	-2.9	+1.7	-4.0	-5.5	+1.5
58	-0.1	-1.0	+0.9	-0.1	-1.5	+1.4
59	-0.4	+0.4	-0.8	-0.8	-3.1	+2.3
61	+0.1	+0.1	0.0	+0.8	+1.5	-0.7
62	-0.6	-0.3	-0.3	-0.8	-1.4	+0.6
64	+3.2	+2.8	+0.4	-3.8	-2.5	-1.3
70	-0.5	-1.5	+1.0	-4.6	-2.6	-2.0
72	+3.2	+0.6	+2.6	-7.5	-6.7	-0.8
75	+3.9	+2.7	+1.2	+7.3	+4.9	+2.4
79	-5.9	-4.6	-1.3	+1.9	+0.8	+1.1
80	+13.9	+9.5	+4.2	-12.5	-8.6	-3.9
84	+3.1	+3.8	-0.7	-4.6	-5.3	+0.7
85	+17.0	+12.1	+4.9	+3.9	+2.2	+1.7
98	-4.6	-9.8	+5.2	+6.2	+4.4	+1.8
111	+8.8	+6.5	+2.3	-9.7	-8.9	-0.8
114	+8.7	+9.4	-0.7	-7.5	-2.3	-5.2
119	-8.2	-4.7	-3.5	-0.9	-0.2	-0.7
120	-0.3	-1.5	+1.2	+1.7	+1.0	+0.7
123	-4.8	-0.5	-4.3	-4.4	-4.6	+0.2
501	+6.8	+6.4	+0.4	-3.8	-4.1	+0.3
740	+10.4	+10.5	-0.1	-2.9	-3.0	+0.1
9574	+14.1	+7.0	+7.1	-13.6	-8.9	-4.7

Table 2.3A

Deflection Prediction Results - Comparison with Observed Values.

$$\bar{x} = \frac{1}{n} \sum_{i=1}^{n} x_i$$

$$\bar{y} = \frac{1}{n} \sum_{i=1}^{n} y_i \qquad 2.61$$

ρ_{xy} can vary from -1 to 1 with zero indicating complete independance.

The degree of correlation may be measured using the criteria (Vaníček and Hamilton, 1972):

$1 \geq \lvert\rho_{xy}\rvert > 0.85$	strong correlation
$0.85 \geq \lvert\rho_{xy}\rvert > 0.40$	correlation
$0.40 \geq \lvert\rho_{xy}\rvert > \lambda$	weak correlation
$\lambda \geq \lvert\rho_{xy}\rvert$	no correlation

where:

$$\lambda = \sqrt{\left(\frac{1 - \rho_{xy}^{2}}{n-2}\right)} \qquad 2.62$$

and n is the number of elements involved in the testing.

The error correlations have been determined in each of the three Eastern Canadian areas investigated, and the coefficients are indicated in Table 2.4. The column headings have the following meanings:

1a: correlation with predicted error in ξ

1b: correlation with predicted error in η

2 : correlation with number of data points in inner zone

3 : correlation with topography roughness.

There is some correlation of the actual errors with the predicted errors, but not sufficient to indicate that a simple scaling of the predicted errors would solve the problem.

Area	1a	1b	2	3
New Brunswick	+0.26	+0.29	+0.08	+0.52
St. Lawrence Valley	+0.12	+0.32	+0.25	+0.20
Gaspé	+0.43	+0.58	-0.20	+0.45
Average	+0.27	+0.40	+0.04	+0.39

Table 2.4

Error Correlations

1a - with predicted error in ξ

1b - with predicted error in η

2 - with number of data points in inner zone

3 - with topography roughness

It had been thought that the small number of gravity stations in the immediate vicinity of the computation point would produce significant errors. This would show as a strong negative correlation in column 2, but this is not the case. It appears that the checks for adequacy of data, incorporated in the programme for gravimetric deflections, have eliminated this factor as a source of error.

The correlation with roughness of topography, although weak by the criterion established above, does require explanation. The roughness of topography is indicated by a factor t, determined as follows:

$$t = \frac{\sum_{i=1}^{n} (\bar{H} - H_i)^2}{n} \qquad 2.63$$

where H_i are the heights (in feet) of the n measured gravity anomalies in the inner zone, and $\bar{H}$ is the mean of H_i:

$$\bar{H} = \frac{1}{n} \sum_{i=1}^{n} H_i \qquad 2.64$$

The reliability of t as an indicator of the roughness of topography (within 30 km of the computation point) will depend upon the number and distribution of the gravity anomalies in the inner zone. A large value for t indicates rough terrain, while a small value indicates the converse. The correlation with terrain roughness should indicate the effect of plumbline curvature, as it is in mountainous terrain that plumbline curvature reaches extreme values (Kobold and Hunziker, 1962). It should be remembered that the free air anomalies, used to compute the modified gravimetric deflections, are themselves highly correlated with elevation (Uotila, 1960), so that the correlation with t may be due, in part, to the influence of this correlation.

Besides the numerical correlations described above, other correlations may be determined by examining the error vectors shown in Figure 2.11. The error vectors appear to be randomly distributed over the region, so that they do not seem to be a function of position. However, in the Gaspé and St. Lawrence areas, the direction of the error vectors is similar to the direction of the actual deflections. As this direction is exclusively away from the land masses towards the open water, it may be concluded that the effect of topography on the observed astro-geodetic deflections (i.e. plumbline curvature) has not been modelled by the prediction technique. In this same area, the distribution of gravity data in the inner zones is generally poorer (see Figures 2.12 and 2.13) than in New Brunswick. This seems to indicate that the elementary procedures for checking the distribution of data (described in section 2.34) are inadequate. However, this type of distribution of gravity data (along main roads and railways) is restricted to parts of Eastern Canada and British Columbia. In the remainder of the country the data is distributed on a more uniform grid, better suited to the needs of this kind of investigation (Nagy, 1973).

None of the above described correlations is strong enough to be used as a basis for a model modifying the predicted errors to correspond better with the actual errors. It appears, therefore, that the attempt to reliably predict the error of a predicted deflection is unsuccessful. However, these predicted deflections can be used for computing geoidal heights, provided they are weighted correctly relative to the observed deflections. The predicted standard deviations cannot be used to determine the weights, as they are too optimistic. However, there is a significant correlation between the RMS actual errors and the RMS predicted

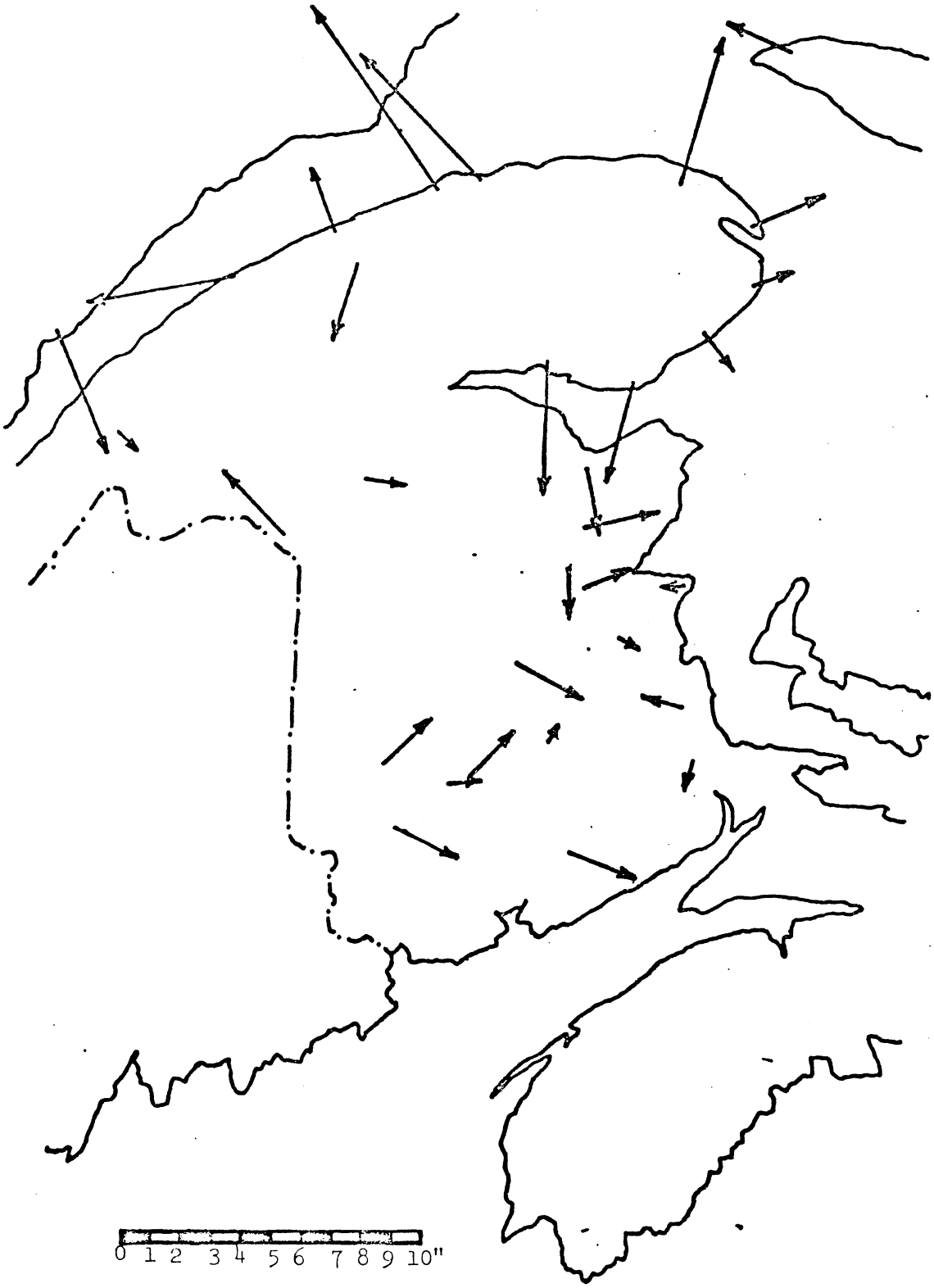

Figure 2.11

Error Vectors (Observed-predicted)

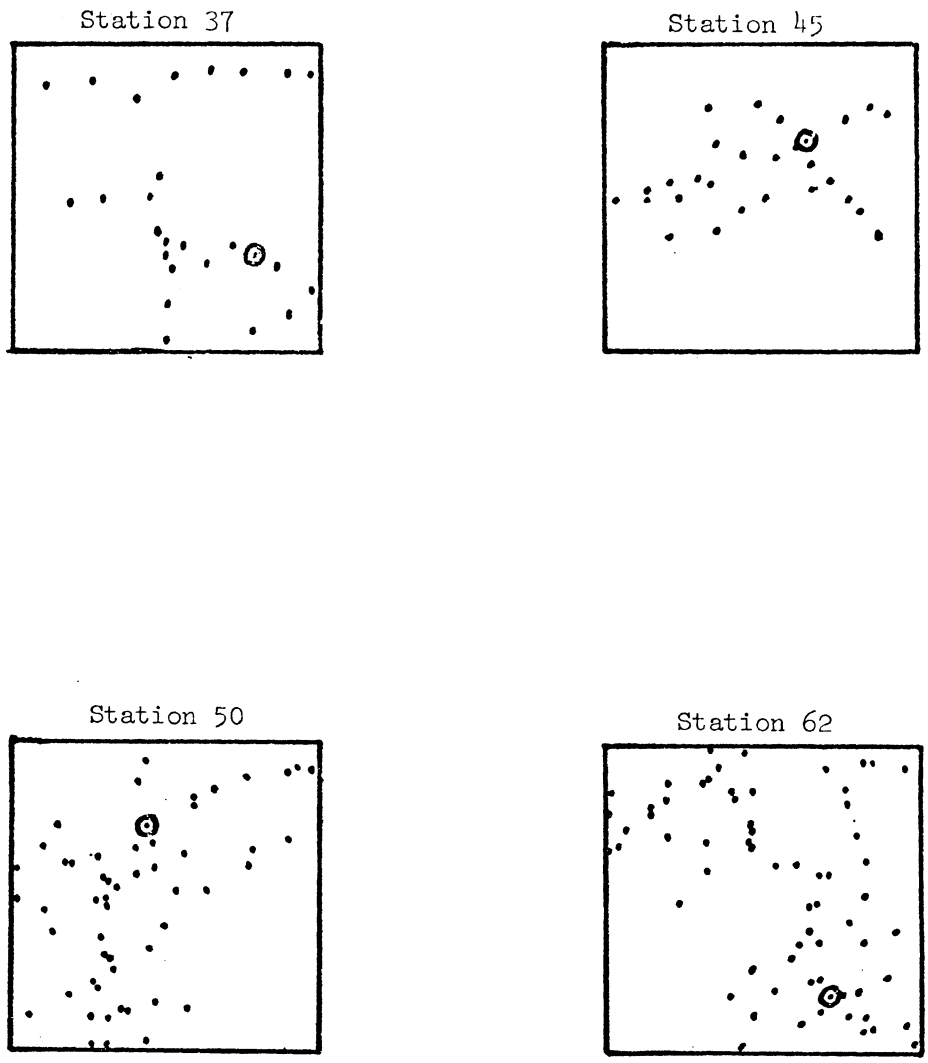

Figure 2.12

Distribution of Gravity Data - New Brunswick

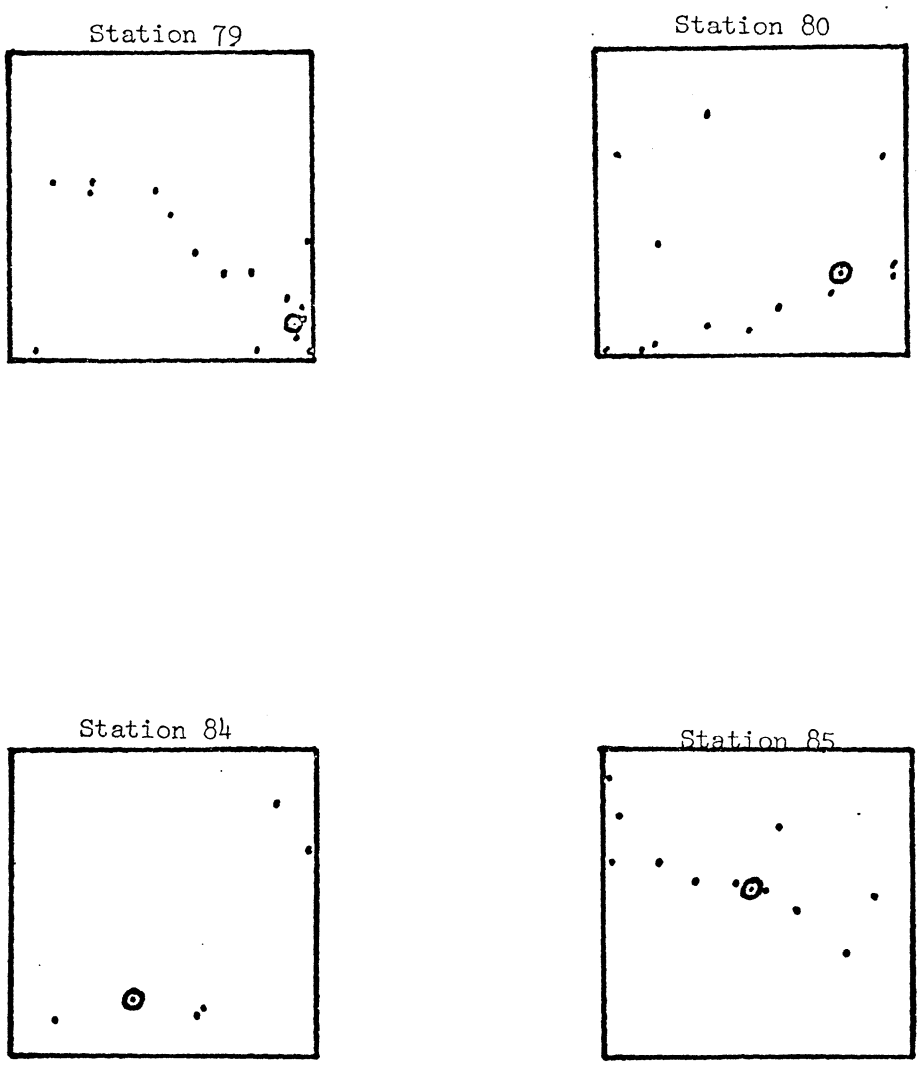

Figure 2-13

Distribution of Gravity Data - Gaspé and St. Lawrence

deflections, for each region (Figure 2.14). A model that does suggest itself is:

$$\text{RMS actual error} = 0''.6 + 0.3\ (\text{RMS predicted deflection}) \qquad 2.65$$

In order to obtain more realistic predicted standard deviations (on the average), the following procedure may be used: All the predicted standard deviations are multiplied by a scale factor, S, given by:

$$S = \frac{\text{"RMS actual error"}}{\text{RMS predicted error}} \qquad 2.66$$

where the "RMS actual error" is given by equation 2.65 and the RMS predicted error is computed from the individual predicted errors, derived using equation 2.58. There will be a separate scale factor for each of σ_ξ, σ_η.

During the course of this study, several gross errors in the point gravity data in Eastern Canada were found. Removal of these incorrect values from the data set resulted in the predicted deflection value at one point changing by 3", to better agree with the observed value, and in other deflection values changing by smaller amounts. Other errors in the data set are known to exist (R.J. Buck, pers. comm., 1974), and correction of these may further improve the results.

In summary, errors in the predicted deflections are due to a combination of:

(1) Errors (and blunders) in the original gravity data.

(2) Inadequate modelling of the gravity field.

(3) Poor distribution of gravity data.

(4) Poor distribution of deflection control stations.

(5) Non-correction of observed deflections for plumbline curvature.

(6) Systematic errors in geodetic co-ordinates.

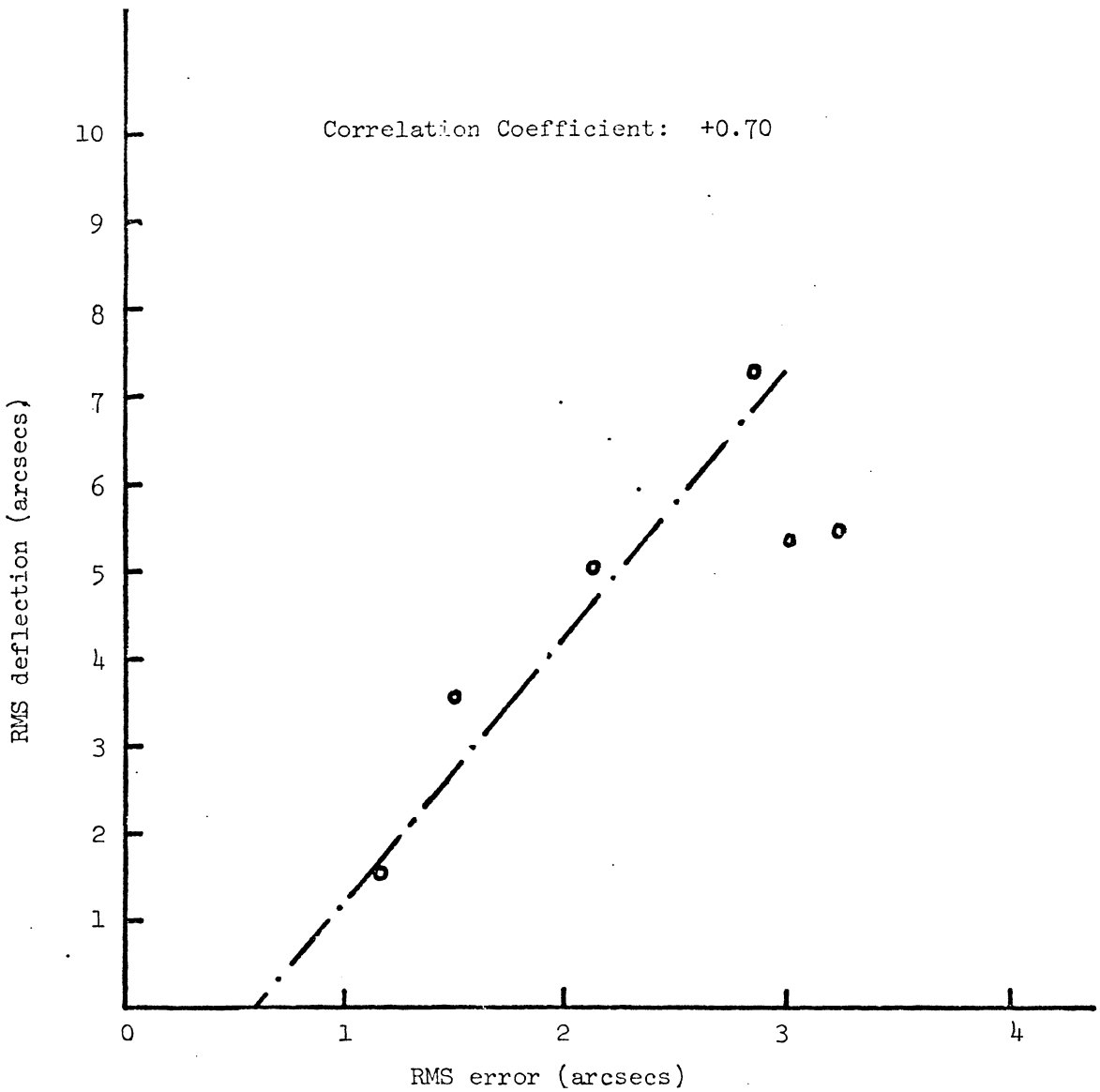

Figure 2.14

RMS Error as a Function of RMS Deflection

Of these, only random errors in the original gravity data, and the effects of the poor control station distribution have been modelled. Consequently, the predicted standard deviations are optimistic and need scaling before being used in combination with observed astrogeodetic deflections of the vertical.

CHAPTER 3

GEOID COMPUTATION

3.1 Survey of Computational Methods

The most commonly used method is that employing Helmert's formula (Heiskanen and Moritz, 1967):

$$N_i = N_{i-1} - \int_{i-1}^{i} (\xi\cos\alpha + \eta\sin\alpha)ds \qquad 3.1$$

where N_i is the geoidal height of the ith station, ξ, η are the deflection components in the meridian and prime vertical, and α is the azimuth of the line connecting the two stations, i-1 and i. In practice, this formula is replaced by:

$$N_i = N_{i-1} - \frac{(\xi_i + \xi_{i-1})\cos\alpha + (\eta_i + \eta_{i-1})\sin\alpha}{2} s \qquad 3.2$$

where ξ_i, η_i and ξ_{i-1}, η_{i-1} are measured at the stations i and i-1, and s is the distance between them.

Variations based upon this technique have been developed by Ney (1955), Rice (1962), Fischer et al (1967), and Lachapelle (1973). These variations all make the initial assumption that the geoid varies linearly between adjacent deflection stations, no matter how far apart these stations may be.

Recently, more sophisticated techniques have been applied to geoid determinations in West Germany and Denmark (Heitz and Tscherning, 1972), based respectively upon the autocorrelation of geoidal heights,

and upon the cross-correlation between geoidal heights and deflections of the vertical. The second of these methods assumes the deflections to be errorless and hence the geoid is made to fit exactly to all the deflections. This results in a large system of equations (as many equations as unknowns) which may be impracticable to solve. The method of Heitz (1969), using an empirical autocorrelation function, requires a system of equations of half the size (as many equations as deflection stations). It would be practicable to use this technique in smaller countries, such as Germany, but impracticable in many other countries, where large numbers of deflections are available.

3.2 The Surface-Fitting Technique

3.21 Model using deflections

This approach was developed at the University of New Brunswick in 1972 and reported in Vaníček and Merry (1973). A two-dimensional polynomial of nth order is used to represent the geoid. The coefficients of this polynomial are determined using a least-squares approximation, in which the quantity to be minimised is the sum of the squares of the weighted discrepancies between the slope of this mathematical surface, given by the derivatives of the polynomial in two orthogonal directions, and the slope of the physical surface of the geoid, given by the two components of the deflection of the vertical. The procedure is then nothing more than fitting a mathematically defined surface to a field of vectors in such a way that the directions of the normals to this surface fit best (in the least squares sense) to the directions of the vectors.

As with all the astrogeodetic techniques only relative geoidal heights may be determined, and some initial height (usually at the initial

point of the horizontal control networks) must be defined.

The development of this model has been described in detail in Vaníček and Merry (1973), but, for the sake of completeness, is re-developed here.

The geoidal height $N(x,y)$ at a point (x,y) may be approximated by the polynomial:

$$P_n(x,y) = \sum_{\substack{i=0 \\ j=0}}^{n} C_{ij}\, x^i y^j \doteq N(x,y) \qquad 3.3$$

The co-ordinates (x,y) may be determined from the geodetic quantities, using the simple transformation:

$$\begin{aligned} x &= R(\phi - \phi_o) \\ y &= R(\lambda - \lambda_o)\cos\phi \end{aligned} \qquad 3.4$$

where (ϕ, λ) are the geodetic latitude and longitude of the point, (ϕ_o, λ_o) are the co-ordinates of an arbitrary origin, and R is a mean radius of curvature of the earth.

The slope of the geoid, with respect to the geodetic reference ellipsoid, is given by the astrogeodetic deflection of the vertical at the geoid. Hence the following equations are valid, for small deflections:

$$\begin{aligned} \frac{\partial P_n}{\partial x} &\doteq \frac{\partial N}{\partial x} = -\tan\xi \doteq -\xi \\ \frac{\partial P_n}{\partial y} &\doteq \frac{\partial N}{\partial y} = -\tan\eta \doteq -\eta \end{aligned} \qquad 3.5$$

Denoting $\frac{\partial P_n}{\partial x}$ and $\frac{\partial P_n}{\partial y}$ by P_{nx} and P_{ny}, respectively, the least squares criterion requires that the following expressions be a minimum:

$$\begin{aligned} \rho_x^2 &= \sum_{\ell} [P_{nx}(x_\ell, y_\ell) + \xi_\ell]^2 \\ \rho_y^2 &= \sum_{\ell} [P_{ny}(x_\ell, y_\ell) + \eta_\ell]^2 \end{aligned} \qquad 3.6$$

where $\sum_{\ell}$ implies the summation over all the involved deflection stations. The partial derivatives are evaluated from the formulae:

$$P_{nx}(x_\ell, y_\ell) = \sum_{\substack{i,j=0 \\ i+j\neq 0}}^{n} C_{ij} i x^{i-1} y^j = \sum_{i,j}' C_{ij} i x^{i-1} y^j$$

$$P_{ny}(x_\ell, y_\ell) = \sum_{i,j}' C_{ij} j x^i y^{j-1} \qquad 3.7$$

with the understanding that, whenever a negative exponent is encountered in the summations, the term should be replaced by zero. The conditions for a minimum can be written as:

$$\frac{\partial \rho_x^2}{\partial C_{ij}} = 0$$

$$\text{for } i,j=0,\ldots,n \qquad 3.8$$

$$\frac{\partial \rho_y^2}{\partial C_{ij}} = 0$$

then:

$$\frac{\partial \rho_x^2}{\partial C_{ij}} = 2 \sum_{\ell} [(P_{nx} + \xi_\ell)\, i x^{i-1} y^j] = 0 \qquad 3.9$$

or:

$$\sum_{\ell} [(\sum_{s,r}' C_{sr} s\, x^{s-1} y^r + \xi_\ell) i x^{i-1} y^j] = 0 \qquad \text{for } \begin{matrix} i=1,\ldots,n \\ j=0,\ldots,n \end{matrix} \qquad 3.10$$

Re-arranging the last equation and using scalar product notation:

$$\langle \sum_{s,r}' C_{sr} s x^{s-1} y^r i x^{i-1}, y^j \rangle = - \langle \xi, i x^{i-1} y^j \rangle \qquad 3.11$$

or

$$i \sum_{s,r}' [C_{sr} s \langle x^{s+i-2}, y^{r+j} \rangle] = - i \langle \xi, x^{i-1} y^j \rangle \qquad 3.12$$

$$\text{for } i=1,\ldots,n;\ j=0,\ldots,n$$

Similarly, for the y-component:

$$j \sum_{s,r}' [C_{sr} r \langle x^{s+i}, y^{r+j-2} \rangle] = - j \langle \eta, x^i y^{j-1} \rangle \qquad 3.13$$

$$\text{for } i=0,\ldots,n;\ j=1,\ldots,n$$

Since both equations have to be satisfied at the same time we have:

$$\sum_{s,r}' [C_{sr}(is \langle x^{s+i-2}, y^{r+j} \rangle + jr \langle x^{s+i}, y^{r+j-2} \rangle)] =$$

$$= - i \langle \xi, x^{i-1} y^j \rangle - j \langle \eta, x^i y^{j-1} \rangle \qquad 3.14$$

Considering different weights $w_\xi(x_\ell, y_\ell)$ and $w_\eta(x_\ell, y_\ell)$ for the quantities ξ, and η, leads to the expression:

$$\sum_{s,r}' [C_{sr}(is \langle w_\xi x^{s+i-2}, y^{r+j} \rangle + jr \langle w_\eta x^{s+i}, y^{r+j-2} \rangle)] =$$

$$= - i \langle w_\xi \xi, x^{i-1} y^j \rangle - j \langle w_\eta \eta, x^i y^{j-1} \rangle$$

$$\text{for } i,j = 0,\ldots,n;\ i+j \neq 0 \qquad 3.15$$

The above system of equations may be written in matrix notation as:

$$A \underset{\sim}{b} = \underset{\sim}{u} \qquad 3.16$$

where the elements of matrix A are given by:

$$a_{km} = is \langle w_\xi x^{s+i-2}, y^{r+j} \rangle + jr \langle w_\eta x^{s+i}, y^{r+j-2} \rangle ; \qquad 3.17$$

the elements of vector $\underset{\sim}{b}$ are the unknown coefficients C_{sr}:

$$b_m = C_{sr} \qquad 3.18$$

and vector $\underset{\sim}{u}$ consists of:

$$u_k = - i \langle w_\xi \xi, x^{i-1} y^j \rangle - j \langle w_\eta \eta, x^i y^{j-1} \rangle \qquad 3.19$$

where:

$$i,j,r,s,=0,\ldots,n;\ i+j \neq 0;\ r+s \neq 0 ,$$

$$k=i+j+ni;\ m=s+r+ns .$$

The unknown coefficients C_{sr} are then obtained from:

$$\underset{\sim}{b} = A^{-1} \underset{\sim}{u} \qquad 3.20$$

since A is positive-definite and can always be inverted, provided that

$$2\ell \geq (n + 1)^2 - 1 \qquad 3.21$$

The weights used are inversely proportional to the estimated a priori variances of the observations, i.e.

$$\begin{aligned} w_\xi &= \sigma_\xi^{-2} A \,, \\ w_\eta &= \sigma_\eta^{-2} A \,, \end{aligned} \qquad 3.22$$

for the observed astrogeodetic deflections, where $\sigma_\xi A$ and $\sigma_\eta A$ are given by equation 2.43, and:

$$\begin{aligned} w_\xi &= (s\sigma_{\tilde{\xi}} A)^{-2} \\ w_\eta &= (s\sigma_{\tilde{\eta}} A)^{-2} \end{aligned} \qquad 3.23$$

for the predicted astrogeodetic deflections where $\sigma_{\tilde{\xi}} A$, $\sigma_{\tilde{\eta}} A$ are determined from equation 2.58, and s from equation 2.66.

The error covariance matrix of the coefficients is found from:

$$\Sigma_b = \sigma_o^2 \, A^{-1} \qquad 3.24$$

where

$$\sigma_o^2 = \frac{\sum_\ell \left[w_\xi (P_{nx} + \xi)^2 + w_\eta (P_{ny} + \eta)^2 \right]}{2\ell - (n + 1)^2 + 1} \qquad 3.25$$

The error covariance matrix, $\Sigma_{\hat{N}}$, for any vector of q estimated geoidal heights, $\hat{\underset{\sim}{N}} = \underset{\sim}{P}_n = (P_n(x_1,y_1),\ldots,P_n(x_q,y_q))$, can be derived as follows. Each $P_n(x_i,y_i)$ is a linear combination of the coefficients, $\underset{\sim}{b}$:

$$\hat{\underset{\sim}{N}} = B_N \, \underset{\sim}{b} \qquad 3.26$$

where B_N is a q x $((n+1)^2-1)$ matrix of mixed algebraic functions. Then the error covariance matrix, applying the law of propagation of covariance, is given by:

$$\Sigma_{\tilde{N}} = B_N \, \Sigma_b \, B_N^T \qquad 3.27$$

3.22 Model using deflections and geoidal heights

This model is an extension of the model described above, in that geoidal heights may be included as additional observations (or weighted constraints) in the solution for the polynomial coefficients. There are two reasons for developing this particular model:

(1) The model of section 3.21 produces a somewhat smoothed version (because of practical limitations on the number of coefficients) of the geoid when it is used over large areas, containing large amounts of deflection data. This smoothed version can serve as a basis for local geoid computations (showing greater detail) in areas where there are sufficient deflections.

(2) There exists the possibility that satellite data may provide geoidal heights to serve as constraints on the solution. The procedure would be as follows:

The satellite determined $(x, y, z)_s$ co-ordinates of a point in a geocentric system are transformed to geodetic $(x, y, z)_G$ co-ordinates, through the relationship:

$$\begin{bmatrix} x \\ y \\ z \end{bmatrix}_G = R \begin{bmatrix} x \\ y \\ z \end{bmatrix}_s + \begin{bmatrix} x_o \\ y_o \\ z_o \end{bmatrix}_G \qquad 3.28$$

where R is an elementary rotation matrix, rotating the geocentric

co-ordinate system parallel to the geodetic, and (x_o, y_o, z_o) are the co-ordinates of the origin of the geocentric system, in the geodetic system (translation components). A scale change between the co-ordinate systems may also be included here.

The ellipsoidal geodetic co-ordinates (ϕ, λ, h) may be obtained via the equations 1.1. Provided the height of the point above the geoid, H, is known (from spirit levelling, for example), then the geoidal height is given by:

$$N \doteq h - H \qquad 3.29$$

It should be noted that the $(x, y, z)_s$ co-ordinates are not the only satellite information that could be used. For example, the satellite geoid could be transformed to geoidal heights related to the geodetic system by means of the differential equation developed in Merry and Vaníček (1974b). These geoidal heights could then be used as constraints.

Both procedures mentioned above are not independant of an initial knowledge of the geoidal heights (referred to the geodetic system), as the rotation and translation components can only be found if several geoidal heights are already known. The procedure could be made iterative, as geoidal heights near the geodetic initial point may be used to determine these transformation parameters, which can then be used, as outlined above, in regions distant from the initial point.

In order to include geoidal heights as constraints, the model of section 3.21 needs to be expanded in the following way:

At the k points at which geoidal heights are known:

$$P_n(x,y) = \sum_{i,j=0}^{n} C_{ij} x^i y^j \doteq N(x,y) \qquad 3.30$$

In matrix notation:

$$D \underset{\sim}{b} = \underset{\sim}{N} + \underset{\sim}{V} \qquad 3.31$$

Considering correlated geoidal heights, the least squares criterion is that:

$$\rho_N^2 = \underset{\sim}{V}^T P \underset{\sim}{V} \qquad 3.32$$

is a minimum, where P is a correlated weight matrix. It has been shown (e.g. Wells and Krakiwsky, 1971) that for equations of the type of 3.31, this criterion is satisfied by the equation:

$$D^T P D \underset{\sim}{b} = D^T P \underset{\sim}{N} \qquad 3.33$$

This equation is of the same dimension as equation 3.16, and they may be added together:

$$D^T P D \underset{\sim}{b} + A \underset{\sim}{b} = D^T P \underset{\sim}{N} + \underset{\sim}{u} \qquad 3.34$$

The solution for the coefficients is then:

$$\underset{\sim}{b} = (D^T P D + A)^{-1}(D^T P \underset{\sim}{N} + \underset{\sim}{u}) \qquad 3.35$$

The components of $\underset{\sim}{b}$, A, and $\underset{\sim}{u}$ are as described in the previous section. The correlated weight matrix P is given by:

$$P = \Sigma_N^{-1} \qquad 3.36$$

i.e. the inverse of the error covariance matrix of the geoidal heights. This error covariance matrix may be obtained from a prior solution for the geoidal heights. The error covariance matrix for the coefficients is given by:

$$\Sigma_b = \sigma_o^2 (D^T P D + A)^{-1} \qquad 3.37$$

where

$$\sigma_o^2 = \frac{\underset{\sim}{V}^T P \underset{\sim}{V} + \sum_{\ell} [w_\xi (P_{nx} + \xi)^2 + w_\eta (P_{ny} + \eta)^2]}{k + 2\ell - (n + 1)^2} \qquad 3.38$$

The error covariance matrix of a string of geoidal heights may be obtained from Σ_b as described in section 3.21.

3.3 Evaluation

3.31 Preliminary testing

The variance factor, σ_o^2, computed through equation 3.25, is an indicator both of the reliability of the initial standard deviations used, and of the completeness of the mathematical model. A variance factor of 1 implies that the initial accuracy estimates were correct, and that the mathematical model is complete (Wells and Krakiwsky, 1971). In the least squares approximation, the mathematical model is not necessarily complete, but the variance factor may still be used to determine the optimum number of polynomial coefficients, in the following way.

By increasing the number of coefficients, the variance factor should decrease, as the model fits the observations better. After a certain number of coefficients are used, a further increase may bring about little change in the variance factor, and hence in the accuracy of the results. This number of coefficients would then be the minimum number that should be used. If, at this stage, $\sigma_o^2 < 1$, then the implication is that the observations are, on average, too pessimistically weighted. The converse is true if $\sigma_o^2 > 1$. It should, however, be remembered that, as the number of coefficients approaches the number of observations, σ_o^2 tends to zero, no matter how the observations are weighted. Hence, the above inequalities may not be too reliable as guidelines.

The variance factor, σ_o^2, as a function of the number of coefficients used for different geoid computations, is shown in Figure 3.1.

Figure 3.1

Variance Factor as a Function of Variation in Polynomial Coefficients

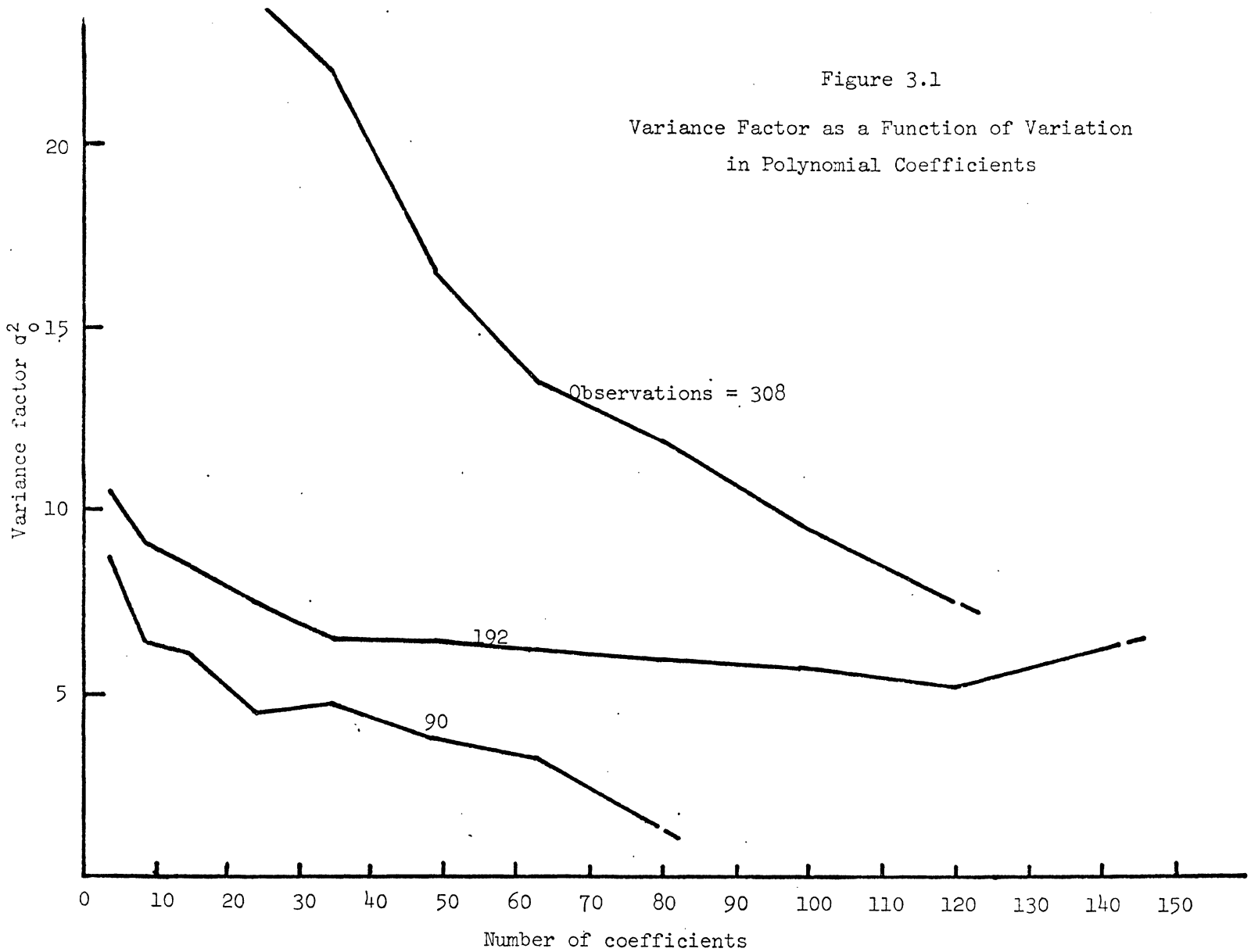

From two of these results, it appears that the optimum number of coefficients is around 30, but this number will increase (as may be expected) with an increasing number of observations. The value of σ_0^2 for this optimum is approximately 6 and, ideally, the number of coefficients (for any computation) should be increased until a variance factor of this order is obtained. Practical problems may not make this possible, as accumulated round-off errors in the computer solution limit the number of coefficients that may be obtained. The value of 6 for the variance factor indicates that the observations have been too optimistically weighted. The reasons for this have been discussed in section 2.42.

3.32 Geoid comparisons

To verify the correctness of the program for this technique, a comparison with the conventional technique, over a limited area, was made using data supplied by the National Geodetic Survey (Rice, personal comm., 1973). Test data at 41 stations on a regular grid inside a 1° x 1° square in Iowa was used, and the results compared to those of Rice (1965). Using 48 coefficients the maximum difference in relative geoidal height was 0.3 m (corresponding to 10% of the actual value). This initial test showed that satisfactory results could be obtained with this method, and further evaluations were performed. These involved computing geoids for different regions of North America and comparing them against other published values (Vaníček and Merry, 1973).

Since the publication of the above paper, considerably more data has become available and a revised astrogeodetic geoidal height chart for North America has been prepared (Figure 3.2). This chart is based upon deflections observed at 3923 points in the U.S.A. and Canada, in the years

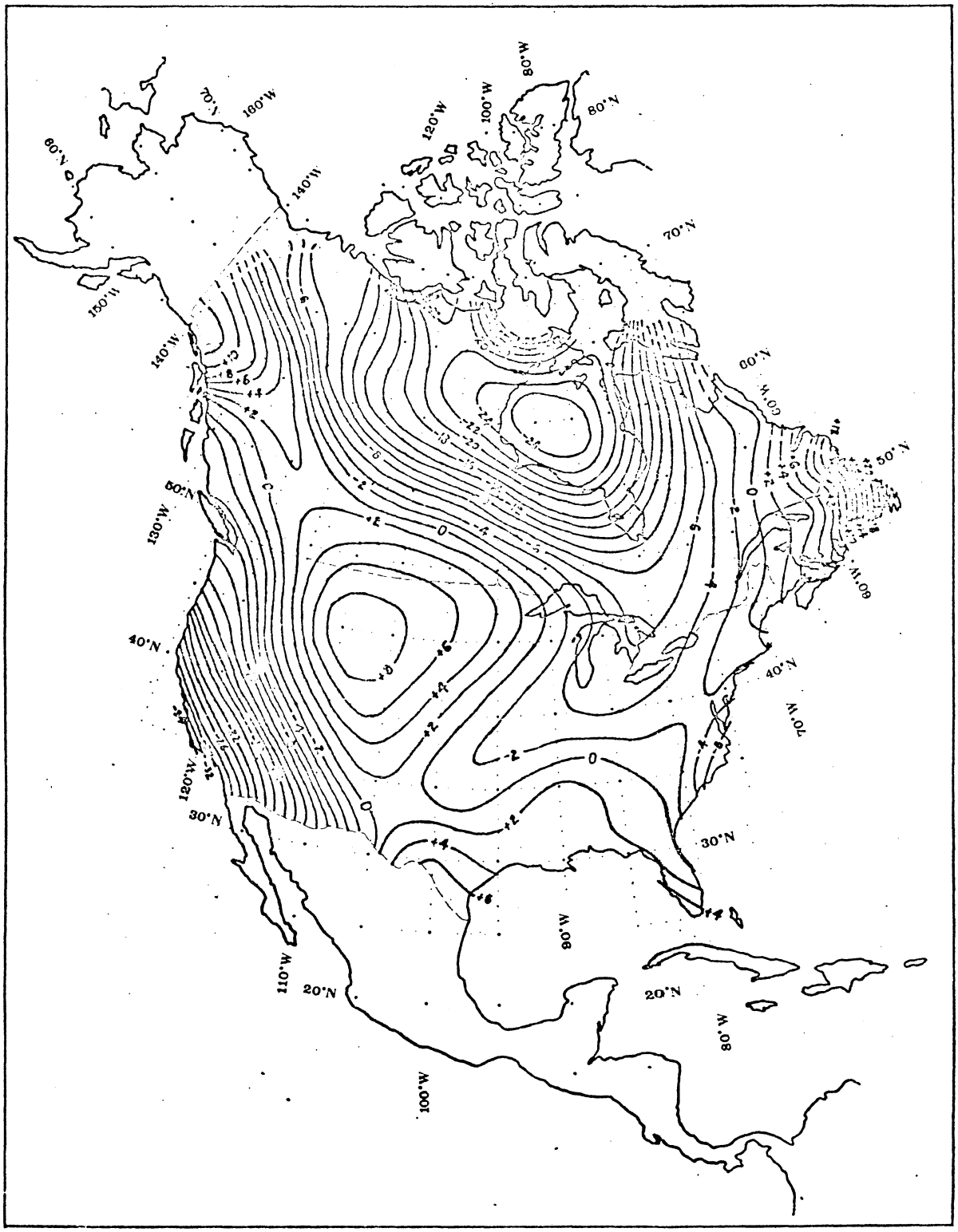

Figure 3.2

UNB74-1 Astrogeodetic Geoid in North America

144 Coefficients 2 metre Contours

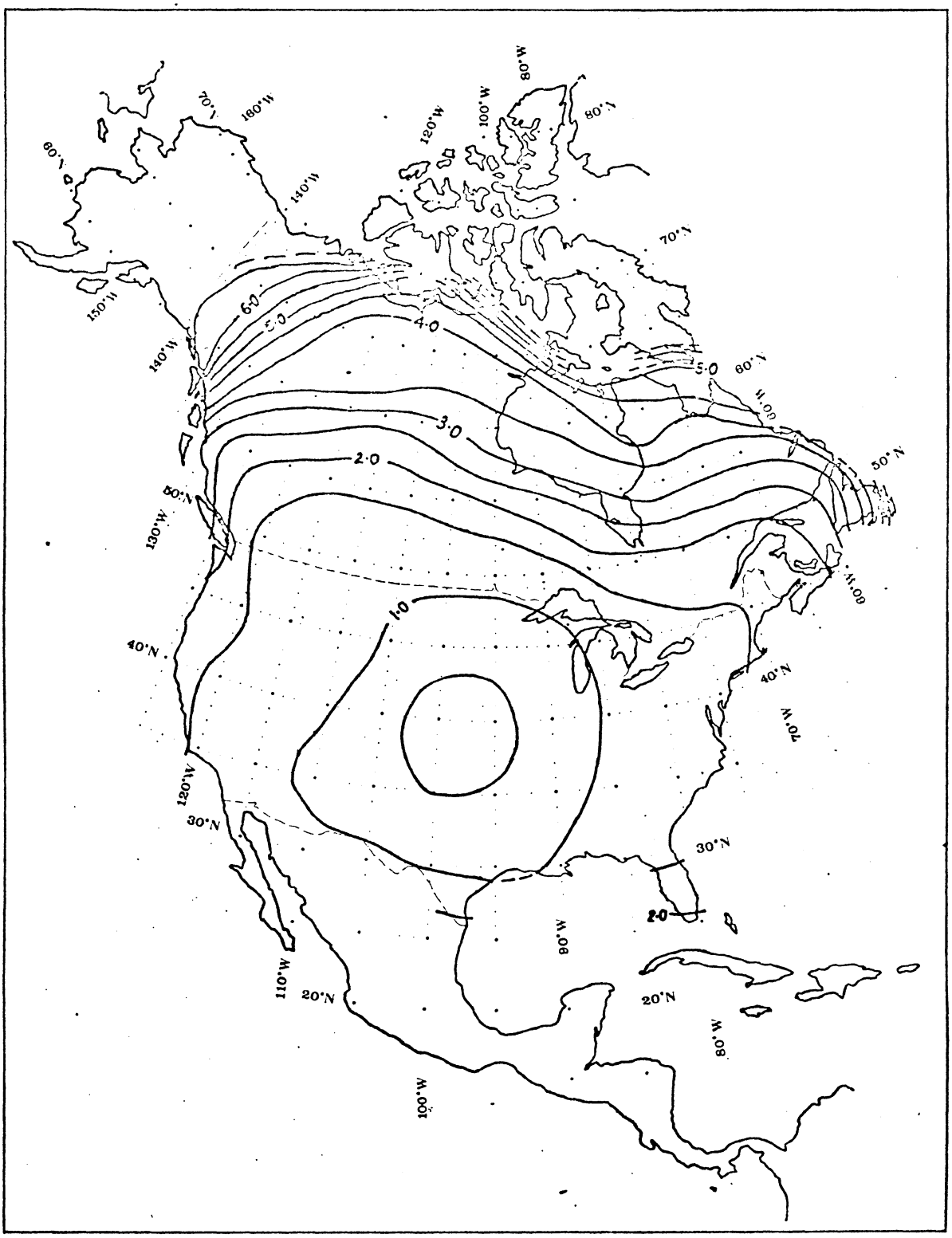

Figure 3.3

UNB74-1 Estimated Standard Deviations

0.5 metre Contours

up to, and including, 1972. It does not use the scattered deflections in Alaska, Mexico and on Ellesmere Island. Besides serving as an update of the chart in Vaníček and Merry (1973), it also has a number of other uses, relevant to this thesis. It serves as a basis for the geoidal height constraints used in section 3.35, and is also a means of evaluating the success of the surface-fitting procedure in a continental context. This evaluation has been performed by comparing the geoid obtained here (denoted UNB74-1) with three other available geoids. These are:

(1) Army Map Service geoid chart of North America (Fischer et al, 1967) - denoted AMS67.

(2) National Geodetic Survey geoidal heights in the U.S.A. (D.A. Rice, pers. comm., 1973) - denoted NGS73.

(3) Computer Sciences Corporation/Goddard Space Flight Centre combined satellite-gravimetric geoid of North America (Vincent et al, 1972) - denoted GSFC72.

Before these comparisons are described, one other note may be made. The estimated standard deviations of the geoidal heights obtained in the UNB74-1 solution (Figure 3.3) serve as an indicator of areas of weakness in the astrogeodetic deflection coverage. In the U.S.A. the weakest areas appear to be in Southern Florida and the State of Washington. In Canada the deflection coverage is only adequate in the southern parts of the Western and Central provinces and in the Maritime provinces. There also appears to be an area of reasonable coverage north of the 60th parallel, west of Hudson Bay. In other areas the deflections are sparsely distributed, especially in the Yukon, portions of the Northwest Territories, the coast of Labrador and the island of Newfoundland. The deflection coverage in the Arctic islands is so scanty that geoidal heights in this

region are meaningless.

(1) The comparison with the AMS67 geoid (Figure 3.4) indicates that the additional data observed since 1967 has brought about significant changes in the shape of the geoid in North America, although some of these changes are due to the difference in the two techniques used. Similar changes may be expected in the UNB74-1 geoid when additional data in Canada is obtained. The RMS difference between the two geoids (measured on a $2^\circ \times 2^\circ$ grid) is ± 7.1 m, and the mean difference is + 4.0 m. This bias (in the AMS67 geoid) has already been reported in Fischer (1971), although a smaller value of + 2 to + 3 m was estimated then.

(2) The NGS73 geoid was computed as point geoidal heights at 2528 deflection stations in the U.S.A., mainly along the High Precision Geodimeter Traverse. The mean difference from the UNB74-1 values is zero, with an RMS difference of 2.2 m. As basically the same data was used in the U.S.A., these differences are due to the differences in the two techniques employed - as mentioned earlier Rice's is based upon Helmert's formula. The maximum differences are in Washington and southern Florida (- 6 m and + 8 m, in the sense: NGS73 minus UNB74-1) - the two areas where the distribution of U.S. deflections is weakest. The Puget Sound deflections (in Washington) are separated from the remainder by several mountain ranges, while the geoidal heights in Florida are based upon deflections along a single line of triangulation.

(3) The GSFC72 geoid was digitised on a $2^\circ \times 2^\circ$ grid for North America, with the values being interpolated from the chart accompanying the report by Vincent et al (1972). These geoidal heights were first transformed to the same datum as UNB74-1, taking into account the change

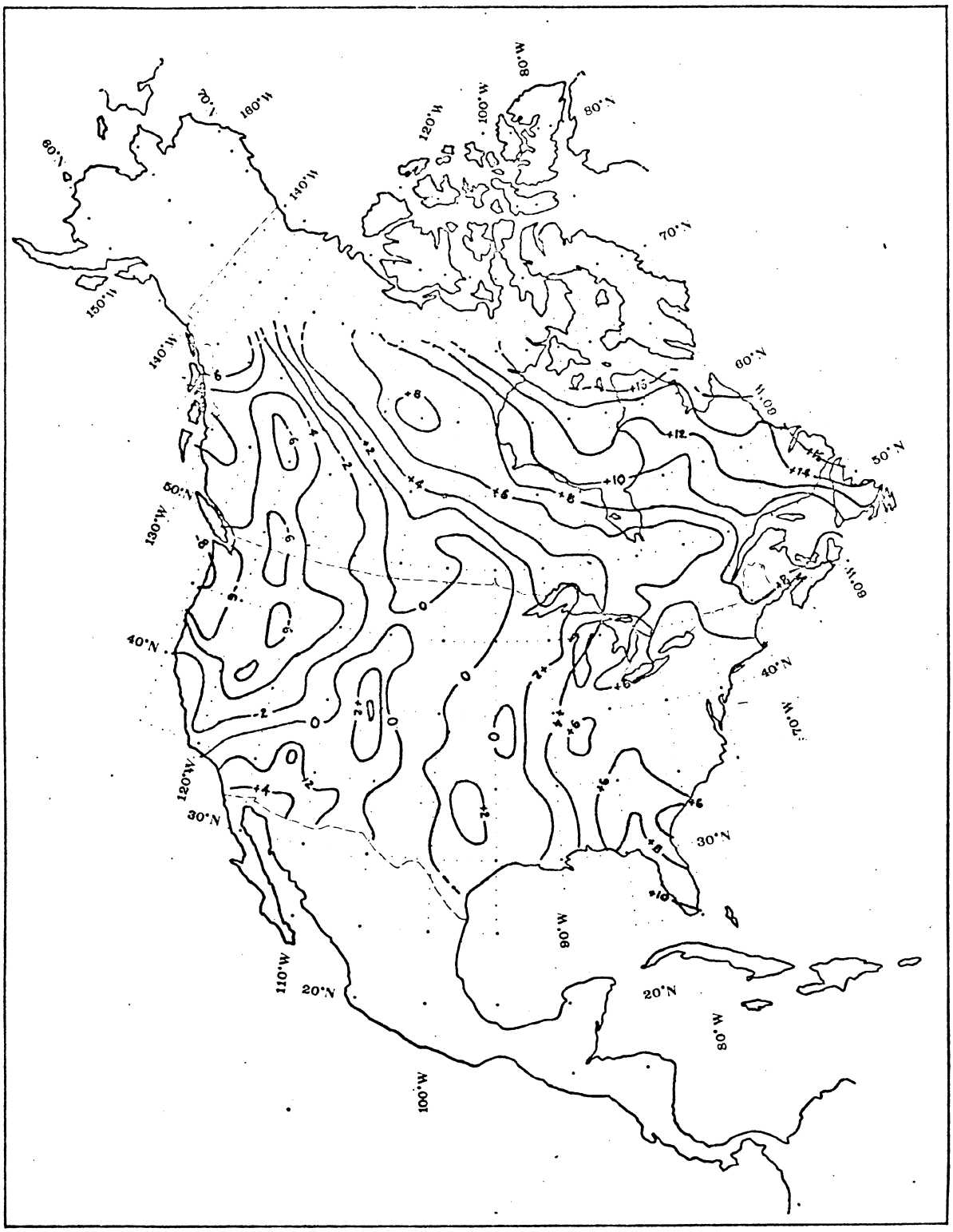

Figure 3.4

AMS67 Minus UNB74-1 Geoid

2 metre Contours

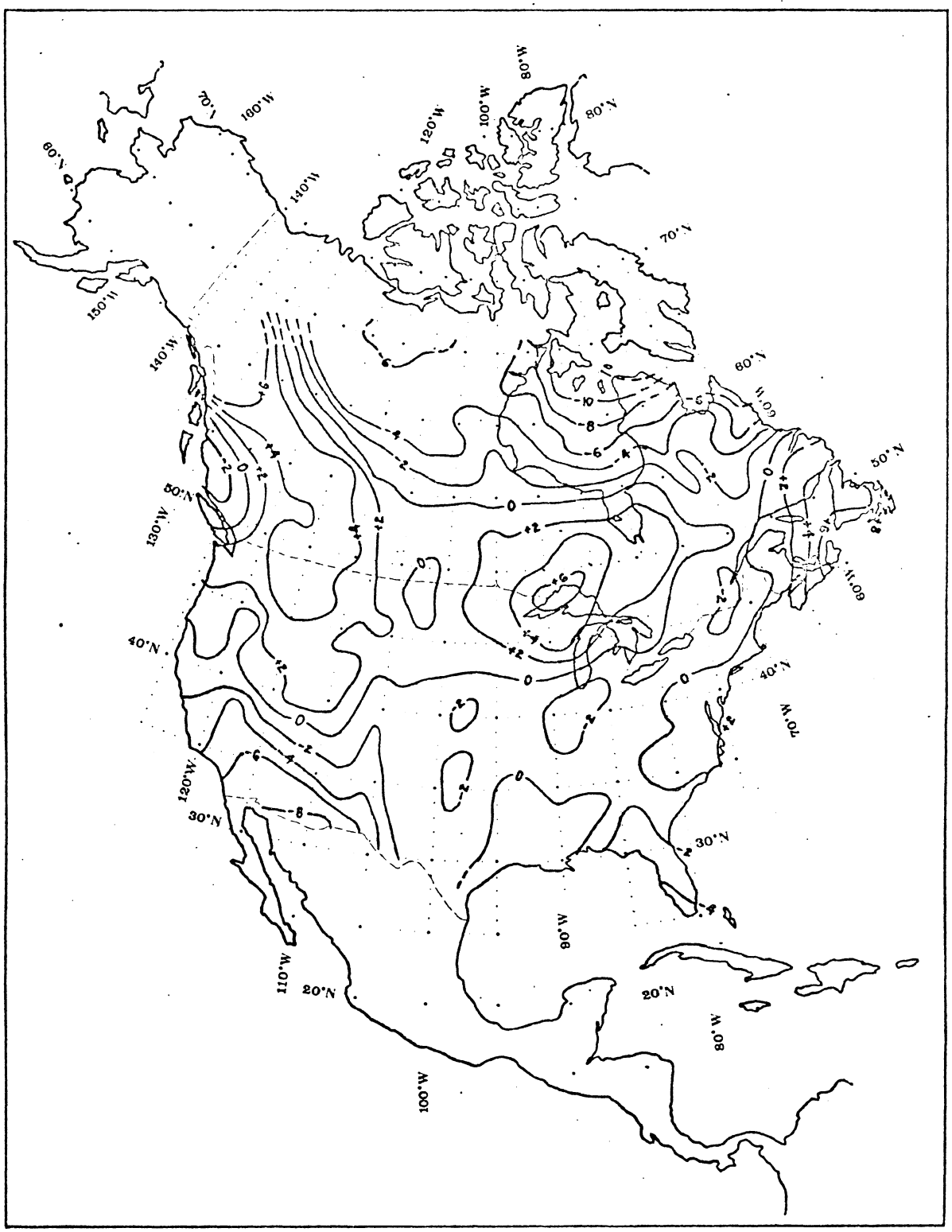

Figure 3.5

UMB74-1 Minus GSFC72 Geoid

2 metre Contours

in size and shape of the reference ellipsoid, and three translation components. These translation components were determined simultaneously in the transformation, using the least squares principle that the distance between the two sets of geoidal heights, after transformation, be a minimum. The procedure is described in more detail in Merry and Vaníček (1974b). The translation components determined, using this procedure, are:

$$\delta x = - \quad 6.5 \text{ m} \pm 0.8 \text{ m}$$

$$\delta y = + 154.3 \text{ m} \pm 0.7 \text{ m}$$

$$\delta z = + 190.0 \text{ m} \pm 0.6 \text{ m}$$

In this case, the mean difference is zero, and the RMS difference is 3.8 m. These values represent the co-ordinates of the centre of the geodetic reference ellipsoid in a cartesian co-ordinate system with origin at the centre of the geocentric reference ellipsoid used for the GSFC72 geoid. The differences between the two geoids, after transformation, are shown in Figure 3.5.

As the GSFC72 geoid is the only external comparison source completely independant from the UNB74-1 geoid (the others share common data), it is worth taking a closer look at the differences especially those exceeding (in absolute value) 5 metres. The effect of the scarcity of astrogeodetic deflection data in the Yukon, Northwest Territories, northern Labrador and Newfoundland is immediately apparent. (It should also be borne in mind that the gravity data in parts of these regions is also scarce.) The two areas of + 5 m difference in western Canada and the north-western U.S.A. are in mountainous regions where both astrogeodetic deflections of the vertical and gravity anomalies are likely to be sparsely distributed. The two remaining features, the high near Lake Superior and

the low in the south-western U.S.A. are more difficult to explain. The Lake Superior high may be due to the paucity of deflection data in that region. However, in the south-western U.S.A., there appears to be adequate coverage of both deflection and gravity data.

3.33 Density and distribution of deflection data

Other investigators, using the linear one-dimensional interpolation of Helmert's formula, have recommended that the spacing between adjacent deflection stations should be of the order of 20 km to 25 km (Rice, 1962; Bomford, 1971; Fryer, 1972). An investigation has been carried out as to whether this figure is applicable to the surface-fitting technique. It is apparent that for this approach the deflection stations should not be concentrated along single chains of triangulation or traverse, but should be well-distributed over the entire region of interest. Well distributed deflections have been predicted, using the methods of Chapter 2, in an area 500 km by 650 km in Labrador/Quebec. Using progressively more deflections in the same area so that the distribution became denser, geoidal heights were computed in the region. The variance factor and RMS predicted standard deviation (computed from 20 selected points) are shown as a function of approximate station spacing in Figure 3.6. Also indicated are the RMS geoidal height differences (computed at the same points) of the various determinations, compared to the final determination. From this figure, it is apparent that a deflection spacing of 40 - 45 km is adequate and that, if possible, the spacing should not exceed 60 km. In general, these results are in agreement with those of other investigators, but a somewhat longer spacing may be used. This is due to the non-linear two-dimensional interpolation implied in the surface-fitting technique, as contrasted to the linear one-dimensional

Figure 3.6

Variation in Deflection Station Spacing

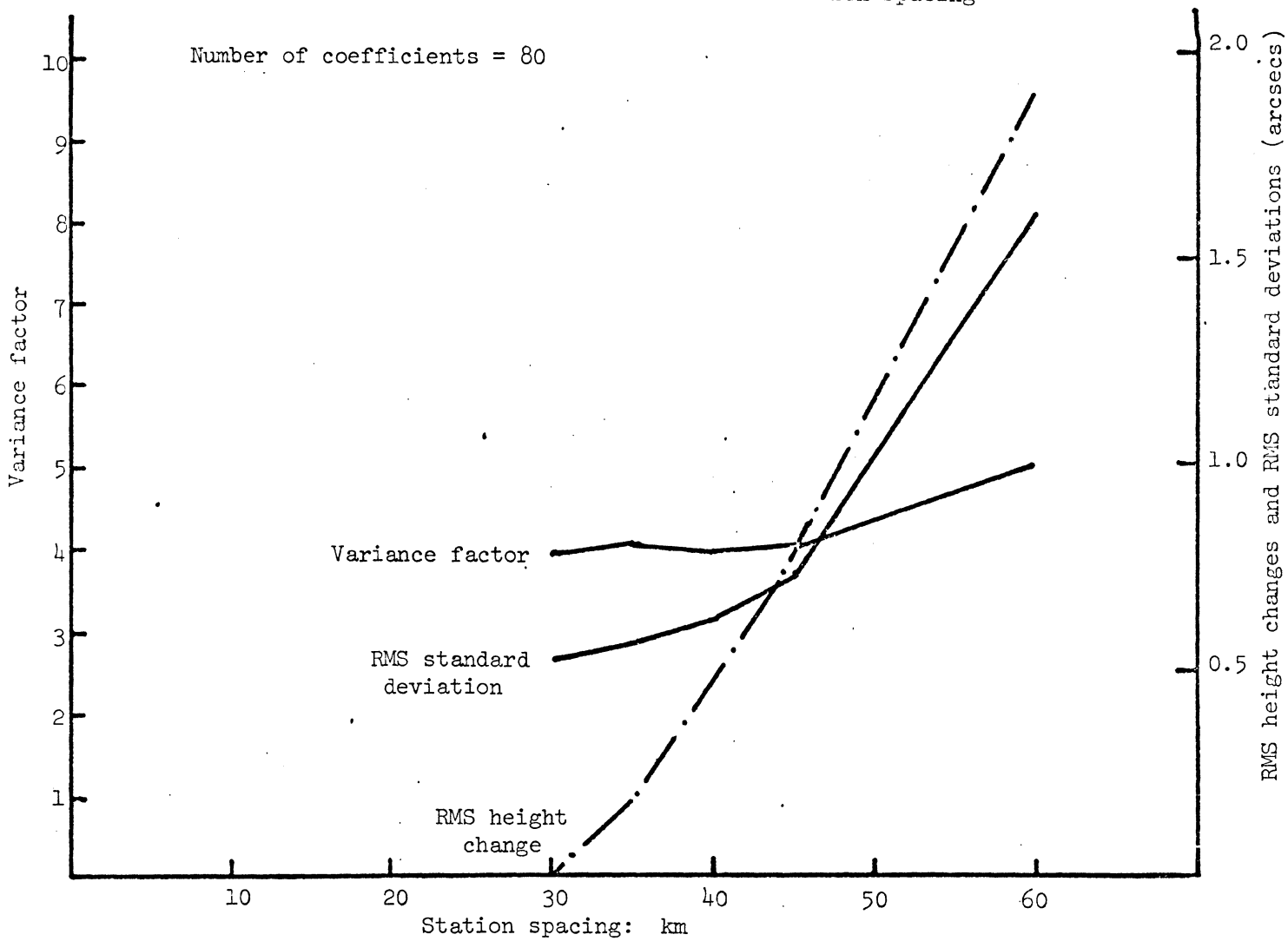

interpolation of Helmert's technique, used by the other investigators.

3.34 Inclusion of predicted deflections

In eastern Canada (east of 75° w) there are approximately 350 stations at which deflections of the vertical have been obtained by astrogeodetic means. These are concentrated in southern Quebec and the Maritime provinces and are very scattered in the remaining regions. However, these scattered deflections are sufficient to allow astrogeodetic deflections to be predicted, using the methods described in the previous chapter. Deflections were predicted at 490 stations in this area, at approximately 50 km spacing, to yield a fairly homogeneous deflection field for eastern Canada. Due to lack of both gravity data and observed deflections, it was not possible to predict deflections in Labrador north of 55° latitude and in Quebec north of 58° latitude. Geoidal heights have been computed in the region using, in one case, only the observed deflections, and, in the other, all the available deflections, including those predicted. The geoidal height of a single point in the centre of the region was held fixed at + 0.97 m, the value obtained from the continental solution, UNB74-1, described in section 3.32.

The results for the two computations are shown in Figures 3.7 and 3.8, and the differences between them in Figure 3.9. The differences between the two geoids are large, reaching a maximum of 9 m in northern Quebec. The mean difference is 3.3 m, with the astrogravimetric geoid being lower than the astrogeodetic. As was to be expected, the differences are smaller in the areas where there were sufficient astrogeodetic deflection stations. Predicted standard deviations of the geoidal heights have also been computed for the two solutions, and these are shown in Figures 3.10

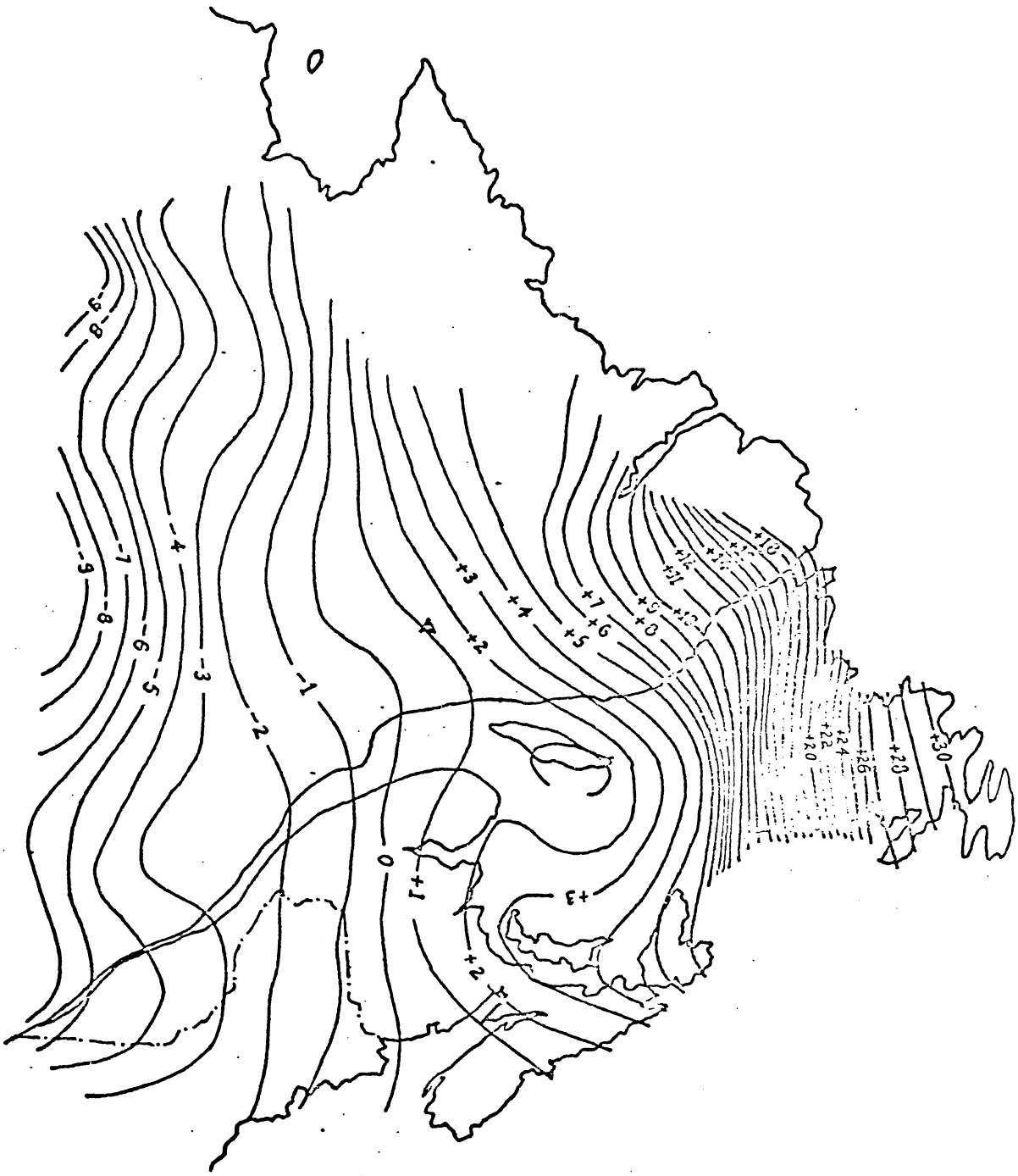

Figure 3.7

Astrogeodetic Geoid in Eastern Canada

(1 metre Contours)

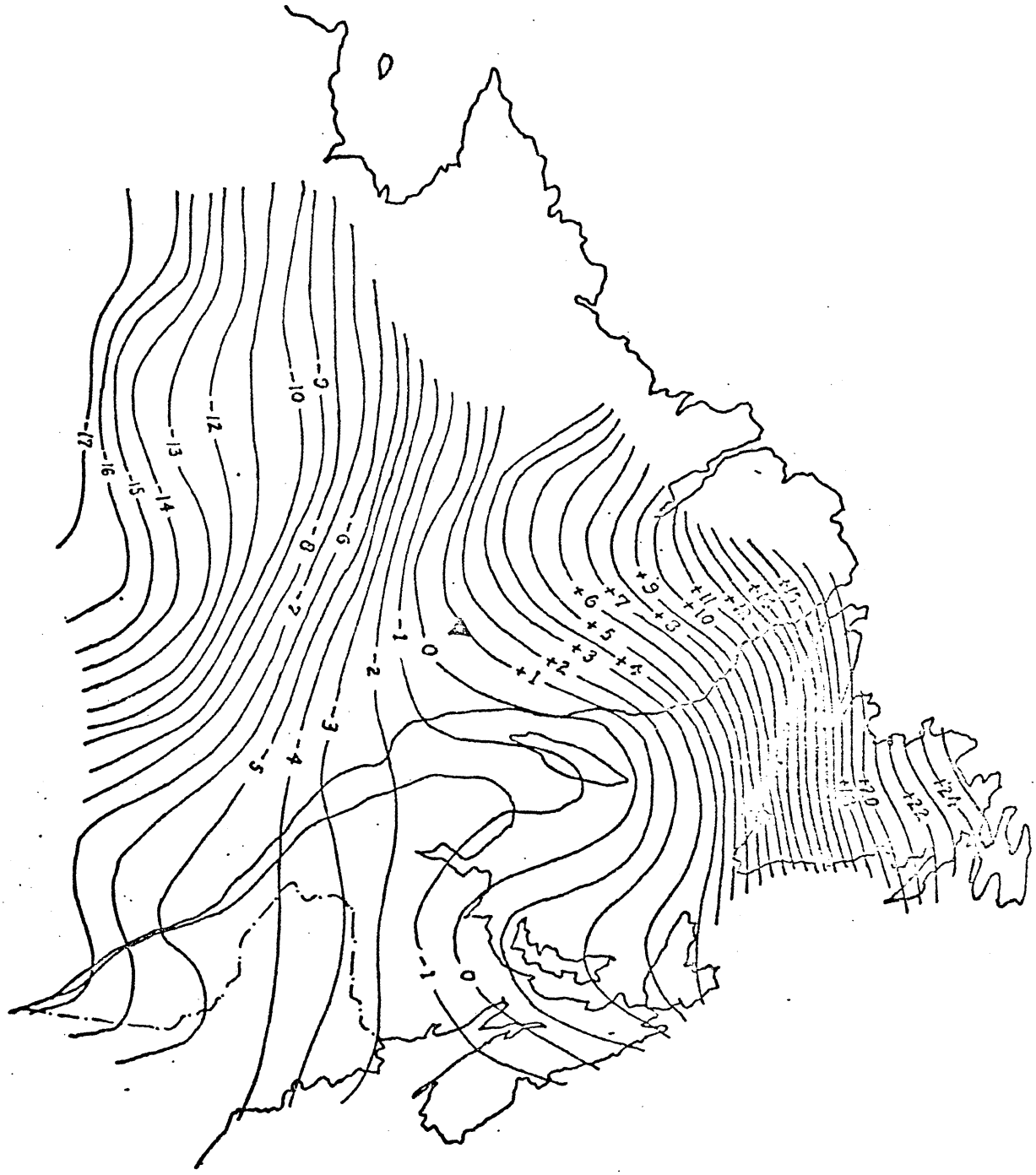

Figure 3.8
Astrogravimetric Geoid in Eastern Canada
(1 metre Contours)

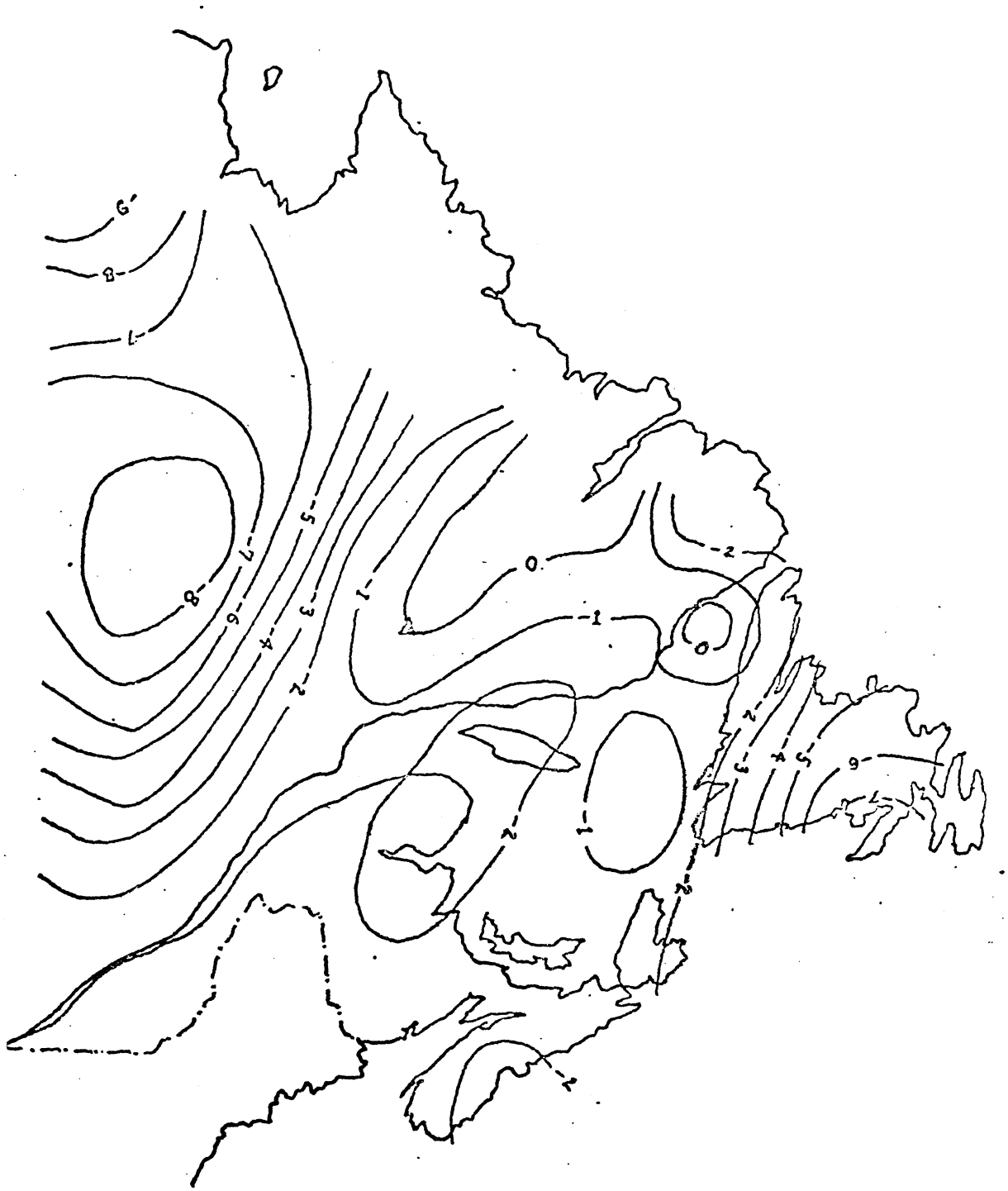

Figure 3.9

Astrogravimetric Minus Astrogeodetic Geoids in Eastern Canada

(1 metre Contours)

Figure 3.10

Standard Deviations - Astrogeodetic Geoid

(0.5 metre Contours)

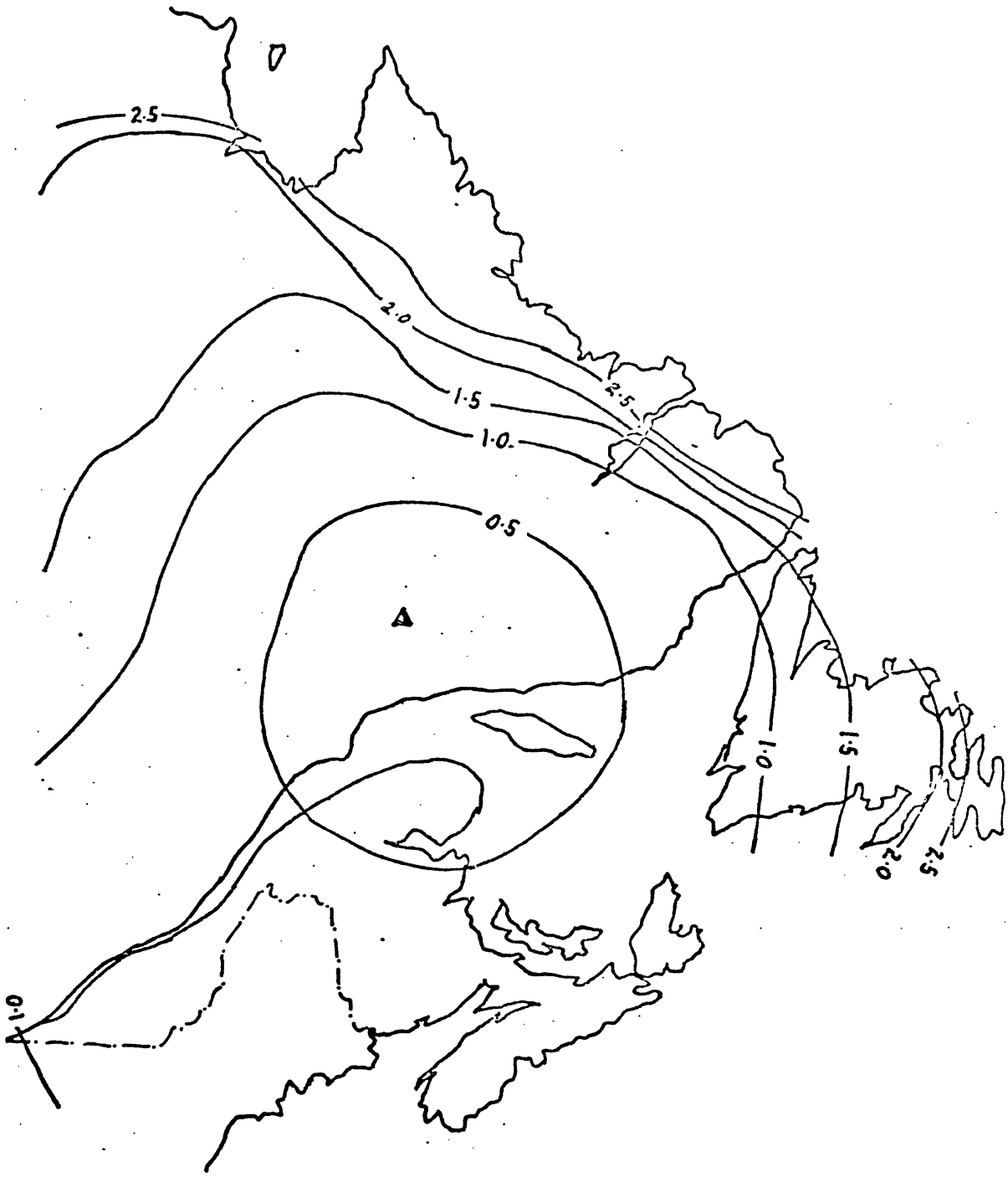

Figure 3.11

Standard Deviations - Astrogravimetric Geoid

(0.5 metre Contours)

and 3.11. It is apparent that the inclusion of predicted deflections has significantly improved the accuracy estimates. This confirms the results obtained for a smaller area and described in Merry and Vaníček (1974c).

From both these figures, the effect of there being only a couple of deflection stations on the Labrador coast is evident in the steep slope of the standard deviation contours in this area. On the other hand, the good deflection coverage in the Maritimes is indicated by the shallow slope in that region.

As an external check, both the geoids described above were compared to a combined satellite-gravimetric geoid, that of Vincent et al (1972). This geoid is considered to have an accuracy of 2 - 3 m on land, and a lower accuracy at sea, so that it is of limited value as a precise external reference. However, at present, it is the best available independant solution. The geoidal heights from this publication were digitised at 1° latitude by 2° longitude intervals for eastern Canada. They were then transformed to the same datum as the astrogeodetic geoidal heights, using the method of Merry and Vaníček (1974b). The RMS differences are then respectively 3.6 m when compared to the astrogeodetic geoid and 3.1 m when compared to the astrogravimetric geoid. There does, therefore, appear to be a slight improvement when the astrogravimetric geoid is used.

3.35 Sequential use of the technique

The mathematical model of section 3.21 has one limitation that is important where detailed variations in the geoidal heights for a local region are required to be known. The geoidal height at the initial point

of a geodetic network is usually defined to be a particular value, and all other geoidal heights are determined relative to this value. In order to determine geoidal heights at other points in the network, all the deflection stations between these points and the initial point must be included in the determination. For a continent the size of North America, this means that a large number of deflections are available for inclusion in the model, and the number of coefficients must be correspondingly increased in order to adequately describe all variations in geoidal heights. A practical limitation is imposed, however, in that round-off errors in the solution (by electronic computer) rapidly accumulate with increase in the degree of the polynomial. This eventually leads to the matrix of normal equations becoming ill-conditioned and impossible to invert (by conventional means). The computer time increases with the square of the number of coefficients and this, too, is a limiting influence. The greatest number of coefficients successfully used for all the astrogeodetic data in North America (as of 1972 and excluding Alaska) is 144. The geoid resulting from this solution is shown in Figure 3.2, and the standard deviations of these geoidal heights are shown in Figure 3.3. It is apparent from a comparison of Figures 3.2 and 3.7 that some detail in eastern Canada has been lost in the continental geoid. One way of obtaining more detail in a particular region is that used in the previous section, in which the geoidal height at a local origin is obtained from a continental geoid and then more detailed geoidal heights, relative to this local origin, are computed for the region of interest. This sequential use of the model of section 3.21 has two drawbacks, however. One is that the point selected as a local origin may not be the most suitable for the region, and discontinuities between the local and continental geoids may

occur at the edges of the local geoid. In the example mentioned above, there are differences reaching 3.5 m at the edges of the local geoid. The second is that the standard deviations obtained in the solution are relative to the local, and not the continental, origin. The estimated variance of the geoidal height at the local origin (from the continental solution) may be added to the variances obtained in the local solution, but this still results in the incongruous situation that the standard deviations of the geoidal heights apparently increase as the continental origin is approached (Figure 3.10).

An alternative approach is to use the mathematical model of section 3.22 for the area of interest. In this procedure, a number of geoidal heights obtained from the continental solution, together with their error covariance matrix, are used as additional observations.

The astrogravimetric geoid in eastern Canada was computed using respectively 4, 10, 15 geoidal heights as constraints. The resultant geoidal heights differ only by a constant shift (of + 5.9 m, + 4.6 m, + 5.8 m) from the astrogravimetric geoid described earlier. The variance factors for the three solutions differed little from each other. Hence, the accuracy of the solution does not appear to be a function of the number of constraints used. The solution itself does depend upon the particular constraints used.

The solution using 10 constraints was selected for further analysis. The constant shift of + 4.6 m has brought the astrogravimetric geoid into better agreement with the local astrogeodetic geoid (as can be seen from Figure 3.9, the astrogravimetric geoid was consistently lower than the astrogeodetic). At the same time it also fits the continental solution better than does the local astrogeodetic geoid.

The continental solution itself would be improved by the inclusion of predicted deflections in areas of poor deflection coverage.

The standard deviations associated with this particular local geoid are depicted in Figure 3.12. These values agree with what would be intuitively expected, that the errors increase with increasing distance from the origin. The slowly varying standard deviation, of approximately 5 m, implies that the geoidal heights relative to one another are well-determined, but that their relationship with the continental origin is less well-known. If only relative geoidal heights are needed (relative in a local sense), then either sequential procedure would suffice. If geoidal heights relative to a distant continental origin are required, then the second technique is preferable.

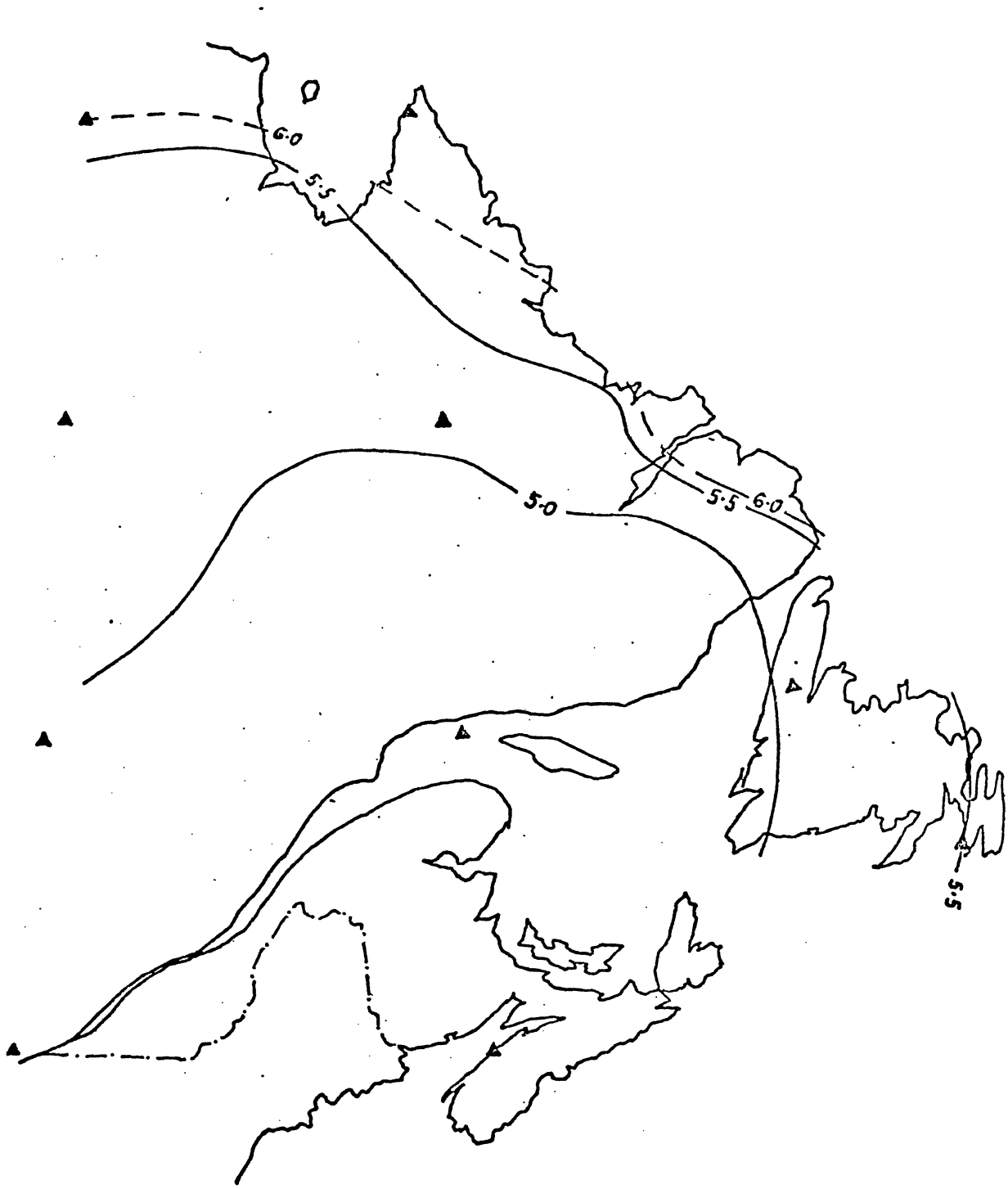

Figure 3.12

Standard Deviations - Astrogravimetric Geoid with 10 Constraints

(0.5 metre Contours)

CHAPTER 4

CONCLUSIONS AND RECOMMENDATIONS

4.1 Deflection Prediction

The method of deflection prediction developed here provides satisfactory results when tested using real data. In the test areas studied, the actual errors in the predicted deflections are, on average, 50% of the magnitude of the deflections themselves. Thus, use of these deflections will result in an improvement over using no deflections at all. It should be noted that this procedure recovers the more important regional trends in the geoid, rather than the very short wavelength details, which have a localised effect (Meissl, 1973). The accuracy requirement of 1" cotgZ for the reduction of directions (described in section 1.3) will be met, in all but extreme cases. Hence these predicted deflections may be used for this purpose.

The prediction of errors in these deflections has been less successful, and further improvement is necessary. Only random errors in the gravity data were taken into account as error sources, and it is apparent that these are not the major source. The possible error sources have been itemised in section 2.54. The most important of these are:

(1) Blunders in the gravity data,

(2) Poor distribution of gravity data,

(3) Plumbline curvature.

None of these errors can be eliminated using the prediction technique

described here.

This procedure is an improvement over that suggested by Molodensky et al (1962), in that it is not limited to interpolation along astrogeodetic profiles. The integration distance needed is half that recommended by other investigators, due to the use of a second-order, two-dimensional correction polynomial. The computation point is not restricted to being on a rectangular grid, but may lie virtually anywhere within the area of interest.

Although, in theory, the size of the area of interest is not limited, for practical computational reasons, the area should not exceed 1000 km by 1000 km. The control stations to be used should be towards the outside of this region, so that no extrapolation takes place. There should be at least ten control stations, well-distributed over the region of interest. No reliable method of evaluating and quantifying distribution has been developed in this thesis, and further investigation in this area is recommended, as the distribution of both gravity and deflection data can influence the results of the prediction. Further assessment and improvement in the quality and quantity of the gravity anomalies in North America is warranted, as errors and gaps in this data can seriously affect the reliability of this prediction method.

4.2 Geoid Computation

Very satisfactory results have been obtained using the surface-fitting procedure. As contrasted to the applications of Helmert's technique, this method takes full advantage of the tri-dimensionality of the geoidal surface. As with the deflection prediction, this method is dependant upon a homogeneous distribution of data. For this procedure

(and those of Heitz and Tscherning (1972)) the deflections of the vertical are most effective if they are observed, and predicted,on a regular grid.

In this technique, deflections need only be available at 40 km to 50 km spacing, a two-fold improvement upon the spacing requirements of the methods based upon Helmert's formula. The method has the additional advantage that geoidal heights, and their associated error covariance matrix, can be computed at any points within the region and not only at deflection stations.

The sequential use of the surface-fitting technique allows more detail of the geoid to be determined in those areas for which there may be a need and for which there is sufficient data. The method using previously determined geoidal heights as quasi-observations is preferable, as more realistic error estimates are obtained. The inclusion of geoidal heights as obtained via satellite determinations (described in section 3.22) was not evaluated as, at the time of writing, sufficient satellite data was not yet available. Further investigations should study whether this approach will strengthen the determination of the geoid in areas of sparse deflection coverage, such as the Canadian Arctic.

Of the two accuracy requirements described in section 1.3, the first has been met for the conterminous U.S.A. and most of Canada, without resorting to gravimetrically predicted deflections. For the second requirement (of 2 metres) additional deflections will be needed before it can be met. Some of these additional deflections will need to be observed deflections (to act as control stations), but the great majority of them will have to be predicted, if this requirement is to practically be met within the next few years. From the National Reports presented to the International Association of Geodesy in Moscow (1971b), it is evident that

the scarcity of deflection data is not a North American problem, but a global one. Thus these comments apply equally well to other areas of the world.

APPENDIX I

THE METHOD OF LEAST SQUARES

In several of the mathematical models used in this thesis, there are more than sufficient observations for a unique solution, and a systematic method to optimise the solution must be found. One such method is that employing the least squares principle. Although it is not the only optimisation method that may be used, it is one of the simplest and most convenient of these methods. Consequently, it has been used extensively in this thesis. The least squares principle may be described as:

(1) minimising the trace of the error covariance matrix,

(2) minimising the distance between two functions.

(1) The first approach, via the field of statistics, is useful for least squares adjustment (Wells and Krakiwsky, 1971), in which the mathematical model relating observed and unobserved parameters is complete, and any discrepancies may be considered to be randomly distributed. The error covariance matrix, of which the trace is to be minimised, is that of the unknown quantities, $\underset{\sim}{x}$, and is given by:

$$\Sigma_{\tilde{x}} = \begin{bmatrix} \sigma_1^2 & \sigma_{12} & - & - & - \\ \sigma_{21} & \sigma_2^2 & & & \\ - & & - & & \\ - & & & - & \\ - & & & & \sigma_n^2 \\ - & & & & \end{bmatrix} \qquad \text{I.1}$$

where σ_i^2 is the variance, and σ_i is the standard deviation of the ith element of $\underset{\sim}{x}$; and σ_{ij} is the error covariance between the ith and j^{th} elements of $\underset{\sim}{x}$.

The standard deviation is a measure of the accuracy, while the error covariance is a measure of the correlation between quantities. They are defined by:

$$\sigma_i^2 = E((x_i - E(x_i))^2) \qquad \text{I.2}$$

$$\sigma_{ij} = E((x_i - E(x_i))(x_j - E(x_j))) \qquad \text{I.3}$$

where E is the expectation operator (Wells and Krakiwsky, 1971).

The further development of least squares adjustment, leading to the solution of sets of normal equations, is not discussed here. For a comprehensive treatment of the subject, see Wells and Krakiwsky (1971).

(2) The second description of the least squares principle is from the field of functional analysis. This principle is used in least squares approximation, where a complicated function is replaced by a simpler one (usually a linear form). The simpler function does not necessarily model the original function completely, but the discrepancies may be treated as being random noise. However, these discrepancies are not generally homogeneous or isotropic, as in the case of least squares adjustment. In this study, the distance to be minimised is the Euclidean distance, $\rho(F, P_n)$, given by:

$$\rho^2(F, P_n) = \langle F(x,y) - P_n(x,y), F(x,y) - P_n(x,y) \rangle \qquad \text{I.4}$$

where the original function $F(x,y)$ is represented by a discrete set of values, and the approximating function, $P_n(x,y)$, is an algebraic polynomial of order n.

The weight function, $w(x,y)$, may be arbitrarily selected. In this investigation, discrete values were used, given by the inverses of the variances of the discrete values of $F(x,y)$. The development of the normal equations for the solution for the coefficients of $P_n(x,y)$ is treated in detail in Vaníček and Wells (1972).

The propagation of errors has also been included in this study, and follows the conventional error covariance propagation theory (Vanicek, 1973). In some instances, practical difficulties have made it possible to propagate only error variances. Estimates of the standard deviations of the original data cannot be made by standard statistical means, such as those of equation I.2, as no repeated observations were made. Consequently, the term "standard deviation" has been somewhat loosely applied to the accuracy estimates (based largely upon the practical experience of others) used for the initial data.

APPENDIX II

DERIVATION OF EXPRESSION FOR MEAN GRAVITY ANOMALY

The mean gravity anomaly $\bar{\Delta}g$ is given by:

$$\bar{\Delta}g = \frac{1}{A} \iint \Delta g \, dA \qquad \text{II.1}$$

For a rectangular area with a local cartesian co-ordinate system (x,y) with origin at the centre and co-ordinates of the four corners: (a,b), (-a,b), (a,-b), (-a,-b):

$$\bar{\Delta}g = \frac{1}{4ab} \int_{-a}^{a} \int_{b}^{b} \Delta g \, dx \, dy \qquad \text{II.2}$$

Δg_i, the anomaly, at the ith point, is approximately given by $\tilde{\Delta}g_i$:

$$\tilde{\Delta}g_i = \sum_{j,k=0}^{2} C_{jk} \, x_i^j \, y_i^k \qquad \text{II.3}$$

Hence, in its fully expanded form, equation II.2 may be written as:

$$\bar{\Delta}g \doteq \frac{1}{4ab} \int_{-a}^{a} \int_{-b}^{b} (C_{oo}+C_{01}y+C_{02}y^2+C_{10}x+C_{11}xy+C_{12}xy^2+C_{20}x^2+C_{21}x^2y+C_{22}x^2y^2) dxdy \qquad \text{II.4}$$

Evaluating each of these simple integrals:

$$\bar{\Delta}g \doteq \frac{1}{4ab} \left(C_{oo}xy + \frac{C_{01}}{2} xy^2 + \frac{C_{02}}{3} xy^3 + \frac{C_{10}}{2} x^2y + \frac{C_{11}}{4} x^2y^2 + \frac{C_{12}}{6} x^2y^3 + \frac{C_{20}}{3} x^3y + \frac{C_{21}}{6} x^3y^2 + \frac{C_{22}}{9} x^3y^3\right) \Bigg|_{x=-a}^{a} \Bigg|_{y=-b}^{b} \qquad \text{II.5}$$

or

$$\bar{\Delta}g \doteq \frac{1}{4ab}\left(4C_{00}ab + \frac{4}{3}C_{02}ab^3 + \frac{4}{3}C_{20}a^3b + \frac{4}{9}C_{22}a^3b^3\right) \qquad \text{II.6}$$

i.e.

$$\bar{\Delta}g \doteq C_{00} + \frac{C_{02}}{3}b^2 + \frac{C_{20}}{3}a^2 + \frac{C_{22}}{9}a^2b^2 \qquad \text{II.7}$$

APPENDIX III

DERIVATION OF EQUATIONS FOR INNER ZONE CONTRIBUTION TO THE GRAVIMETRIC DEFLECTIONS OF THE VERTICAL

Let the inner zone ($1/3^\circ \times 1/3^\circ$) limits be given by: ϕ_1, ϕ_2, λ_1, λ_2 ($\lambda_2 > \lambda_1$, $\phi_2 > \phi_1$). The Vening-Meinesz integral is then:

$$\xi_3 = \frac{1}{4\pi G} \int_{\lambda=\lambda_1}^{\lambda_2} \int_{\phi=\phi_1}^{\phi_2} \Delta g \cos\alpha \cos\phi \frac{dS(\psi)}{d\psi} d\phi d\lambda$$

$$\eta_3 = \frac{1}{4\pi G} \int_{\lambda=\lambda_1}^{\lambda_2} \int_{\phi=\phi_1}^{\phi_2} \Delta g \sin\alpha \cos\phi \frac{dS(\psi)}{d\psi} d\phi d\lambda \qquad \text{III.1}$$

where G is the mean gravity, Δg the free-air anomaly, α the azimuth of the line connecting the computation point with the dummy point in the integration and ψ is the angular distance between these two points.

In the inner zone, ψ is small, and $\frac{dS(\psi)}{d\psi}$ approaches infinity. Then, $\frac{dS(\psi)}{d\psi}$ can be approximated by:

$$\frac{dS(\psi)}{d\psi} \doteq \frac{1}{2(\psi/2)^2} + 8\psi - 6 - 3\,\frac{1 - \psi/2}{\psi} + 3\psi\, \ln[\psi/2 + (\psi/2)^2] \qquad \text{III.2}$$

In the particular case of a $1/3^\circ \times 1/3^\circ$ block, $\psi < 0.01$ radians and:

$$\frac{dS(\psi)}{d\psi} \doteq -\frac{2}{\psi^2} - \frac{3}{\psi} \qquad \text{III.3}$$

with a maximum error of 0.03%. In the integration, ϕ, λ, can be replaced by plane rectangular co-ordinates x, y with origin (x_o, y_o) at the computation point. Then

$$dx = Rd\phi$$

$$dy = R\cos\phi\, d\lambda$$

$$\psi \doteq s/R$$

$$s = \sqrt{(x^2 + y^2)}$$

where R is a mean radius of curvature for the earth. Considering, for the moment, only the ξ-component, and replacing $\cos\alpha$ by x/s we can rewrite equation III.1 as:

$$\xi_3 \doteq -\frac{1}{4\pi G}\int_{y=y_1}^{y_2}\int_{x=x_1}^{x_2} \Delta g\left(\frac{2R^2}{s^2} + \frac{3R}{s}\right)\cos\alpha\,\frac{dxdy}{R^2} \qquad \text{III.4}$$

$$= -\frac{1}{2\pi G}\int_{y=y_1}^{y_2}\int_{x=x_1}^{x_2} \left[\Delta g\cdot x(x^2 + y^2)^{-3/2} + 3/2\ \Delta g\frac{x(x^2+y^2)^{-1}}{R}\right]dxdy$$

Integration of the above expression over the inner zone requires Δg values to be known over the entire zone. This is not generally the case, and Δg at any point in the zone must be approximated. Δg can be written in the form:

$$\Delta g = \Delta g_o + xg_x + yg_y + \ldots\ (0) \qquad \text{III.5}$$

where Δg_o is the gravity anomaly at the computation point (x_o, y_o) and

$$g_x = \left.\frac{\partial \Delta g}{\partial x}\right|_{\substack{x=x_o\\ y=y_o}}, \qquad g_y = \left.\frac{\partial \Delta g}{\partial y}\right|_{\substack{x=x_o\\ y=y_o}}$$

are the horizontal derivatives of the gravity anomalies at the computation point. This approximation uses just these first three terms in the Taylor series and is equivalent to fitting a plane to the gravity anomalies in the inner zone. Then, for the meridian component:

$$\xi_3 = \frac{-1}{2\pi G}\int_{y=y_1}^{y_2}\int_{x=x_1}^{x_2} (\Delta g_o + xg_x + yg_y)\left(x(x^2 + y^2)^{-3/2} + \frac{3}{2R}\,x(x^2 + y^2)^{-1}\right)dxdy$$

or

$$\xi_3 = -\frac{1}{2\pi G}\sum_{j=1}^{6} I_j \qquad \text{III.}$$

where

$$I_1 = \Delta g_o \iint_A x(x^2 + y^2)^{-3/2}\, dxdy$$

$$I_2 = g_x \iint_A x^2(x^2 + y^2)^{-3/2} dxdy$$

$$I_3 = g_y \iint_A xy(x^2 + y^2)^{-3/2}\, dxdy$$

$$I_4 = \frac{3\Delta g_o}{2R} \iint_A x(x^2 + y^2)^{-1}\, dxdy$$

$$I_5 = \frac{3g_x}{2R} \iint_A x^2(x^2 + y^2)^{-1}\, dxdy$$

$$I_6 = \frac{3g_y}{2R} \iint_A xy(x^2 + y^2)^{-1}\, dxdy$$

and the integration is carried out for the whole area A of the inner zone. The solution of these integrals is a non-trivial problem and is described below:

$$I_1 = \Delta g_o \int_{y_1}^{y_2} \frac{-dy}{\sqrt{(x^2 + y^2)}} \Big|_{x=x_1}^{x_2} = -\Delta g_o\, \ln(y + \sqrt{(x^2 + y^2)}) \Big|_{x=x_1}^{x_2} \Big|_{y=y_1}^{y_2} \qquad \text{III.7}$$

$$I_2 = g_x \left\{\int_{y_1}^{y_2} \frac{-xdy}{\sqrt{(x^2 + y^2)}} + \int_{y_1}^{y_2} \ln(x + \sqrt{(x^2 + y^2)})dy\right\} \Big|_{x=x_1}^{x_2}$$

III.8

$$= -g_x x\, \ln(y + (x^2 + y^2)) \Big|_{x=x_1}^{x_2} \Big|_{y=y_1}^{y_2} + g_x \int_{y_1}^{y_2} \ln(x + (x^2 + y^2))dy \Big|_{x_1}^{x_2}$$

The second part of this expression is evaluated separately:

$$\int_{y_1}^{y_2} \ln(x + \sqrt{(x^2 + y^2)})dy = \int_{y_1}^{y_2} \ln x\, dy + \int_{y_1}^{y_2} \ln(1 + \sqrt{(1 + \frac{y^2}{x^2})})dy$$

$$= y \ln x + \int_{y_1}^{y_2} \ln(1 + \sqrt{(1 + \frac{y^2}{x^2})})\, dy \qquad \text{III.9}$$

Putting $1 + \frac{y^2}{x^2} = t^2$, then $dy = \frac{x^2\, t dt}{x\sqrt{(t^2 - 1)}}$ and

$$\int_{y_1}^{y_2} \ln(1 + \sqrt{(1 + \frac{y^2}{x^2})})dy = \int_{y_1}^{y_2} \ln(t + 1) \frac{tx}{\sqrt{(t^2 - 1)}} dt$$

$$= \ln(t + 1) \int_{y_1}^{y_2} \frac{tx}{\sqrt{(t^2 - 1)}} dt - \int_{y_1}^{y_2} \frac{1}{t + 1} (\frac{tx^{dt}}{\sqrt{(t^2 - 1)}} dt$$

$$= x \ln(t + 1) \sqrt{(t^2 - 1)} \Big|_{y_1}^{y_2} - x \int_{y_1}^{y_2} \frac{\sqrt{(t^2 - 1)}}{t + 1} dt \qquad \text{III.10}$$

Now

$$\int_{y_1}^{y_2} \frac{\sqrt{(t^2 - 1)}}{t + 1} dt = \int_{y_1}^{y_2} \sqrt{(\frac{t - 1}{t + 1})}dt = \sqrt{(t - 1)}\, \sqrt{(t + 1)} \Big|_{y_1}^{y_2} - \int_{y_1}^{y_2} \frac{dt}{\sqrt{(t-1)}\sqrt{(t+1)}}$$

$$= \sqrt{(t - 1)}\sqrt{(t + 1)} \Big|_{y_1}^{y_2} - \int_{y_1}^{y_2} \frac{dt}{\sqrt{(t^2 - 1)}} = \sqrt{(t-1)}\sqrt{(t+1)} \Big|_{y_1}^{y_2} - \ln(t + \sqrt{(t^2 - 1)} \Big|_{y_1}^{y_2}$$

III.11

Back-substituting in equation III.10

$$\int_{y_1}^{y_2} \ln(1 + \sqrt{(1 + \frac{y^2}{x^2})})dy = x[\sqrt{(t^2 - 1)}(\ln(t + 1) - 1) + \ln(t + \sqrt{(t^2 - 1)})] \Big|_{y_1}^{y_2}$$

Substituting for $t = \sqrt{(1 + \frac{y^2}{x^2})}$ and rearranging terms:

$$\int_{y_1}^{y_2} \ln(x + \sqrt{(x^2 + y^2)})dy = [y \ln(x + \sqrt{(x^2 + y^2)}) - y + x \ln(y + \sqrt{(x^2+y^2)}) -$$

$$- x \ln x] \Big|_{y_1}^{y_2}$$

Substituting in equation III.8

$$I_2 = g_x \{y \ln(x + \sqrt{(x^2 + y^2)}) - y - x \ln x\}\Big|_{x=x_1}^{x_2} \Big|_{y=y_1}^{y_2} \qquad \text{III.8}$$

The evaluation of the third integral is straightforward:

$$I_3 = g_y \int_{y_1}^{y_2} \frac{-y dy}{\sqrt{(x^2 + y^2)}} \Big|_{x=x_1}^{x_2} = - g_y \sqrt{(x^2 + y^2)} \Big|_{x=x_1}^{x_2} \Big|_{y=y_1}^{y_2} \qquad \text{III.12}$$

Further:

$$I_4 = \frac{3\Delta g_o}{4R} \int_{y_1}^{y_2} \ln(x^2 + y^2) dy \Big|_{x_1}^{x_2}$$

$$= \frac{3\Delta g_o}{4R} \{y \ln(x^2 + y^2) - y + x \arctan \frac{y}{x}\}\Big|_{x=x_1}^{x_2} \Big|_{y=y_1}^{y_2} \qquad \text{III.13}$$

$$I_5 = \frac{3g_x}{2R} \int_{y_1}^{y_2} (x - y \arctan \frac{x}{y})\, dy \Big|_{x=x_1}^{x_2}$$

$$= \frac{3g_x}{2R} \{xy \Big|_{y_1}^{y_2} - \int_{y_1}^{y_2} y \operatorname{arccot} \frac{y}{x}\, dy\} \Big|_{x_1}^{x_2}$$

$$= \frac{3g_x}{2R} \{xy \Big|_{y_1}^{y_2} - \frac{y^2}{2} \operatorname{arccot} \frac{y}{x} \Big|_{y_1}^{y_2} + \frac{x}{2} \int_{y_1}^{y_2} \frac{y^2}{y^2 + x^2} dy\} \Big|_{x=x_1}^{x_2}$$

$$= \frac{3g_x}{2R} \{\frac{xy}{2} - \frac{y^2}{2} \operatorname{arccot} \frac{y}{x} + \frac{x^2}{2} \arctan \frac{y}{x}\} \Big|_{x=x_1}^{x_2} \Big|_{y=y_1}^{y_2} \qquad \text{III.14}$$

$$I_6 = \frac{3g_y}{2R} \int_{y_1}^{y_2} \frac{y}{2} \ln(x^2 + y^2) dy \Big|_{x=x_1}^{x_2}$$

$$= \frac{3g_y}{8R} \{(x^2 + y^2) \ln(x^2 + y^2) - y^2\} \Big|_{x=x_1}^{x_2} \Big|_{y=y_1}^{y_2} \qquad \text{III.15}$$

(The integral identities used above are taken from: Selby, S.M. (editor) Standard Mathematical Tables. Chemical Rubber Company, 1972). Evaluating the above equations for the indicated limits, the equation for ξ_3 becomes:

$$\xi_3 = -\frac{1}{2\pi G}(\Delta g f_1 + g_x f_2 + g_y f_3) - \frac{3}{4\pi GR}(\Delta g g_1 + \frac{1}{2} g_x g_2 + \frac{1}{4} g_y g_3) \qquad \text{III.16}$$

where

$$f_1 = \ln(y_2 + \sqrt{(x^2 + y^2)}) - \ln(y_2 + \sqrt{(x_2^2 + y_2^2)}) - \ln(y_1 + \sqrt{(x_1^2 + y_1^2)})$$

$$\ln(y_1 + \sqrt{(x_2^2 + y_1^2)})$$

$$f_2 = y_2 \ln(x_2 + \sqrt{(x_2^2 + y_2^2)}) - y_2 \ln(x_1 + \sqrt{(x_1^2 + y_2^2)}) - y_1 \ln(x_2 + \sqrt{(x_2^2 + y_1^2)}) +$$

$$+ y_1 \ln(x_1 + \sqrt{(x_1^2 + y_1^2)})$$

$$f_3 = \sqrt{(x_1^2 + y_2^2)} - \sqrt{(x_2^2 + y_2^2)} - \sqrt{(x_1^2 + y_1^2)} + \sqrt{(x_2^2 + y_1^2)}$$

$$g_1 = \frac{1}{2}(y_2 \ln(x_2^2 + y_2^2 + y_1 \ln(x_1^2 + y_1^2 - y_2 \ln(x_1^2 + y_2^2) - y_1 \ln(x_2^2 + y_1^2)) +$$

$$+ x_2 \arctan\frac{y_2}{x_2} + x_1 \arctan\frac{y_1}{x_1} - x_2 \arctan\frac{y_1}{x_2} - x_1 \arctan\frac{y_2}{x_1}$$

$$g_2 = x_2 y_2 - y_2^2 \arctan\frac{x_2}{y_2} + x_2^2 \arctan\frac{y_2}{x_2} - x_1 y_2 + y_2^2 \arctan\frac{x_1}{y_2} - x_1^2 \arctan$$

$$\frac{y_2}{x_1} - x_2 y_1 + y_1^2 \arctan\frac{x_2}{y_1} - x_2^2 \arctan\frac{y_1}{x_2} + x_1 y_1 - y_1^2 \arctan\frac{x_1}{y_1} +$$

$$+ x_1^2 \arctan\frac{y_1}{x_1}$$

$$g_3 = (x_2^2 + y_2^2) \ln(x_2^2 + y_2^2) - (x_1^2 + y_2^2) \ln(x_1^2 + y_2^2) - (x_2^2 + y_1^2) \ln(x_2^2 + y_1^2) +$$

$$+ (x_1^2 + y_1^2) \ln(x_1^2 + y_1^2)$$

For η_3, a similar equation can be written, where, $\sin\alpha$ is replaced by y/s:

$$\eta_3 = -\frac{1}{2\pi G}(\Delta g f_1' + g_y f_2' + g_x f_3') - \frac{3}{4\pi GR}(\Delta g g_1' + \frac{1}{2} g_y g_z' + \frac{1}{4} g_x g'_z)$$

Here, the equations for f_1', f_2', f_3', g_1', g_2', g_3' are identical to those for f_1, f_2, f_3, g_1, g_2, g_3, except that x and y are everywhere interchanged.

The above analytical expressions for ξ_3, η_3 are correct to within 0.03% for the case where it is sufficient to model the local gravity anomalies by a plane. If a more complex modelling is required, then many additional integrals would have to be evaluated. The density of gravity data presently available does not warrant the additional effort involved.

APPENDIX IV

PROGRAMME DESCRIPTIONS

This appendix briefly summarises the purpose, and data used, for the major programmes used in the preparation of the thesis. It is not intended that this act as programme documentation, as full documentation of these programmes is available from the Surveying Engineering Department Computer Programme Library, and from the author. All programmes have been written in IBM FORTRAN IV for the IBM 370/158 installation at the University of New Brunswick Computer Centre.

(1) MEAN: Computes mean gravity anomalies (for arbitrary size blocks), using an analytical integration of a second-order polynomial, fitted to point gravity anomalies. The data consists of point gravity anomalies, together with their position (latitude and longitude) and estimates of their height accuracy. The data set should reside on tape, in the format used by the Earth Physics Branch, Dept. of Energy, Mines & Resources, Ottawa. Output is onto printer, with an optional output onto disc, and consists of: Position of the centre of each block, mean gravity anomaly, and estimate of its standard deviation.

(2) PRED: Computes predicted mean gravity anomalies (for arbitrary block sizes), using the weighted arithmetic mean of adjacent "observed" mean gravity anomalies (obtained via MEAN). The data consists of mean gravity anomalies (of the same size block), together with

the position of the centre of each block, and estimated standard deviations, read from disc. Output is onto printer (also optionally onto disc), and consists of both predicted and observed anomalies, block centre positions, and estimated standard deviations.

(3) INTDOV: Computes predicted astrogeodetic deflections using modified gravimetric deflections and two-dimensional correction polynomials. Input data consists of: Station numbers and positions of points at which deflections are to be predicted (on cards); station numbers, observed astrogeodetic deflection components, their positions and estimated standard deviations; $1^\circ \times 1^\circ$ free-air gravity anomalies, $1/3^\circ \times 1/3^\circ$ free-air gravity anomalies, point free-air gravity anomalies, together with their positions and error estimates (all from disc). Output consists of: Station numbers, predicted astrogeodetic deflection components, their positions, and estimated standard deviations. Output is by line printer, but the results may also be punched. An American National Standard FORTRAN version of this programme is also available.

(4) ANGEOID: Computes geoidal heights using a surface-fitting technique with deflections of the vertical. Input consists of: Station numbers, positions, deflection components, estimated standard deviations, all from disc. Output consists of: Station numbers, geoidal heights, residuals (at all deflection stations), and positions, geoidal heights, and estimated standard deviations of the geoidal heights, on a rectangular grid, all by line printer. Optionally, the grid values may also be punched, and

polynomial coefficients and their associated error covariance matrix written on disc.

(5) CONGA: Is a modification of ANGEOID in which additional input data, consisting of geoidal heights and their position and error covariance matrix, is used. This data is read from cards. The output is identical to that of ANGEOID.

(6) TRANS: Computes translation components between different geodetic datums. Input data consists of: Size and shape parameters for both datums, positions, geoidal heights and their estimated standard deviations, for both datums, and is read from cards. The positions on both datums should form matching pairs. Output consists of: Residuals, variance factor, translation components, and their error covariance matrix, on the line printer.

(7) DOVEGUN2: Is a modification of DOVEGUN1 (written by D.B. Thomson and A. Hamilton). It computes selected geoidal heights, deflections of the vertical, and their error covariance matrices, from the polynomial coefficients, and their error covariance matrix, produced by ANGEOID. Input consists of the above-mentioned coefficients and matrix, from disc files, and station numbers and positions, read from cards. Output consists of: Station numbers, positions, geoidal heights, deflection components, and error covariance matrices, on the line printer. Optionally, positions, geoidal heights and their error covariance matrix may be punched.

APPENDIX V

DATA BASE DESCRIPTION

This section briefly describes the data base developed using the raw data supplied by Geodetic Survey of Canada, Earth Physics Branch, and Defense Mapping Agency. This raw data has been modfied for use in INTDOV and ANGEOID, using some of the programmes described in the previous appendix. A more detailed description is available in the Surveying Engineering Computer Library. The data is of two types: Astrogeodetic deflections of the vertical, and free-air gravity anomalies. All the data sets reside on the disc: SEGEOD, at the University of New Brunswick Computer Centre, and are sequential data sets.

(1) Astrogeodetic Deflection data: consists of two data sets: USA.DEFL, and CANA.DEFL. The first of these contains the deflections in the United States; the second, those in Canada. Each data record contains the following information. Station number; latitude; longitude; deflection in meridian (ξ); deflection in prime vertical (η); standard deviation of ξ; standard deviation of η. (Note: Longitude measured positive EAST.)

(2) The free-air gravity anomalies are of three classes. Point anomalies; $1/3^\circ \times 1/3^\circ$ mean anomalies; $1^\circ \times 1^\circ$ mean anomalies. The mean anomaly data sets consist of observed and predicted mean anomalies (see section 2.2 of this thesis for details). Due to the large amount of data, the classes have been broken down geographically into smaller data sets.

Each data record, in these sets, contains the following. Latitude; longitude (these for the mid-point of the block, for the mean anomalies); gravity anomaly; standard deviation of gravity anomaly. (Note: Longitude measured positive WEST.)

The geographical breakdown of the classes is outlined below, in terms of latitude (ϕ) and longitude (λ) limits.

(1) Point anomalies:

PNT.EAST:	$42° \leq \phi < 65°$	$52° \leq \lambda < 75°$
PNT.CENTRE:	$42° \leq \phi < 65°$	$72° \leq \lambda < 90°$
PNT.PRAIR:	$49° \leq \phi < 65°$	$90° \leq \lambda < 120°$
PNT.WECO:	$49° \leq \phi < 65°$	$115° \leq \lambda < 140°$
PNT.NWT:	$60° \leq \phi < 70°$	$90° \leq \lambda < 140°$
PNT.HUDBAY:	$50° \leq \phi < 65°$	$70° \leq \lambda < 100°$

(2) $1/3° \times 1/3°$ mean anomalies:

PRED3.EAST:	$40° \leq \phi < 65°$	$50° \leq \lambda < 80°$
PRED3.CENTRE:	$40° \leq \phi < 65°$	$73° \leq \lambda < 95°$
PRED3.PRAIR:	$47° \leq \phi < 65°$	$90° \leq \lambda < 120°$
PRED3.WECO:	$47° \leq \phi < 65°$	$115° \leq \lambda < 145°$
PRED3.NWT:	$60° \leq \phi < 70°$	$90° \leq \lambda < 145°$
PRED3.HUDBAY	$50° \leq \phi < 65°$	$70° \leq \lambda < 100°$

(3) $1° \times 1°$ mean anomalies:

PRED1:	$40° \leq \phi < 85°$	$50° \leq \lambda < 145°$

REFERENCES

Bacon, C.J. (1966). Deflections of the vertical from mountain net adjustment. M.Sc. Thesis, Department of Surveying Engineering, University of New Brunswick.

Bender, P.L., C.O. Alley, D.G. Currie, J.E. Faller (1968). Satellite geodesy using laser range measurements only. J. of Geophys. Res. Vol. 73, No. 16.

Bomford, G. (1971). Geodesy. Third Edition. Oxford University Press, Oxford.

Buck, R.J., and J.G. Tanner (1972). Storage and retrieval of gravity data. Bulletin Géodésique, No. 103.

Decker, B.L. (1972). Present day accuracy of the earth's gravitational field. Paper presented at Int. Symp. on Earth Gravity Models and Related Problems, St. Louis.

Derenyi, E.E. (1965). Deflections of the vertical in central New Brunswick. M.Sc. Thesis, Department of Civil Engineering, University of New Brunswick.

Dept. of Energy, Mines & Resources (1972). Workshop Report on Horizontal and Vertical Control Surveys in the Hinterland Areas, Ottawa.

Dufour, H.M. (1968). The whole geodesy without ellipsoid. Bulletin Géodésique, No. 88

Fischer, I. (1960). A map of geoidal contours in North America. Bulletin Géodésique, No. 57.

Fischer, I. (1965). Gravimetric interpolation of deflections of the vertical by electronic computer. Paper presented to special study group 5-29, IAG, Uppsala.

Fischer, I., M. Slutsky, R. Shirley, P. Wyatt (1967). Geoid charts of North and Central America. Army Map Service Tech. Rep. No. 62.

Fischer, I. (1971). Interpolation of deflections of the vertical. Report of Special Study Group 5-29 to the 15th General Assembly, IAG, Moscow.

Fryer, J.G. (1971). The geoid in Australia - 1971. Dept. of National Development, Division of National Mapping, Tech. Rep. No. 13.

Gaposchkin, E.M. and K. Lambeck (1969). Smithsonian standard earth II. S.A.O. Spec. Rep. No. 315.

Heiskanen, W.A. and Vening-Meinesz (1958). The earth and its gravity field. McGraw-Hill, New York.

Heiskanen, W.A. and H. Mortiz (1967). Physical geodesy. W.H. Freeman, San Francisco.

Heitz, S. (1969). An astrogeodetic determination of the geoid for West Germany. Verlag des Inst. Fur Angewandte Geodasie, Reich II, Heft Nr. 24.

Heitz, S. and Tscherning, C.C. (1972). Comparison of two methods of astrogeodetic geoid determination based on least-squares prediction and collocation. Tellus, Vol. 24, No. 3.

Hoskinson, A.J. and J.A. Duerksen (1952). Manual of geodetic astronomy. U.S. Dept. of Commerce, Coast and Geodetic Survey, Spec. Publ. No. 237.

Hotine, M. (1969). Mathematical geodesy. ESSA Monograph 2, Washington.

REFERENCES - cont'd

Hradilek, L. (1968). Spatial triangulation in mountain regions. Acta Universitatis Carolinae, Geographica No. 1.

International Association of Geodesy (1971a). Geodetic System 1967. Special Publication No. 3.

International Association of Geodesy (1971b). Proceedings of the 15th general assembly. IAG. Moscow.

Kaula, W.M. (1957). Accuracy of the gravimetrically computed deflections of the vertical. Trans. of the AGU, Vol.38

Kaula, W.M. (1966). Theory of satellite geodesy. Blaisdell, Waltham.

Klinkenberg, H. (1972). New specifications for control surveys in Canada. Paper presented at Canadian Inst. of Surveying Annual Meeting, Quebec.

Kobold, F. and E. Hunziker (1962). Communication sur la courbure de la verticale. Bulletin Géodésique, No. 65.

Krakiwsky, E.J. and Konecny, G. (1971). Analysis of the primary and secondary control networks - Implications for a readjustment to satellite control. The Canadian Surveyor, Vol. 25, No. 2.

Lachappelle (1973). A study of the geoid in Canada. Univ. of Oxford. Department of Surveying and Geodesy, M.Sc. Thesis.

Lambeck, K. (1971). The relations of some geodetic datums to a global geocentric reference system. Bulletin Géodésique, No. 99.

Lauritzen, S.L. (1973). The probabilistic background of some statistical methods in physical geodesy. Publ. of the Danish Geodetic Inst., no. 48.

Lisitzin, E. and J.G. Pattulo (1961). The principal factors influencing the seasonal oscillation of sea level. Journal of Geoph. Res., Vol. 66, No. 3.

McLellan, C.D. (1974). Geodetic networks in Canada. Presented at Int. Symp. on Problems Related to the Redefinition of North American Geodetic Networks, Fredericton.

Meissl, P. (1973). Distortions of terrestrial networks caused by geoid errors. Bolletino di Geodesia e Scienze Affine, Vol. 32, No. 2.

Melchior, P. (1966). The earth tides. Pergamon Press.

Merry, C.L. and P. Vaníček (1973). Horizontal control and the geoid in Canada. The Canadian Surveyor, Vol. 27, No. 1.

Merry, C.L. and P. Vaníček (1974a). A method for astrogravimetric geoid determination. Dept. of Surveying Engineering Technical Report No. 27, University of New Brunswick.

Merry, C.L. and P. Vaníček (1974b). The geoid and datum translation components. The Canadian Surveyor, Vol. 28, No. 1.

Merry, C.L. and P. Vanicek (1974c). A technique for determining the geoid from a combination of Astrogeodetic and gravimetric deflections. Paper presented at Int. Symp. on Problems Related to the Redefinition of North American Geodetic Networks, Fredericton.

Molodensky, M.S., V.F. Eremeev, M.I. Yurkina (1962). Methods for the study of the external gravitational field and figure of the earth. Israel program for Scientific Translations, Jerusalem.

Moritz, H. (1972). Advanced least squares methods. Ohio State Univ., Department of Geodetic Science, Report No. 175.

Mueller, I.I. (1964). Interpolation of deflections of the vertical by means of a torsion balance. Ann. Acad. Scient. Fennicae, A.III, 78.

REFERENCES - cont'd

Mueller, I.I. (1969). Spherical and practical astronomy as applied to geodesy. F. Ungar, New York.

Mueller, I.I., J.P. Reilly, T. Soler (1972). Geodetic satellite observations in North America (solution NA-9). Ohio State Univ. Dept. of Geodetic Science Rep. No. 187.

Nagy, D. (1963). Gravimetric Deflections of the vertical by digital computer. Public. of the Dominion Observatory, Vol. 27, No. 1

Nagy, D. (1973). Free air anomaly map of Canada from piece-wise surface fittings over half-degree blocks. The Canadian Surveyor, Vol. 27, No. 4.

Ndyetabula, S.L.P. (1974). A study on the curvature of the lines of force of gravity. M.Sc. thesis, Dept. of Surveying Engineering, University of New Brunswick.

Ney, C.H. (1955). Contours of the geoid for Southeastern Canada. Bulletin Géodésique, No. 23.

Rapp, R.H. (1972). A 300 n.m. terrestrial gravity field. Paper presented at 53rd annual meeting, AGU, Washington.

Rice, D.A. (1952). Deflections of the vertical from gravity anomalies. Bulletin Géodésique, No. 25.

Rice, D.A. (1962). A geoidal section in the United States. Bulletin Géodésique, No. 65.

Rice, D.A. (1965). The development of geoidal sections in the central United States. Aus der Geodatischen Lehre und Forschung.

Seppelin, T.O. (1971). 1° x 1° mean free-air gravity anomalies. ACIC Reference publication No. 29, St. Louis.

Seppelin, T.O. (1974). The department of Defense world geodetic system 1972. Presented at Int. Symp. on Problems Related to the Redefinition of North American Geodetic Networks, Fredericton.

Simmons, L.G. (1950). How accurate is first-order triangulation? The Journal, Coast and Geodetic Survey, No. 3.

Stoyko, A. (1962). Heure definitive (TU2) des Signaux Horaires en 1962. Bulletin Horaire, No. 19 (series G).

Szabo, B. (1962). Comparison of the deflection of the vertical components computed by astrogeodetic, gravimetric and topographic isostatic techniques. Bulletin Géodésique, No. 65.

Strange, W.E. and G.P.Woollard (1964). Anomaly selection for deflection interpolation. Hawaii Inst. of Geophysics, Report No. 64-12.

Thomson, D.B. and E.J. Krakiwsky (1974). Combination of terrestrial and satellite networks. University of New Brunswick, Dept. of Surveying Engineering, Tech. Report No. 30.

Uotila, U.A. (1960). Investigations on the gravity field and shape of the earth. Ann. Acad. Scient. Fennicae, A.III, 55.

Vaníček, P., J.D. Boal, T.A. Porter (1972). Proposals for a more modern system of heights for Canada. Surveys and Mapping Branch, Tech. Rep. No. 72-3.

Vaníček, P. and A.C. Hamilton (1972). Further analysis of vertical control movement observations in the Lac St. Jean area, Quebec. Can. J. of Earth Sciences, Vol. 9, No. 9.

Vaníček, P. and D.E. Wells (1972). The least-squares approximation and related topics. Dept. of Surveying Engineering Lecture Notes No. 22, University of New Brunswick.

REFERENCES - cont'd

Vaníček, P. (1973). Introduction to adjustment calculus. Univ. of New Brunswick, Dept. of Surveying Engineering Lecture Notes No. 35.

Vaníček, P. and C.L. Merry (1973). Determination of the geoid from deflections of the vertical using a least-squares surface fitting technique. Bulletin Géodésique, No. 109.

Vaníček, P. and D.E. Wells (1974). Positioning of geodetic datums. Paper presented at Int. Symp. on Problems Related to the Redefinition of North American Geodetic Networks, Fredericton.

Vincent, S., W.E. Strange, J.G. Marsh (1972). A detailed gravimetric geoid of North America, North Atlantic, Eurasia and Australia. Paper presented at Int. Symp. on Earth Gravity Models and Related Problems, St. Louis.

Wells, D.E. and E.J. Krakiwsky (1971). The method of least squares. University of New Brunswick, Dept. of Surveying Engineering Lecture Notes. No. 18.

Wells, D.E. (1974). Electromagnetic metrology, Hilbert space optimisation, and their application to Doppler geodetic control. Ph.D. thesis, Dept. of Surveying Engineering, University of New Brunswick.